

# **The role of the testicular microenvironment in inducing a testis-specific phenotype of testicular macrophages**

Inaugural Dissertation

submitted to the

Faculty of Medicine

in partial fulfillment of requirements

for the PhD-Degree

of the Faculty of Veterinary Medicine and Medicine

of the Justus Liebig University Giessen

by

Yalong Yang

of

Henan, China

Giessen 2021

From the Department of Anatomy and Cell Biology  
Director/Chairman: Prof. Dr. Wolfgang Kummer  
of the Faculty of Medicine of the Justus Liebig University Giessen

First Supervisor and Committee Member: Prof. Dr. Andreas Meinhardt

Second Supervisor and Committee Member: Prof. Dr. Gerhard Schuler

Committee Members:

Prof. Dr. Norbert Weißmann

Prof. Dr. Georgios Scheiner-Bobis

Date of Doctoral Defense: 27.05.2021

# CONTENTS

## CONTENTS

<u>CONTENTS</u> .....	I
<u>ABBREVIATIONS</u> .....	-1-
<u>1. INTRODUCTION</u> .....	-4-
<u>1.1 The testis as an immune privileged organ</u> .....	-4-
<u>1.1.1 Anatomy of the testis and interaction of different cells</u> .....	-4-
<u>1.1.2 Testicular immune privilege</u> .....	-6-
<u>1.2 Testicular macrophages play an important role in the immunosuppressed microenvironment of the testis</u> .....	-8-
<u>1.2.1 Role of macrophages in balancing the innate immunity</u> .....	-8-
<u>1.2.2 Tissue-resident macrophages and testicular macrophages</u> .....	-10-
<u>1.3 Growth factors induce different macrophage immune profiles</u> .....	-13-
<u>1.4 The cross-talk between inflammation and metabolism</u> .....	-16-
<u>1.4.1 The metabolism profiles of different phenotypes of macrophages</u> .....	-16-
<u>1.4.2 Metabolism of cholesterol in macrophages during inflammation</u> .....	-17-
<u>1.4.3 Relationship between male reproduction and 25HC</u> .....	-19-
<u>1.5 Regulations of interferon and interferon related genes in macrophages</u> .....	-19-
<u>1.5.1 Interferons</u> .....	-19-
<u>1.5.2 Role of IFN-<math>\beta</math> in immune regulation</u> .....	-20-
<u>1.5.3 Functions of IRFs in inflammation</u> .....	-22-
<u>1.6 Aim of the study</u> .....	-23-
<u>2. MATERIALS AND METHODS</u> .....	-25-
<u>2.1 Materials</u> .....	-25-
<u>2.1.1 Equipment</u> .....	-25-
<u>2.1.2 Chemicals</u> .....	-26-
<u>2.1.3 Cell culture reagents</u> .....	-28-
<u>2.1.4 Kits</u> .....	-29-

# CONTENTS

<u>2.1.5 Experimental antibodies.....</u>	-29-
<u>2.1.5.1 Antibodies for flow cytometry.....</u>	-29-
<u>2.1.5.2 Antibodies for immunoblotting.....</u>	-30-
<u>2.1.6 Primers.....</u>	-31-
<u>2.1.7 Miscellaneous .....</u>	-32-
<u>2.2 METHODS.....</u>	-33-
<u>2.2.1 Animals.....</u>	-33-
<u>2.2.2 Bone marrow derived macrophage (BMDM) culture.....</u>	-33-
<u>2.2.3 Flow Cytometry (FC) assay.....</u>	-34-
<u>2.2.3.1 Flow Cytometry assay with BMDM.....</u>	-34-
<u>2.2.3.2 Flow Cytometry assay with samples extracted from organs.....</u>	-35-
<u>2.2.4 Protein extraction from cells.....</u>	-35-
<u>2.2.5 Enzyme-linked immunosorbent assay (ELISA) of inflammatory cytokines.....</u>	-36-
<u>2.2.6 Cell viability analyzed by MTT assay.....</u>	-36-
<u>2.2.7 cDNA synthesis and qRT-PCR assay.....</u>	-37-
<u>2.2.7.1 Total mRNA isolation.....</u>	-37-
<u>2.2.7.2 DNA digestion.....</u>	-37-
<u>2.2.7.3 cDNA synthesis.....</u>	-37-
<u>2.2.7.4 Polymerase chain reaction (PCR).....</u>	-38-
<u>2.2.7.5 Agarose gel electrophoresis.....</u>	-38-
<u>2.2.7.6 Real-time reverse transcription- Polymerase chain reaction (qRT-PCR).....</u>	-39-
<u>2.2.7.7 Genotyping of Irf7 knockout mice.....</u>	-40-
<u>2.2.8 Mouse testicular macrophages (mTM) isolation.....</u>	-41-
<u>2.2.8.1 Reagent and instrument .....</u>	-41-
<u>2.2.8.2 Preparation of single cell suspension using a percoll gradient.....</u>	-41-
<u>2.2.8.3 MicroBead selection .....</u>	-42-
<u>2.2.9 Immunofluorescent (IF).....</u>	-42-
<u>2.2.10 Isolation of peritoneal macrophages.....</u>	-42-

# CONTENTS

2.2.11 Immunoblotting.....	-43-
2.2.11.1 Buffers and solutions .....	-43-
2.2.11.2 Western blotting (WB) .....	-45-
2.2.12. Immunohistochemistry (IHC).....	-45-
2.2.13 Hematoxylin and Eosin ( HE ) Staining.....	-46-
2.3 Statistical methods.....	-46-
3. RESULTS.....	-47-
3.1 Testicular macrophages showed specific immunosuppressive characteristics.....	-47-
3.1.1 TM isolation by microbeads.....	-47-
3.1.2 TM show specific profiles compared to peritoneal macrophages.....	-48-
3.1.3 TM display a significantly different gene expression profile compared to microglia.....	-49-
3.2 25HC displays anti-inflammatory functions to a similar extent as corticosterone.....	-50-
3.2.1 Optimization of the culture system of bone marrow derived macrophages.....	-50-
3.2.2 High amounts of 25HC are produced in the testis.....	-51-
3.2.3 25HC was cytotoxic to BMDM in a dose and time depend manner.....	-52-
3.2.4 25HC has anti-inflammatory effects on BMDM at the protein levels.....	-52-
3.2.5 25HC shows anti-inflammatory effects at the gene expression level.....	-53-
3.2.6 Inhibition of 25HC has no obvious effects on macrophage phenotypes.....	-54-
3.3 25HC down-regulates the relevant transcription factors.....	-57-
3.4 BMDM show diametrically opposite inflammatory responses characteristics following M-CSF and GM-CSF stimulation.....	-58-
3.4.1 M-CSF derived macrophages show higher expression of anti-inflammatory genes than GM-CSF derived macrophages.....	-58-
3.4.2 Production of TNF- $\alpha$ and IL-10 is differently regulated by CSF.....	-59-
3.4.3 M-CSF/CSF1R inhibition study.....	-60-
3.4.3.1 Cytotoxicity of PLX-3397 (Pexidartinib) on matured BMDM.....	-60-
3.4.3.2 PLX blocked the activation of CSF1R targeted proteins upon LPS	

# CONTENTS

<u>stimulation</u> .....	-61-
3.4.3.3 PLX, by blocking CSF1R, suppressed the production of TNF- $\alpha$ .....	-62-
3.4.3.4 PLX inhibits the modulation of CSF1R-stimulated pro-/anti-inflammatory <u>genes</u> .....	-63-
3.5 Inflammatory response induced by M-CSF and GM-CSF are differently modulated by <u>25HC</u> .....	-63-
3.5.1 25HC suppresses TNF- $\alpha$ in GM-CSF derived macrophages.....	-64-
3.5.2 25HC differently regulates anti-inflammatory genes in M-CSF and GM-CSF <u>derived macrophages</u> .....	-64-
3.5.3 Pro-inflammatory genes are mostly down-regulated by 25HC in M-CSF <u>derived macrophages</u> .....	-66-
3.5.4 IFN- $\beta$ is differently regulated by 25HC and CSF.....	-67-
3.6 Relationship between IFN- $\beta$ , IRF7 and inflammatory response.....	-69-
3.6.1 M-CSF induces a higher expression of <i>Ifn-<math>\beta</math></i> than GM-CSF.....	-69-
3.6.2 IFN1R inhibitor study.....	-70-
3.7 IRF7 deficiency in mice modulates immune cells <i>in vivo</i> .....	-72-
3.7.1 Verification of Irf7 knock out by PCR.....	-73-
3.7.2 Mice deficient of Irf7 show no change in the ratio of body/testis weight.....	-73-
3.7.3 IRF7 deficient mice show normal structure histology.....	-74-
3.7.4 Irf7 knock out influences leukocyte modulation <i>in vivo</i> .....	-75-
3.7.5 Irf7 modulates the inflammatory response of BMDM.....	-85-
4. DISCUSSION.....	-90-
4.1 Testicular macrophage shows specific immune characteristics.....	-90-
4.2 25HC displays dual functions in inflammation.....	-91-
4.3 M-CSF induces an immunosuppressive environment in the testis.....	-95-
4.4 IRF7 causes a tolerant immune phenotype in macrophages.....	-98-
5. SUMMARY.....	-103-
6. ZUSAMMENFASSUNG.....	-104-

# CONTENTS

<u>7. REFERENCE</u> .....	-105-
<u>8. ACKNOWLEDGEMENTS</u> .....	-117-
<u>9. CURRICULUM VITAE</u> .....	-119-
<u>10. EHRENWÖRTLICHE ERKLÄRUNG</u> .....	-120-

## ABBREVIATIONS

### ABBREVIATIONS

ANOVA	Analysis of variance
APS	Ammonium persulfate
BMDM	Bone marrow derived macrophages
BSA	Bovine serum albumin
BTB	Blood testis barrier
°C	Degree Celsius
cDNA	Complementary DNA
CD32	Cluster of differentiation 32
CD45	Cluster of differentiation 45
CSF1	Colony stimulating factor 1
25HC	25-hydroxycholesterol
DCs	Dendritic cells
DAPI	4', 6'-diamino-2-phenylindole
DNA	Deoxyribonucleic acid
DNase	Deoxyribonuclease
dNTPs	2'-deoxynucleoside-5'-triphosphates
EDTA	Ethylene diamine tetraacetic acid
ELISA	Enzyme-linked immunosorbent assay
FCS	Fetal calf serum
GM-CSF	Granulocyte-macrophage colony stimulating factor
IFN- $\beta$	Interferon- $\beta$
IL-1 $\beta$	Interleukin 1 $\beta$
IL-10	Interleukin 10
kD	Kilo Dalton
LH	Luteinizing hormone
LPS	Lipopolysaccharide
M	Molar
M-CSF	Macrophage colony stimulating factor



## ABBREVIATIONS

MEM	Minimum essential medium
mg	Milligram
MHC	Major histocompatibility complex
min	Minute
mL	Milliliter
mM	Milimolar
MW	Molecular weight
NaCl	Sodium chloride
NF- $\kappa$ B	Nuclear factor-kB
NO	Nitric oxide
NOS	Nitric oxide synthase
OD	Optical density
PAGE	Polyacrylamide gel electrophoresis
PBS	Phosphate buffered saline
PCR	Polymerase chain reaction
PRR	Pattern-recognition receptors
P/S	Penicillin/Streptomycin
RE	Relative expression
RNA	Ribonucleic acid
RNase	Ribonuclease
rt-PCR	Real-time polymerase chain reaction
qRT-PCR	Quantitative real-time PCR
rpm	Revolutions per minute
RT	Room temperature
SDS	Sodiumdodecylsulphate
sec	Second
TAE	Tris acetate EDTA
TBS	Tris buffered saline
TGF- $\beta$	Transforming growth factor $\beta$
TLR	Toll-like receptor

## ABBREVIATIONS

TM	Testicular macrophages
TNF- $\alpha$	Tumor necrosis factor alpha
Tris	Tris (hydroxymethyl) amino methane
$\mu$	Micro
$\mu\text{g}$	Microgram
$\mu\text{l}$	Microliter
$\mu\text{M}$	Micromolar
V	Volt
v/v	Volume per volume
w/v	Weight per volume

# INTRODUCTION

## 1. INTRODUCTION

### 1.1 The testis as an immune privileged organ

#### 1.1.1 Anatomy of the testis and interaction of different cells

The testis is the male reproductive gland or gonad in all mammals, including humans. The functions of the testis are to produce both sperm and androgens, primarily testosterone. Testosterone release is mainly controlled by the anterior pituitary gland derived luteinizing hormone (LH); whereas spermatogenesis is mainly regulated both by the anterior pituitary gland derived follicle-stimulating hormone (FSH) and gonadal testosterone<sup>1-2</sup>.

Human testes are a pair of oval-shaped organs, and each testis weighs about 25g, is 2-3cm in diameter and 4-4.5cm long. Each testis is covered by the tunica albuginea, a fibrous capsule, and is divided into around 350 wedge-shaped lobules. Within each lobule, there are 2-9 coiled tubules, called seminiferous tubules, which produce sperm cells. The septa dividing lobes all converge in one area at the dorsal side of each testis to form the mediastinum testis<sup>1-3</sup>.

The testis mainly consists of three types of cells, namely germ cells which differentiate into mature spermatozoa, Sertoli cells (SC) which support and nourish the developing germ cells, and Leydig cells (LC) which are involved in testosterone synthesis<sup>2-4</sup>. The spermatogonial stem cells migrate to the fetal testis from the embryonic yolk sac and differentiate into spermatozoa. SC, which are interspersed between the germinal epithelial cells within the seminiferous tubules, are analogous to the granulosa cells in the ovary. LC, which are located beneath the tunica albuginea, in the septal walls, and mostly between the tubules, are analogous to the hormone-secreting interstitial cells of the ovary. LC are irregularly shaped and have more than one nucleus. They are surrounded by numerous blood and lymphatic vessels, as well as nerve fibers. LC occupy 10-20% of the interstitial compartment<sup>2-4</sup>.

The interstitial compartment of the testis, which constitutes the area outside of the testis cords/seminiferous tubules, represents about 12-15% of the total testicular volume in humans. The interstitial compartment is composed of several cell types. The tubular compartment is separated from the interstitium via the collagen- and laminin-containing basement membrane, which is overlaid by peritubular cells that physically separate the two compartments<sup>3-4</sup>. Although the basic architecture of the testis is fairly similar among different mammal species, there are still some structural and cellular differences in the interstitium<sup>4-5</sup>. For instance, in the

# INTRODUCTION

human testis, a multi-cell-layered peritubular wall is present, in contrast to a single-cell-layered wall found in rodents<sup>5</sup>. Additionally, the human testis contains mast cells in the interstitium, which are rarely found in rodent testis<sup>6</sup>.

Within the interstitial compartment of both human and rodent testes, there are various somatic cell types, including peritubular cells, vascular endothelial cells, vascular smooth muscle cells, LC and immune cells. Under normal conditions, immune cells are mostly composed of testicular macrophages, accounting for around 20% of interstitial cells<sup>6-7</sup>. For every 10-50 LC present, one macrophage can be found<sup>7</sup>. The macrophages probably influence the function of the LC, in particular their proliferation, differentiation, and steroid production, through the secretion of cytokines. Several observations suggest that there is extensive and intimate cross-talk between these two cell types, which is probably facilitated by the unique intercytoplasmic digitations that physically connect these two cell types<sup>6-7</sup>. CSF1, which is known to regulate the function and survival of cells of the phagocytic mononuclear lineage is produced in the testis by for example LC<sup>8-11</sup>. All together, these data indicate the regulation between TM and LC.

Besides the LC-produced CSF1, also testosterone regulates testicular macrophage functions. Rettew and colleagues found that the *in vitro* administration of testosterone to macrophages resulted in a diminished production of pro-inflammatory cytokines<sup>12</sup>. Testosterone can maintain a negative feedback of macrophages by reducing the production of 25-hydroxycholesterol (25HC), a precursor of testosterone and stimulant for LC steroidogenesis<sup>12</sup>. However, Wang and colleagues showed that corticosterone and to a lesser extent testosterone in the interstitial fluid helps to maintain an immunosuppressive M2-like testicular macrophage (TM) profile leading to an increased expression of CD163, a higher secretion of IL-10 and lower secretion of TNF- $\alpha$ <sup>13</sup>. The different conclusions between two studies may due to different experimental models, the administration of two different CSFs for macrophages *in vitro* models, and different cell types and also other elusive reasons.

The interactions that exist in the testis among different cells, particularly TM, LC, and sperm cells, are rather complex. Depletion of LC in the testis whether by the specific cytotoxin ethane dimethane sulphonate (EDS) or by withdrawal of LH, leads to a significant progressive depletion of resident macrophages<sup>14-17</sup>. Tony DeFalco and colleagues found that one type of TM, which lies on the surface of the seminiferous tubules, appears to be necessary for the proliferation and differentiation of undifferentiated spermatogonia in the interstitium<sup>18</sup>. Moreover, stereological analysis indicated that both LC and TM are affected by gonadotropin

# INTRODUCTION

overstimulation, which can also lead to testosterone deficiency<sup>19</sup>. Evidence indicates that the underlying interactions that exist among TM, LC and sperm cells are not one-way dependent and further research is still needed to reveal the role of the testicular immune system in spermatogenesis.

## 1.1.2 Testicular immune privilege

Immune privileged organs are operationally defined as sites in the body where foreign tissue grafts can survive for extended, often indefinite periods<sup>20</sup>. Similar grafts placed at regular non-privileged sites in the body are acutely rejected<sup>20</sup>. In brief, immune privileged organs can tolerate antigens which would induce an immune response in other non-privileged organs. The central nervous system (CNS), including the brain, and the spinal cord, are regarded as immune privileged organs/systems<sup>20-21</sup>. With the development of refined methods, new studies found that immune privileged organs can still mount an immune response that can induce inflammation<sup>21</sup>. The induced inflammation is often of a weaker type than in non-privileged organs. Accumulating evidence shows that within immune-privileged organs, complex mechanisms in the immunosuppressive microenvironment exist that are diverted towards the resolution than the induction of inflammation<sup>21-22</sup>.

The testis is regarded as an immune-tolerant organ as it has the capacity to tolerate neo-antigens appearing on the developing germ cells in puberty, at a time when the immune system is already established<sup>22-23</sup>. The testicular immune tolerance mechanism has always been a key issue in the field of male reproduction. It is particularly important to understand the regulatory mechanisms of the immune system in the testis. Considering that plenty of neo-autoantigens are expressed during spermatogenesis, the immune tolerant status of the testis is critical in protecting the germ cells from auto-immune attacks<sup>3, 22-23</sup>. In 1767, John Hunter was the first to notice this specific immune tolerance, when he transplanted an intact testis from a cock into the abdominal cavity of a hen. Two centuries later, Head and colleagues transplanted skin and parathyroid allografts into the interstitial area of the testis, where the transplants survived for a longer period than orthotropic grafts. On the other hand, in some pathological conditions, the testicular immune privilege is undermined, followed by the production of anti-sperm antibodies (ASAs), which could lead to male infertility by affecting the sperm's fertilizing capacity and the number of mature sperm as well<sup>3, 22-25</sup>. Hence, testicular immune privilege is considered critical to guarantee human and other mammalian reproductive capabilities. A number of recent studies have shown that multiple mechanisms are involved in maintaining the testicular immune privilege, such as the blood-testis-barrier

# INTRODUCTION

(BTB)/ Sertoli cell barrier (SCB), immunosuppression by local microenvironmental factors and systemic immune tolerance<sup>23-25</sup>.

The SC provide structural and nutritional support for the development of germ cells<sup>2</sup>. The seminiferous tubule is surrounded either by a single layer (as in rats and mice) or multiple layers (as in human) of mesenchymal myoid peritubular cells (PTC)<sup>2-4</sup>. The SCB is formed by tight, adherent, and gap junctions that exist between SC in the seminiferous tubules. Germ cells expressing auto-antigens are separated from interstitial leukocytes by the SCB, which was previously believed to be the only factor responsible for maintaining the immune privilege in the testis<sup>3-5</sup>. Of note, Tung and colleagues showed that critical neo-antigens (Ags), such as the testis-specific isoform of lactate dehydrogenase 3 (LDH3) found in meiotic and post-meiotic germ cells sequestered behind the SCB, are phagocytosed and transported by SC through the SCB to the interstitial space<sup>26</sup>. Egressed Ags still maintain systemic tolerance which is probably dependent on regulatory T cells (Tregs) or some other mechanisms<sup>26</sup>. For a long period, the sole importance of SCB in maintaining the testicular immune privilege was widely accepted. However, some studies showed that patients with oligozoospermia or azoospermia have an intact SCB, so once again the reasons responsible for oligozoospermia or azoospermia were questioned<sup>3, 27</sup>.

Several factors come into play to ensure that the testicular immune privileged status is maintained including the chronic neo-antigen exposure which might induce immune tolerance, as well as the local immunosuppressive microenvironment. Emerging evidence indicates that the testicular somatic cells and some cytokines (e.g. corticosterone) could contribute to the tolerant microenvironment that shifts the TM phenotype to an immunosuppressive one<sup>13, 22-25</sup>. Ming and colleagues found that in the testicular interstitial fluid, corticosterone but not testosterone was a key factor in maintaining the M2 phenotype profile of TM<sup>13</sup>. Many other studies have shown that transforming growth factor beta (TGF- $\beta$ ), activin A, 25HC, and chemokine (C-C motif) ligand 2/ monocyte chemoattractant protein 1 (CCL2/ MCP1), which is found in the testicular interstitial space, have immunosuppressive functions<sup>27-29</sup>. Transplantation of macrophages between different organs in the mouse, for example from the peritoneum to the pleural cavity, led to the rapid adaption of peritoneal macrophages to the new environment with a specific pleural phenotype and gene profile<sup>36</sup>. This provides evidence that the local microenvironment is more powerful than systemic settings in maintaining and inducing differentiated resident macrophages. Similar evidence showed that microglia are IL-34 dependent and are regulated by TGF- $\beta$  through the transcription factors SMAD<sup>29-32</sup>.

# INTRODUCTION

Alveolar macrophages in the lung can be induced by CSF2 and are regulated by other factors via the PPAR $\gamma$  pathway<sup>29-32</sup>. Whether specific pathways or transcription factors found in the testis also have an important role in maintaining the immunosuppressive microenvironment in the testis is yet to be investigated.

## **1.2 Testicular macrophages play an important role in the immunosuppressed microenvironment of the testis**

### **1.2.1 Role of macrophages in balancing the innate immunity**

Macrophages- “the large eaters” according to its Greek origin- were first discovered by Ilya Mechnikov in 1882 in the larvae of starfish upon insertion of thorns of a tangerine tree and later in *Daphnia Magna* or the common water flea infected with fungal spores as cells responsible for the process of phagocytosis of exogenous particles. In 1908 he received the Noble Prize in Physiology or Medicine for this discovery. The macrophage is one type of white blood cells, that engulfs and digests cellular debris, exogenous particles, microbes, cancer cells, as well as abnormal cells, which is termed as phagocytosis<sup>33</sup>.

Macrophages are sentinels of the innate immune system that are distributed in all tissues and organs. Macrophages are a heterogeneous population of immune cells, playing critical and diverse functions in homeostatic and immune response. In the 1900s, Charles Mills and colleagues first identified the fundamentals of the M1/M2 phenotype based on the different pathways of arginine metabolism<sup>34</sup>. M1 macrophages produce toxic nitric oxide (NO), while M2 macrophages produce ornithine and urea. Mills also identified the most important and basic dichotomy in macrophage functions, whereas M1 macrophages kill (pathogens, infected cells, or tumor cells) and M2 macrophages heal (wound repair or tumor growth)<sup>34-35</sup>. M1 macrophages are regarded as pro-inflammatory while M2 macrophages are regarded as anti-inflammatory/pro-resolving. However, macrophages can differentiate into many more phenotypes allowing them to adapt to different stimuli and various microenvironments<sup>36</sup>

According to the original description, the main characteristic of M1 macrophages is their ability to start and sustain inflammatory responses, secrete pro-inflammatory cytokines, activate endothelial cells, and induce the recruitment and activation of other immune cells into lesions, like T and B cells. On the other hand, M2 macrophages are characterized by their ability to promote the resolution of inflammation, phagocytose apoptotic cells, drive collagen deposition in lesions, coordinate tissue integrity, and release anti-inflammatory mediators,

## INTRODUCTION

such as IL-10 to terminate the inflammation<sup>35-36</sup>. Depending on the specific signaling pathways and markers, macrophages can be generally distinguished into M1 or M2 phenotype (**Table 1**). Well-designed experiments provide evidence that the choice of classical markers or genes used to identify the phenotypes of macrophage depends on the microenvironmental context as well as other factors<sup>37-38</sup>.

Phenotype	Signaling pathway	Gene	Comment
M1	STAT1 and STAT3	NOS2	Highly induced in M1 activation
		IL12b	Highly induced in M1 activation
		SOCS3	Induced by IL-6 and many other factors
		COX2	Highly induced in M1 activation
		IL23a (IL23p19)	Highly induced in M1 activation
M2	STAT6	SOCS2	Not macrophage-specific but highly induced by IL-4 and IL-13
		Chi3l3(Ym1)	Not expressed in human but highly induced by IL-4 and IL-13
		CXCL13	Th2 cell response
		KLF4	Transcription factor induced by IL-4
		CCL12	Th2 cell response
Context-dependent	—	Arg1	Both STAT6 and STAT3 can induce
		IL-10	Not all but most macrophages can be induced in different contexts
		Mrc1	Expressed in many subtypes of macrophages but highly induced in an M2 context

**Table 1. Gene expression and signaling pathways of M1/M2 macrophages.** Modified from Murray PJ, Wynn TA<sup>158</sup>.

Nowadays, it is generally accepted that the polarized macrophages are referred to as M1-like or M2-like macrophages, with the tendency to induce or to resolve inflammation respectively, rather than being referred to as M1 or M2 macrophages<sup>37-38</sup>. Moreover, macrophages can be classified into more subtypes according to their specific function, gene expression, cytokine production, and type of stimulation. Accordingly, they can be divided into atypical, M1, TAM (tumor-associated macrophage), and tissue resident M2, M2a, M2b, M2c, and M2d subtypes



# INTRODUCTION

(Figure 1). However, further investigations into macrophage subtypes and profiles are still needed<sup>39</sup>.

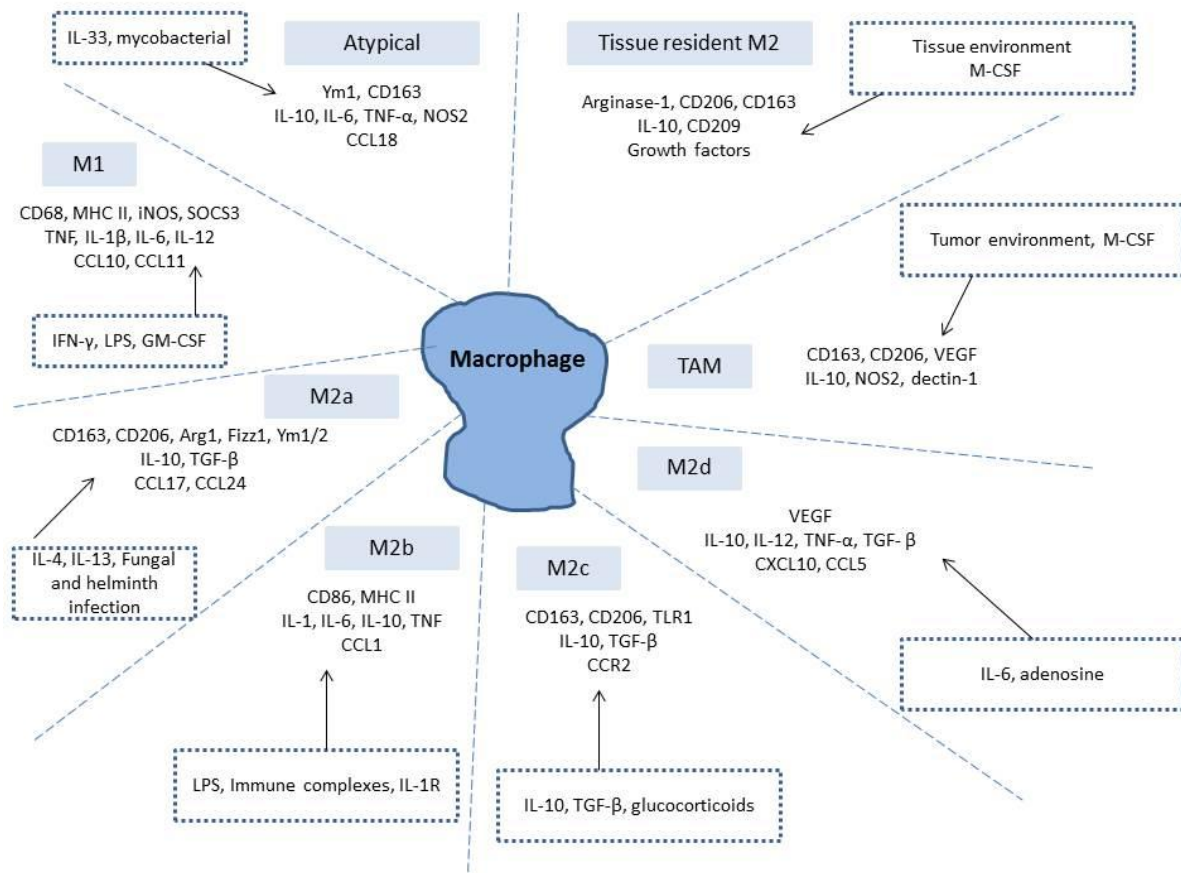


**Figure 1. Subtypes and main characteristics of macrophages.** Adapted from Röszer T<sup>159</sup>.

## 1.2.2 Tissue-resident macrophages and testicular macrophages

Macrophages are present in all vertebrate organs, throughout their life span, and are considered as ubiquitous innate immune cells. Tissue-resident macrophages are a heterogeneous population of immune cells, which also exhibit non-immune functions in order to maintain homeostasis<sup>40</sup>. Tissue macrophages are generated during embryogenesis. Fetal macrophages develop independently of c-Myb, a transcription factor required for hematopoietic stem cells (HSC)<sup>40</sup>. HSC arise in the aorto-gonad-mesonephros region on embryonic day 10.5 (E10.5) and migrate to the fetal liver to initiate definitive hematopoiesis. During late embryogenesis, hematopoiesis then shifts to the bone marrow (BM), where all lineages of the definitive hematopoiesis, including blood monocytes, are generated. Tissue macrophages could arise from BM and blood monocytes under defined conditions and the environment<sup>40-42</sup>.

## INTRODUCTION

Fate mapping studies of organ resident macrophages revealed the origin of tissue macrophages. For example, microglia in the brain originated from the yolk sac, Kupffer cells in the liver from the yolk sac and embryonic HSC, alveolar macrophages in the lung and red pulp macrophages in the spleen from embryonic HSC, and Langerhans cells in the skin from the yolk sac and embryonic HSC<sup>41-42</sup>. Further analyses have revealed that tissue-resident macrophages can self-renew and can persist for a long period of time without requiring HSC replenishment<sup>41-44</sup>. New data recently showed that, after birth, in the heart, maybe also in other organs, resident macrophages can slowly self-renew also from BM progenitors<sup>44</sup>.

Moreover, the tissue environment can drive the selection and function of DNA enhancers which control tissue-specific macrophage identities<sup>45</sup>. By comparing the transcriptomes and enhancers between microglia and resident macrophages in the peritoneal cavity, it was found that distinct tissue environments can divergently regulate gene expression by differentially activating a common enhancer repertoire and by inducing the expression of divergent secondary transcription factors that collaborate with the macrophage lineage-determining factor PU.1 to establish tissue-specific enhancers<sup>45-47</sup>. It is now widely accepted that the organ-specific environment containing specific local factors can induce targeted genes or transcription factors that model the tissue-specific phenotype of resident macrophages<sup>47</sup>.

Testicular macrophages (TM) are abundant in the testis, accounting for around 20% of interstitial cells<sup>6-7</sup>. According to recent studies, testicular macrophages could be divided into two different populations - interstitial macrophages and peritubular macrophages - due to their distinct tissue localization and morphology<sup>48-51</sup>. Recent studies revealed that interstitial macrophages are derived from embryonic progenitors, especially from the yolk sac, whereas peritubular macrophages are exclusively derived from bone marrow-derived progenitors, before puberty<sup>51-53</sup>. Analysis of fate-mapping studies using specific cell markers (CD64 and major histocompatibility complex class II (MHC II)) expressed on peritubular and interstitial macrophages in the testis, showed that 14%-30% of peritubular macrophages are replaced by BM-derived macrophages during life, compared to only 3%-5% of interstitial macrophages<sup>44,48</sup>. More recently, Mossadegh-Keller and Sieweke provided a more detailed characterization of these two populations of TM, showing that interstitial TM are M-CSFR<sup>+</sup>CD64<sup>hi</sup>MHCII<sup>-</sup> cells while peritubular TM are M-CSFR<sup>lo</sup>CD64<sup>lo</sup>MHCII<sup>+</sup> cells<sup>48</sup>. More specific cell markers, such as CD38, Gpr18 and Fpr2 as novel M1 markers, Egr2 and c-Myc as M2 markers, and Lyve1 as an interstitial macrophage marker<sup>53</sup> can be used to further distinguish between different populations of resident macrophages<sup>52</sup>.

## INTRODUCTION

TM and LC play essential roles in controlling concerted interactions of endocrine hormones involved in spermatogenesis. 25HC, for instance, produced by TM, is regarded as the key factor for the synthesis of testosterone by LC<sup>4,12</sup>. As the first line of defense for innate immunity, macrophages can recognize antigens allowing them to induce inflammation. However, TM do not target sperms expressing neo-antigens which arise after puberty, and this tolerance is critical in order to preserve the reproductive capability<sup>22-23, 28</sup>. However, clinical studies revealed that patients with azoospermia or oligozoospermia show no obvious inflammation or damage in the testis<sup>3,7</sup>. Some well-designed studies showed that in pathological situations, immunological tolerance of TM to sperm in the testis is compromised, which can lead to azoospermia, oligozoospermia as well as other sperm dysfunctions<sup>3,7,54</sup>. But comprehensive testicular immune profiles have not been extensively studied until now. Such investigations are nevertheless needed to understand how macrophages in the testis are able to tolerate neo-antigens appearing after puberty, which could give guidance towards clinical treatment of azoospermia or oligozoospermia. Considering SC and LC are regarded as indispensable for proper sperm formation and function, and due to their close association with TM, it was hypothesized that immunosuppression in the testis is also regulated by testicular somatic cells<sup>10, 54</sup>.

The molecular mechanisms that define a specific TM profile are still poorly understood. Ming and colleagues showed that corticosterone in the interstitial fluid could induce immunosuppression in bone marrow derived macrophages (BMDM), and its inhibition in TM could enhance inflammatory responses<sup>13</sup>. Activin A, TGF- $\beta$ , IFN- $\beta$ , and 25HC were also found in the testis and can play a role in regulating and balancing the immune responses in some *ex vivo* models<sup>23-24, 28</sup>. However, whether these factors and the underlying mechanisms can induce and maintain a specific TM profile in the testis still remains elusive<sup>55</sup>.

Over the past decades, many experiments were carried out to decipher the mechanisms and determine the key factors responsible for inducing and maintaining specific macrophage profiles. Initially BMDM or macrophage cell lines were used followed primary macrophages which were treated by specific factors to further investigate their function. These studies took advantage of common procedures, like enzymatic digestion of organs or tissues and harvesting specific cells using fluorescence-activated cell sorting (FACS) or density gradient centrifugation. Some of these studies also relied on the attachment capability of macrophages in order to isolate TM. In 2002, Bryniarski et al. utilized the different buoyant densities of the different cells in the testis, as well as other characteristics, like esterase activity and FcR

# INTRODUCTION

expression, in order to enrich TM<sup>56</sup>. They found that cells present in different fractions differ in their cytokine production, and that TM present in the intermediate fraction are able to produce IL-6 and TNF- $\alpha$ . Further studies revealed that the isolation of resident macrophages using enzymatic digestion may cause irreversible changes to macrophages, which must be considered in studies addressing macrophages in inflammatory settings<sup>56-58</sup>. Studies showed that once naive macrophages were activated towards the M1 phenotype, mitochondrial function is irreversibly impaired. Mitochondrial function is regarded to be important for M2 re-polarization and the production of M2-specific cytokines<sup>59</sup>. Some studies done in the testis showed that TM that were enzymatically obtained produced significantly more pro-inflammatory cytokines (IL-6 and TNF- $\alpha$ ) than TM that were mechanically isolated, and this effect was in fact long-lasting<sup>57-58</sup>. Further studies have used FACS in order to harvest pure resident macrophages, but this method also has some limitations. FACS utilizes high pressure which can compromise cell viability in downstream experiments. The ideal method and procedure to study and isolate organ macrophages should not affect the differentiation, viability or activation of macrophages. When it comes to TM, the activation by enzymes can be avoided, because the testis can be easily dispersed as a single cell solution after decapsulation using mechanical separation. Attachment-detachment methods can be used to obtain TM from rats with a purity above 90%<sup>13</sup>. However, this method could not be applied successfully for TM from mice, due to the relatively small size of mouse organs and a fewer number of macrophages. Hence, an efficient and general method to yield pure testicular macrophages is still lacking.

## 1.3 Growth factors induce different macrophage immune profiles

Macrophage colony-stimulating factor (M-CSF) and granulocyte-M-CSF (GM-CSF) are two critical factors for macrophage differentiation, maturation, survival, and function<sup>60</sup>. It has been shown that the M-CSF receptor, CSF1R, is mainly expressed on macrophages. In hematopoiesis, CSF1R is upregulated during monocytic differentiation, but is downregulated during granulopoiesis<sup>60-62</sup>. CSF1R is predominantly expressed on committed macrophage precursors, monocytes, and tissue macrophages. However, GM-CSF has a low basal circulating level and is elevated during inflammatory reactions. A recent study found that GM-CSF is highly expressed in monocyte-derived or inflammatory dendritic cells (DCs)<sup>60</sup>. On the other hand, the GM-CSF receptor, CSF2R, also known as Cluster of Differentiation 116 (CD116), stimulates the production of white blood cells. The receptor is expressed on myeloblasts, mature neutrophils, but not on erythroid or megakaryocytic lineage cells<sup>60</sup>. In

## INTRODUCTION

2008, a previously undescribed ligand was identified, interleukin-34 (IL-34), which increases monocyte viability, but does not affect other monocyte characteristics<sup>61</sup>. In a separate functional screening, and using a collection of extracellular domains of transmembrane proteins, Lin et al. also discovered the receptor for IL-34, which was a known cytokine receptor, CSF1R<sup>61</sup>. By utilizing *Csf1*<sup>-/-</sup> and *Csf1r*<sup>-/-</sup> mice, IL-34 was confirmed to be a novel functional ligand required for macrophage survival, especially in the brain. IL-34 is not detectable in the circulation but is expressed in low concentrations in wild type mouse organs. Recent evidence showed that IL-34 could also act via an additional receptor, receptor-type protein tyrosine phosphatase- $\xi$  (PTP- $\xi$ )<sup>62-64</sup>. IL-34 and CSF1 have similar structures and combination patterns with their receptor CSF1R. But their combinations with receptor still have small variations: binding of CSF1 to the CSF1R occurs only via the D2 and D3 domains; rotation of binding area has space difference, and IL-34 is more rigid compared to CSF1 which is more plastic<sup>64-65</sup>. Many experiments were carried out to decipher the role and function of IL-34 in tissue-resident macrophages. During the last decade, studies have shown that there is a functional overlap between IL-34 and CSF1, but both cytokines show differential expression and spatiotemporal patterns. IL-34 acts as an important local factor in the brain to maintain specific microglia profiles<sup>63, 65-68</sup>. However, studies done in our lab, using *Csf1*<sup>-/-</sup> and *Il-34*<sup>-/-</sup> null mice, have shown that TM are exclusively CSF1-dependent (unpublished).

Tenosynovial giant cell tumor (TGCT) is mainly derived from osteoblasts that are CSF1R-expressing macrophages. This disease is controlled by CSF1/CSF1R. Pexidartinib/PLX-3397 is a potent selective inhibitor of CSF1R or M-CSFR and c-Kit, with IC50s of 20 and 10nM, respectively. Pexidartinib/PLX-3397 exhibits a 10- to 100-fold selectivity for c-Kit and CSF1R over other related kinases, such as FLT3, KDR (VEGFR2), LCK, FLT1 (VEGFR1) and NTRK3 (TRKC), with IC50s of 160, 350, 860, 880, and 890nM, respectively. Pexidartinib/PLX-3397 has been approved by the FDA for the treatment of TGCT in the clinic<sup>69-71</sup>. Depletion of microglia by oral administration of Pexidartinib/PLX-3397 to mice showed that the activation of CSF1R is one of the critical factors in the brain needed to maintain the specific immune profiles of microglia<sup>67</sup>. In 2019, Merry and colleagues used oral administration of Pexidartinib/PLX-3397 in mice to delete adipose tissue macrophages without affecting glucose homeostasis<sup>70</sup>. Moreover, Nissen showed in 2018 that PLX-5622, a highly selective CSF1R inhibitor that can pass the blood-brain-barrier, is able to attenuate experimental autoimmune encephalomyelitis. The use of PLX-5622 allows the elimination of microglia before and during the establishment of experimental autoimmune

## INTRODUCTION

encephalomyelitis<sup>69</sup>. The use of CSF1R inhibitors provides the possibility to uncover the CSF1R functions in many organs<sup>70-71</sup>. It should be noted though, that only a comparatively small number of *in vitro* experiments was carried out using these inhibitors.

Many studies have tried to decipher the mechanisms responsible for the induction of the M1 or M2 phenotype, and many important factors were identified. However, ongoing studies have revealed conflicting results regarding the factors involved, and this was mostly attributed to the use of different types of cells, different organs, as well as the source of M-CSF or GM-CSF used in *in vitro* experiments. Van den Bossche et al. have shown that once macrophages were induced towards the pro-inflammatory phenotype, by stimulation with LPS and specific viruses, mitochondrial dysfunction would prevent re-polarization towards the anti-inflammatory phenotype with specific factors such as IL-4<sup>59</sup>. This finding could explain the different results obtained regarding inflammation responses, glucose metabolism, and differentiation status in peritoneal macrophages or GM-CSF-BMDM.

Since then, studies have compared the difference between M-CSF and GM-CSF-derived-macrophages with a number of target cells, including bone marrow stem cells, blood monocytes, and peritoneal macrophages. Studies have shown that M-CSF derived macrophages have a similar profile like the M2-anti-inflammatory phenotype, while GM-CSF derived macrophages show a greater tendency to induce inflammation as M1-pro-inflammatory macrophages do<sup>73-74</sup>. Lacey and colleagues compared the individual global gene expression profiles of GM-CSF or M-CSF derived macrophages from murine bone marrow cells. They found that only 17% of genes were differentially regulated by the two CSFs. Time-dependent differences in cytokine gene expression revealed that type I IFN-dependent genes/IFN-regulated factors (IRF) were dramatically differentially regulated by the two CSFs<sup>75</sup>.

In 2009, Fleetwood and colleagues compared M-CSF and GM-CSF derived macrophages, focusing on genes dependent on type I IFN signaling. They found that *Stat1*, *Stat2*, *Irf7*, *Ccl5*, *Ccl12*, and *Cxcl10* were differentially regulated. Following LPS stimulation, BMDM derived from M-CSF produced a higher level of IFN- $\beta$  than BMDM derived from GM-CSF. Through autocrine and paracrine loops, this may regulate the production of the M1 and M2 signature cytokines IL-12p70 and IL-10<sup>76</sup>. A similar study also showed that GM-CSF and M-CSF differentially influence Theiler's Murine Encephalomyelitis virus replication as well as other virological parameters and responses<sup>77</sup>. Inhibiting GM-CSF or GM-CSFR $\alpha$  can ameliorate rheumatoid arthritis (RA) to a similar extent as anti-TNF or anti-IL-6 therapy<sup>77</sup>. However,

# INTRODUCTION

inhibition of GM-CSF or GM-CSFR $\alpha$  mainly reduces the monocyte-DC response to inflammation<sup>60</sup>.

Additionally, Anna Ohradanova-Repic and colleagues showed that M-CSF and GM-CSF derived macrophages exhibit dichotomous effects on T cell activity, which is dependent on extracellular purine metabolism<sup>78</sup>. More and more studies are focusing on the underlying mechanisms of how CSFs can induce different inflammation and metabolism. Na and colleagues for example found that GM-CSF derived macrophages increase the extent of acute glycolysis and the activation of 3-hydroxy-3-methyl-glutaryl-CoA reductase, the rate-limiting enzyme of the mevalonate pathway. Inhibition of acute glycolysis or 3-hydroxy-3-methyl-glutaryl-CoA reductase abrogated the inflammatory effects induced by GM-CSF<sup>79</sup>. By applying liquid chromatography-mass spectrometry, Lukic et al. found that upon LPS/bacterial stimuli, macrophages derived by GM-CSF or M-CSF treatment exhibit differences in the lipid metabolism, especially in the eicosanoid metabolism<sup>80</sup>. Likewise signaling by mechanistic target of rapamycin complex 1 (mTORC1) and the anabolic metabolism were shown to be important for M-CSF-dependent myelopoiesis, involving glucose metabolism, transcription factor activation, such as Myc and IRFs, and sterol biosynthesis<sup>81</sup>.

In summary, CSFs are regarded as local factors that regulate macrophage function and phenotype. Whether M2-like TM are also regulated by M-CSF, IFN- $\beta$ , and even downstream transcription factors, such as IRFs, has to be investigated yet.

## 1.4 The cross-talk between inflammation and metabolism

### 1.4.1 The metabolism profiles of different phenotypes of macrophages

Studies revealed that M1 macrophages display enhanced glycolysis which is accompanied by decreased oxygen consumption<sup>82</sup>. Macrophage polarization towards the M1 or M2 phenotype depends on differences in the metabolization of arginine. Further studies revealed that pro-inflammatory M1 macrophages utilize glycolysis and the pentose phosphate pathway to meet their rapid energy requirements. In M1 macrophages the Krebs cycle is broken, and oxidative phosphorylation (OXPHOS), as well as fatty acid oxidation (FAO), are down-regulated. In contrast, in M2 macrophages the Krebs cycle is intact. The metabolic activity of M2 macrophages is characterized by enhanced FAO and OXPHOS<sup>82-84</sup>.

# INTRODUCTION

Many studies have shown that M1 and M2 macrophages display dramatic differences in cell metabolism and energy consumption patterns<sup>75,82-83</sup>. In particular, M1 macrophages rely mainly on glycolysis for rapid killing, while M2 cells are more dependent on OXPHOS for sustained energy production<sup>82-84</sup>. More recently, a study showed that high glucose levels can affect the expression of TLR4 on BMDM, their capacity to secrete NO as well as the phosphorylation of p46 SAPK/JNK, p42 ERK MAPK, pAKT and pPKC- $\delta$ , which all have a role in regulating inflammatory responses<sup>85</sup>.

Viola et al. recently revealed that M1 and M2 macrophages not only have different metabolic signatures, and that these adaptations can sustain the polarization of macrophages. Of note, transcriptional regulation of lipid metabolism is tightly controlled by sterol receptor element-binding protein (SREBP) and liver X receptors (LXRs), which are highly expressed in macrophages and could regulate the release of inflammatory cytokines. SREBP or LXRs are oppositely activated in M1 and M2 macrophages, respectively. Additionally, LXR expression in M2 is tightly linked to lipid metabolism<sup>86</sup>. Numerous studies provided that different macrophage phenotypes have different metabolic profiles.

## **1.4.2 Metabolism of cholesterol in macrophages during inflammation**

The fundamental function of macrophages is phagocytosis, which is a form of endocytosis involving the exchange of membranes, including a considerable amount of cholesterol and its derivatives<sup>33</sup>. Therefore, many studies have investigated the close association between cholesterol metabolism and macrophage function.

Cholesterol, which makes up the majority of all sterols in mammals, plays an important role in maintaining cell homeostasis<sup>87</sup>. Cholesterol is synthesized by all animals and is an essential structural component of animal cell membranes, constituting about 20% of lipids in the plasma membrane<sup>87</sup>. Cholesterol also acts as a precursor for the biosynthesis of steroid hormones, bile acids, vitamin D, and cortisol, which has long been known for its ability to regulate immune responses<sup>87</sup>. Recent findings show that in addition to their role in maintaining basic metabolic processes, oxidated sterols (oxysterols) are also involved in the signaling pathways that can regulate inflammation through their influence on the status and function of macrophages, mast cells, T cells, and B cells<sup>87-88</sup>. Among the oxysterols, 24HC, 25HC, and 27HC are the main products of the membrane-associated enzymes cholesterol 24-hydroxylase (CH24H), CH25H and CH27H, respectively. Unlike CH24H and CH27H, which are cytochrome P450 family proteins, CH25H belongs to a small family of enzymes that



## INTRODUCTION

utilize diiron cofactors to catalyze the hydroxylation of hydrophobic substrates and is also one of the IFN-stimulated genes (ISGs)<sup>88-89</sup>. 25HC is found to exert a stronger negative feedback of cholesterol metabolism than the cholesterol itself<sup>90-91</sup>. Under normal conditions, levels of CH25H and its product 25HC are low or undetectable. But both can be rapidly induced in the heart, brain, muscle, kidney, lung, and most notably the liver upon exposure to a TLR4 agonist<sup>88-92</sup>. Many studies have also shown that macrophages and DCs are potential major sources for the production of 25HC<sup>92-93</sup>.

Most of the studies investigating 25HC and its role in immune responses were addressed in the viral infections. CH25H and its enzymatic product, 25HC were shown to inhibit Zika virus signaling as well as Lassa Virus entrance in mice and non-human primates via type I interferon (IFN) stimulation<sup>94-95</sup>. In 2010, Park and Scott reported that CH25H expression was TLR- and IFN-dependent. Numerous studies have shown afterwards that IFNAR-JAK-STAT signaling is the cardinal pathway through which ISG are induced in antiviral responses<sup>96-98</sup>. Whether 25HC displays anti-viral functions by inhibiting entry or replication of viruses has yet to be determined<sup>99</sup>.

Bauman and colleagues have shown that 25HC produced by macrophages in response to TLR activation suppresses the production of immunoglobulin A in B cells. This provided a mechanism for local and systemic negative regulation of adaptive immune responses by the innate immune system<sup>100</sup>. Notably, an inflammatory repressor, activating transcription factor 3 (ATF3) in an interferon-dependent manner, could potentially inhibit the immune-stimulated production of 25HC. This indicates that the production of 25HC can be induced by interferons<sup>98-102</sup>. Of note, focusing on foam cell formation in atherosclerosis, studies have shown that 25HC plays a double-edged sword role in macrophage polarization and function. It can amplify inflammation via AP-1, and on the other hand it can repress phagocytosis<sup>103-104</sup>. Park and Scott later showed that following TLR3 and TLR4 activation, CH25H and IFN can be rapidly produced by macrophages and DC via TRIF signaling. IFN then activates IFNAR/JAK/STAT1 signaling which can lead to further production of CH25H. This indicates that CH25H and its product 25HC, may regulate innate immune responses via interferons<sup>102</sup>.

Previous studies showed that 25HC exhibits both pro- and anti-inflammatory regulation of macrophages in different conditions. For instance, 25HC suppresses the production of IL-1 $\beta$  by blocking the activation of the sterol regulatory enhancer binding protein (SREBP) which regulates cholesterol biosynthesis and inflammasome activity<sup>105-107</sup>. However, *in vitro* studies report that high concentrations of 25HC can augment the production of IL-6, IL-8, and

# INTRODUCTION

CXCL5<sup>108</sup>. One of the regulatory pathways of 25HC has been described, starting with the activation of TLR3/4 to TRIF accumulation, which is followed by phosphorylation of IRFs. IRFs then bind with NF- $\kappa$ B, which is followed by the production of (IFN- $\alpha$  and IFN- $\beta$ ). This leads to the activation of IRF1R and Janus kinase/signal transducer and activator of transcription1 (JAK/STAT1) which activates the expression of CH25H and the production of 25HC<sup>92</sup>. However, the function of 25HC on IFNs and inflammation remains elusive. Of note, we could find that previous studies with opposite results had used different concentrations of 25HC, namely from micro molarity to nano molarity. There is evidence suggesting that the ability of 25HC to steer the immune response into an anti- or pro-inflammatory direction, depends on many factors including the cellular and immunological context<sup>100-108</sup>. Altogether, these studies suggest that a highly complex regulation exists that is not fully understood yet.

## 1.4.3 Relationship between male reproduction and 25HC

As mentioned previously, macrophages in the testis have a close association with LC. Previous studies have shown that TM can release a lipophilic factor that stimulates testosterone production by LC. This factor was thought to be physiologically important because depletion of TM from the testis resulted in altered testosterone secretion and reduced fertility. In 2000, Nes et al. used gas chromatography/mass spectrometry and nuclear magnetic resonance spectroscopy for the identification of this factor as the lipophilic substance 25HC<sup>109</sup>. Later on, Lukyanenko et al. found that different concentrations of 25HC produced by TM have opposing effects on LC<sup>110</sup>. As discussed before, interstitial TM are strongly associated with LC through specialized cytoplasmic inter-digitations, which are required for normal LC function. TM could facilitate LC steroidogenesis by secreting 25HC, an intermediate in testosterone biosynthesis. Kimura and colleagues found that M2-like macrophage polarization required Lamtor1 and mTORC1 which is needed for 25HC synthesis<sup>111</sup>. Whether 25HC in the testis acts as a key microenvironmental factor in maintaining a specific M2-like profile in TM in addition to assist in the production of sex hormone from LC, is still unclear.

## 1.5 Regulations of interferon and interferon related genes in macrophages

### 1.5.1 Interferons

In 1957, Alick Isaacs and Jean Lindenmann termed a protein ‘interferon’ because of its ability to interfere with virus replication. We now have a deeper insight into interferons (IFN) with more than 60 years of extensive research. IFN belong to the large class of proteins known as

# INTRODUCTION

cytokines. These molecules are used for communication between cells and to activate the immune response in order to eradicate pathogens<sup>112-114</sup>. In addition to their ability to inhibit virus replication, IFN have various immune-modulating functions. IFN can activate immune cells, such as natural killer cells and macrophages by upregulating the expression of major histocompatibility complex (MHC) antigens<sup>113-114</sup>. Moreover, they can activate the adaptive immune system, promoting the development of high-affinity antigen-specific T and B cell responses and immunological memory<sup>114</sup>. In mammals, around twenty distinct IFN genes and proteins have been identified. They are typically classified into three groups: Type I IFN, Type II IFN, and Type III IFN, among which IFN- $\beta$  belongs to type I IFN and has been shown to widely regulate the immune system and also has been therapeutically tested in different diseases and disorders including cancer<sup>112-113</sup>. The canonical type I IFN-induced signaling pathway was described more than three decades ago. In short, the binding of IFN $\alpha/\beta$  to IFN1R activates JAK1 and tyrosine kinase 2. This leads to the phosphorylation of STAT (p-STAT) which then translocates into the nucleus and binds to IFN-regulatory factors (IRF) to form IFN-stimulated gene factors (ISGF). ISGF bind to IFN-stimulated response elements (ISRE) and induce target gene expression<sup>115-117</sup>. ISGF inhibit viral infection through several mechanisms, including inhibition of viral transcription, translation and replication, the degradation of viral nucleic acids, and the alteration of cellular lipid metabolism, in which CH25H plays an important role<sup>118</sup>.

## 1.5.2 Role of IFN- $\beta$ in immune regulation

Although typically elicited by viruses, type I IFN can also be induced by bacterial infections. Macrophages are regarded as the main source of IFN- $\beta$ <sup>117</sup>. Pathogens can induce pattern-recognition receptor (PRR) signaling which leads to IFN secretion. However, IFN can induce different inflammatory responses that are cell type- and context-dependent<sup>119</sup>. Germline-encoded PRR are essential in protecting a vertebrate from microorganisms. Toll-like receptors (TLR) are the most important PRR. The signaling pathway of different subtypes of TLR relies on four basic adaptor molecules: MyD88, TIR-associated protein (TIRAP)/MyD88-adaptor-like (MAL), TIR-domain-containing adaptor protein-inducing IFN- $\beta$  (TRIF)/TIR-domain-containing molecule1 (TICAM1) and TRIF-related adaptor molecule (TRAM)<sup>120-121</sup>. Activation of TLR3, TLR4, TLR7, and TLR9, but not TLR2, induces type I IFN production in addition to other pro-inflammatory signals. Even in MyD88<sup>-/-</sup> cells, TRIF can trigger IFN- $\beta$ -inducible gene expression, such as IRFs. TRIF interacts with receptor-interacting protein 1, which is responsible for the activation of NF- $\kappa$ B<sup>122</sup>. TRIF activates TRAF family-member-

## INTRODUCTION

associated NF- $\kappa$ B activator binding kinase 1 (TBK1) via TRAF3<sup>123-124</sup>. TBK1 is a member of the inducible I $\kappa$ B kinase family, and these kinases directly phosphorylate IRF3 and IRF7<sup>125-126</sup>. Phosphorylated IRF3 and IRF7 then translocate into the nucleus and initiate the production of type I interferons. This mode of activation of TRIF and production of type I interferons is mainly found in virus-induced responses<sup>125-127</sup>.

Some studies showed that macrophages and monocytes from mice or human, pre-treated with IFN, can suppress the production of pro- and mature IL-1 $\beta$  and enhance the production of IL-10<sup>125</sup>. Moreover, several cytosolic interferon-related PRR have been implicated in inflammasome complex formation and inflammatory caspase-1 activation<sup>126</sup>.

Similar to macrophages, DCs are another major type of APC, which can produce a huge amount of IFN- $\beta$  upon inflammatory stimulation like with LPS<sup>120</sup>. Studies showed that IFN- $\beta$  can induce the expression of MHC class I molecules in DCs, enhance DC maturation and activation, and ultimately promote Th1 responses via the activation of TLR7, MyD88, and IRF1<sup>127</sup>. IFN- $\beta$  can shape the adaptive immune response by activating and priming T cells, especially Th1 and Th17 cells<sup>128</sup>. Numerous studies showed that IFN- $\beta$  can elicit different responses of Th1 and IL-10-producing CD4<sup>+</sup> T cells due to different conditions including incubation time. Type I IFN enhance proliferation and prevents apoptosis of primary B cells, even in the absence of mitogenic stimuli, and can generally enhance B cell development and function<sup>125-127</sup>.

TLR can sense a variety of bacterial and viral ligands, which include LPS (TLR4), peptidoglycan (TLR2), Pam3CSK4 (TLR1/2), dsRNA and poly (I:C) (TLR3), ssRNA (TLR7/8), and CpG ODN (TLR9). LPS was extensively studied for its ability to activate IFN- $\beta$  and TLR4, including MyD88-dependent and MyD88-independent (TRIF-dependent) signaling pathways. TRIF is the key protein for inducing IFN- $\beta$  together with TRAM and TBK1 adaptor molecules in the cytoplasm<sup>125-127</sup>. The kinase TBK1 phosphorylates transcription factor IRF3, which then dimerizes and translocates into the nucleus to induce IFN- $\beta$  expression. LPS-induced IFN- $\beta$  is secreted into the extracellular milieu and binds to IFN1R, and then activates the JAK-STAT1/2 pathway, which will then act on with IFN-stimulated response elements (ISRE)<sup>125</sup>.

In contrast to bacteria or LPS stimulation, viruses induce IFN- $\beta$  through the TLR3/TRIF/TBK1/IKKi pathway. The phosphorylation cascade of proteins leads to the phosphorylation of IRF7 and/or IRF3. By using Irf3 and Irf7 knock out mice, studies showed

# INTRODUCTION

that Irf3 and Irf7 are necessary for the production of IFN- $\beta$  in viral and Malaria infections<sup>126-127</sup>. IFN- $\beta$  is an important immune cytokine and regulates not only the innate immune system but also the adaptive immune response. In addition, IFN- $\beta$  can display both pro- and anti-inflammatory profiles that are controlled by the microenvironment as well as other conditions<sup>128-129</sup>.

A central facet of the IFN-mediated suppressive effect in inflammation is the down-regulation of inflammasome activity and interleukin-1 (IL-1) production, and this inflammatory suppression was found to be related to the regulation of metabolism<sup>128</sup>. Reboldi and colleagues used Ch25h<sup>-/-</sup> mice to show that 25HC is involved in the regulation of IL-1 together with IFNs<sup>128</sup>. Considering 25HC has important anti-viral features, and regulates macrophages, and CH25H is the key IFN-stimulated gene, it becomes clear that the metabolism of cholesterol is intimately related to IFN signaling.

In 1999, the different responses to interferon consensus sequence binding protein (ICSBP, a member of IRFs) by GM-CSF and M-CSF were discovered. In Icsbp<sup>-/-</sup> bone marrow cells, GM-CSF hyper-activates BMDM, while M-CSF markedly reduces the activation of BMDM, indicating that M-CSF and GM-CSF have opposite effects on IFN production and the activation of IRFs<sup>129</sup>. Because IRF7 is expressed predominantly in lymphoid tissues and can be strongly induced by TLR, studies have focused on the relationship between IRFs and the differentiation of immune cells. Additionally, IRF7 was found to be essential for the differentiation from monocyte to macrophage with the expression of CD11b and CD11c<sup>130</sup>.

The introduction of an IFN1R inhibitor provided many possibilities for investigating the functions of IFNs, especially type I interferons. B18R is a soluble vaccinia virus-encoded type I-IFN receptor inhibitor, previously shown to have potent IFN neutralizing effects<sup>131-132</sup>. Studies have shown that B18R can sufficiently inhibit IFN1R by reducing the expression of type I IFN<sup>133</sup>, which provides a potential method to study the function of IFNs.

## 1.5.3 Functions of IRFs in inflammation

IRFs are transcriptional mediators, which can be induced by bacteria or viruses. In mammals, the IRF family consists of nine members: IRF1, IRF2, IRF3, IRF4, IRF5, IRF6, IRF7, IRF8 (ICSBP), and IRF9 (ISGF3 $\gamma$ /p48). IFN regulatory factor (IRF) 7 is regarded as the master regulator of type I IFN-dependent immune responses. The antiviral response of IFNs needs timely termination via extensive negative regulation in order to minimize the inflammatory

# INTRODUCTION

damage. Studies showed that together with the fork-head family of transcription factors, IRF7 could act as a negative regulator of IFN responses<sup>134</sup>.

IRF7, together with IRF3, are regarded as important transcription factors (TFs) to regulate the production of IFN. However, by using *Irf7*<sup>-/-</sup> mice, the function of IRF7 was shown to be more important than IRF3 in terms of immune balance<sup>135</sup>. Owens and colleagues found out that DCs from the spleen of *Irf7*<sup>-/-</sup> mice showed enhanced activation in response to microbial stimuli. This enhanced activation, however, could not be rescued in *Irf7*<sup>-/-</sup> mice by providing extra IFN<sup>135</sup>. IRF7 is further shown to be critical for regulating type I interferons in the virus infections via the activation of DC-MyD88-independent and CD8<sup>+</sup> T cell-MyD88-dependent pathways. This has been shown by using *Irf7*<sup>-/-</sup> mice<sup>136</sup>.

As mentioned earlier, microglia is a typical resident macrophage. Numerous studies have shown that local microenvironmental factors, such as TGF- $\beta$  and IL-34, play important roles in maintaining its phenotype. In 2014, Cohen and colleagues, by using genome-wide expression analysis and chromatin immunoprecipitation followed by next-generation sequencing, showed that the phenotypical switch from pro- to anti-inflammatory (M1-to-M2) macrophages is controlled by the transcription factor IRF7<sup>137</sup>. Moreover, IRF7 in the brain is down-regulated by the TGF $\beta$ 1 pathway, and this downregulation can be reversed by IFN- $\beta$ <sup>137</sup>, indicating that in the brain, microglia is dependent on the suppression of IRF7 by TGF- $\beta$ . However, the function of IRF7 in other resident macrophages is still unknown and needs to be addressed.

## 1.6 Aim of the study

Factors in the tissue microenvironment such as TGF- $\beta$  and CSF play a critical role in generating specific phenotypes of resident macrophages. TM displays specific phenotype that can balance the activation of inflammatory response to antigens and the immune tolerance against spermatozoon. The dysregulation of TM can cause male infertility, but the underlying mechanisms are not clear. Recent evidence indicated that the microenvironment of the testis, like in other organs, maybe the principal reason responsible for maintaining an organ specific immune profile. M-CSF, IFN- $\beta$ , 25HC and transcription factor IRF7 have been studied to regulate macrophage functions individually in different settings. The possible cross-communication between these factors in order to regulate TM profiles and functions, especially in the testis, has not been established.

## INTRODUCTION

The aim of this study was to investigate the functions of M-CSF, IFN- $\beta$  and 25HC, together with the downstream transcription factor IRF7 in the testis and in the process of maintaining specific TM immune profile. The investigation aims to uncover the possible cross-communication between these factors and their role in regulating TM profile with metabolism and inflammation, paving the way for novel clinical treatments for metabolic disorders and infertility.

# MATERIALS AND METHODS

## 2. MATERIALS AND METHODS

### 2.1 Materials

#### 2.1.1 Equipment

Cell culture CO <sub>2</sub> incubator	Binder, Tuttlingen, Germany
Desktop centrifuge Biofuge Fresco	Heraeus, Hanau, Germany
Electronic balance SPB50	Ohaus, Giessen, Germany
Fluorescent microscope Axioplan 2 Imaging	Carl Zeiss, Göttingen, Germany
FUSION-FX7 Advance	PEQLAB, Erlangen, Germany
Flow cytometer	Miltenyi Biotec, Bergisch Gladbach, Germany
FlowJo software version 10	Tree Star, Ashland, USA
Gel Jet Imager 2000 documentation system	Intas, Göttingen, Germany
GraphPad Prism 8	San Diego, CA, USA
Heat block DB-2A	Techne, Cambridge, UK
Horizontal mini electrophoresis system	PEQLAB, Erlangen, Germany
Hybond ECL nitrocellulose membrane	Amersham, Freiburg, Germany
iCycler iQ <sup>®</sup> System	Bio-Rad, München, Germany
Microwave oven	Samsung, Schwalbach, Germany
Mini centrifuge Galaxy	VWR, Darmstadt, Germany
Mini-rocker shaker MR-1	PEQLAB, Erlangen, Germany
Mixer Mill MM 300	Retsch, Haan, Germany
NanoDrop ND 2000	Thermo Fisher, Waltham, USA
PCR thermocycler	Biozyme, Oldendor, Germany
Power supply units	PEQLAB, Erlangen, Germany
SDS gel electrophoresis chambers	Consurs, Reiskirchen, Germany



## MATERIALS AND METHODS

Semi-dry-electroblotter	PEQLAB, Erlangen, Germany
TCS SP2 confocal laser scanning microscope	Leica, Wetzlar, Germany
Typhoon 9100	GE Healthcare, Freiburg, Germany
Thermo Shaker	PEQLAB, Erlangen, Germany
Tristar LB941	Berthold, Bad Wildbad, Germany
UV visible spectrophotometer Ultrospec 2100	Biochrom, Cambridge, UK
Vertical electrophoresis system	PEQLAB, Erlangen, Germany
FACS Aira II	BD BioSciences, San Diego, USA

### 2.1.2 Chemicals

37% Formaldehyde solution	Sigma-Aldrich, Steinheim, Germany
Acrylamide 30% (w/v)	Roth, Karlsruhe, Germany
Agarose	Invitrogen, Karlsruhe, Germany
Bromophenol blue sodium salt	Sigma-Aldrich, Steinheim, Germany
Calcium chloride	Merck, Darmstadt, Germany
Dimethylsulfoxide	Roth, Karlsruhe, Germany
Dithiothreitol (DTT)	Roth, Karlsruhe, Germany
DNA ladder (100 bp)	Promega, Mannheim, Germany
Ethanol	Sigma-Aldrich, Steinheim, Germany
Ethidium bromide	Roth, Karlsruhe, Germany
Ethylene diaminetetraacetic acid disodium salt	Merck, Darmstadt, Germany
Enhanced chemiluminescence (ECL) reagents	Amersham, Freiburg, Germany
Formamide	Merck, Darmstadt, Germany
Glycerol	Merck, Darmstadt, Germany
Glycine	Sigma-Aldrich, Steinheim, Germany
Glycogen	Invitrogen, Karlsruhe, Germany

## MATERIALS AND METHODS

Halt Phosphatase Inhibitor Cocktail	Thermo Fisher, Waltham, USA
Igepal CA-630 (NP-40)	Sigma-Aldrich, Steinheim, Germany
Lipopolysaccharide (LPS)	Sigma-Aldrich, Steinheim, Germany
Magnesium chloride	Merck, Darmstadt, Germany
Magnesium sulfate	Sigma-Aldrich, Steinheim, Germany
2-Mercaptoethanol	Sigma-Aldrich, Steinheim, Germany
Methanol	Sigma-Aldrich, Steinheim, Germany
Non-fat dry milk	Roth, Karlsruhe, Germany
N, N, N', N'-Tetramethylethylenediamin (TEMED)	Roth, Karlsruhe, Germany
Paraformaldehyde	Merck, Darmstadt, Germany
Picric acid	Merck, Darmstadt, Germany
Phenylmethylsulfonyl fluoride (PMF)	Sigma-Aldrich, Steinheim, Germany
Ponceau S	Roth, Karlsruhe, Germany
Potassium chloride	Merck, Darmstadt, Germany
Proteinase inhibitor cocktail	Sigma-Aldrich, Steinheim, Germany
Roti®-Phenol	Roth, Karlsruhe, Germany
Sodium acetate	Roth, Karlsruhe, Germany
Sodium chloride	Roth, Karlsruhe, Germany
Sodium dodecyl sulfate (SDS)	Merck, Darmstadt, Germany
Sodium deoxycholate	Roth, Karlsruhe, Germany
Tris (hydroxymethyl) aminomethane	Roth, Karlsruhe, Germany
TRIS-Hydrochloricacid	Roth, Karlsruhe, Germany
Triton X-100	Roth, Karlsruhe, Germany
Tween-20	Sigma-Aldrich, Steinheim, Germany
Uranyl acetate dehydrate	Merck, Darmstadt, Germany

## MATERIALS AND METHODS

Urea	Merck, Darmstadt, Germany
Xylazine	Bayer, Leverkusen, Germany
DNase I	Invitrogen, Carlsbad, Germany
Desoxyribonukleosidtriphosphate (dNTP)	Promega, Mannheim, Germany
M-MLV RT	Promega, Mannheim, Germany
Oligo dT	Promega, Mannheim, Germany
RNase A	Invitrogen, Karlsruhe, Germany
SuperScript® II Reverse Transcriptase	Invitrogen, Karlsruhe, Germany
SYBR green	Bio-Rad, München, Germany
Taq polymerase	Promega, Mannheim, Germany

### 2.1.3 Cell culture reagents

Bovine serum albumin (endotoxin free)	Invitrogen, Karlsruhe, Germany
Albumin, Rind, Fraktion V, pH 7.0 (BSA)	Serva, Heidelberg, Germany
DMEM-F12	Gibco, Darmstadt, Germany
Fetal bovine serum (FBS)	Gibco, Darmstadt, Germany
Goat serum	Dako, Glostrup, Denmark
GM-CSF	PeptoTech, Hamburg, Germany
Mouse M-CSF premium grade	Miltenyi Biotec, Bergisch Gladbach, Germany
Penicillin/Streptomycin (100×)	Gibco, Darmstadt, Germany
DPBS	Gibco, Darmstadt, Germany
RPMI 1640 medium	Gibco, Darmstadt, Germany
Trypsin/EDTA	Gibco, Darmstadt, Germany
4-(2-hydroxyethyl)-1-piperazineethanesulfonic acid (HEPES)	Gibco, Darmstadt, Germany
Sodium Pyruvate MEM 100MM	Gibco, Darmstadt, Germany

## MATERIALS AND METHODS

MEM Non-essential Amino Acid Solution (100×)	Sigma-Aldrich, Steinheim, Germany
Gentamicin	Sigma-Aldrich, Steinheim, Germany
2-Mercaptoethanol	Gibco, Darmstadt, Germany
Nigericin (sodium salt)	Cayman, Hamburg, Germany
25-hydroxy Cholesterol (25HC)	Cayman, Hamburg, Germany
Macrophage Detachment solution	PromoCell, Heidelberg, Germany
PLX-3397 (Pexidartinib)	MedChemExpress, New Jersey, USA
B18R	R&D system, Minneapolis, USA

### 2.1.4 Kits

Pierce BCA Protein Assay Kit	Thermo Fisher, Waltham, USA
Mouse IL-10 ELISA Set	BD Bioscience, Heidelberg, Germany
Mouse TNF (mono/mono) ELISA Set	BD Bioscience, Heidelberg, Germany
TMB Substrate Reagent Set	BD Bioscience, Heidelberg, Germany
RNase-Free DNase Set	Qiagen, Hilden, Germany
RNeasy Micro kit	Qiagen, Hilden, Germany
MyTaq Extract-PCR Kit	BIOLINE, London, UK
AEC Chromogen Kit	Sigma-Aldrich, Steinheim, Germany

### 2.1.5 Experimental antibodies

#### 2.1.5.1 Antibodies for flow cytometry

Antigen Flow Cytometry	Conjugated Fluorochrome	Manufacturer	Clone	Cat. Number
CD103	BV510	Biolegend	2E7	121423
CD11b	Per/Cy5.5	Biolegend	M1/70	101228
CD11b	BV570	Biolegend	M1/70	101233
CD11c	PE/Cy7	Biolegend	N418	117317
CD11c	PE	Biolegend	N418	117308
CD19	PE Cy7	Biolegend	6D5	115520

## MATERIALS AND METHODS

CD206	Alexa 647	Biologend	C068C2	141711
CD206	BV 421	Biologend	C068C2	141717
CD3	Alexa Flour 488	Biologend	HTK888	400923
CD32	-	BD Pharmingen	D34-485	550271
CD45	PE	Biologend	30-F11	12-0451-82
CD45	PE Dazzle 594	Biologend	30-F11	103146
CD64	PE	Biologend	X54-5/7.1	139303
CD64	PerCP Cy5.5	Biologend	X54-5/7.1	139308
Clec4a4	PE	Biologend	33D1	124905
CX3CR1	PE/Cy7	Biologend	AFS98	135529
eflour 450	eflour 450	eBioscience	-	4297348
F4/80	Alexa 488	Biologend	BM8	123120
F4/80	PE Cy5	Biologend	BM8	123112
FSV700	Alexa 700	BD Horizon	-	564997
GR1	Brilliant Violet 510	Biologend	RB6-8C5	108438
Ly6C	FITC	Biologend	HK1.4	128005
Ly6C	BV605	Biologend	HK1.4	128035
Ly6G	Pacific Blue	Biologend	1A8	127612
MerTK	PE	Biologend	2B10C42	151505
MerTK	APC	Biologend	2B10C42	151508
MHC II	APC	Biologend	AF6-120-1	116418
MHC II	BV510	Biologend	M5/114.15.2	107635
SiglecF	BV 421	Biologend	S17007L	155509

**Table 2.** Information of antibodies used for flow cytometry.

### 2.1.5.2 Antibodies for immunoblotting

Primary antibodies for WB	Manufacturer	Clone	Cat. Number
Akt	Cell Signaling Technology	-	9272
phospho-Akt (Ser473) XP	Cell Signaling Technology	D9E	4060
phospho-SAPK/JNK (Thr183/Tyr185)	Cell Signaling Technology	-	9251
phospho-Stat3	Cell Signaling	D3A7	9145

## MATERIALS AND METHODS

(Tyr705)	Technology		
Stat1	Cell Signaling Technology	9H2	9176
phospho-Stat1 (Tyr701)	Cell Signaling Technology	58D6	9167
Cleaved Caspase-1 (Asp297)	Cell Signaling Technology	D57A2	4199
Cleaved-IL-1 $\beta$ (Asp116)	Cell Signaling Technology	D3A3Z	83186
$\beta$ -actin	Sigma-Aldrich	AC-15	A5441

**Table 3.** Information of primary antibodies used for Western Blotting.

Secondary antibodies for WB	Manufacturer	Conjugated	Cat. Number
anti-mouse IgG	Cell Signaling Technology	HRP	7076
anti-rabbit IgG	Cell Signaling Technology	HRP	7074
anti-rat IgG	Thermo Fisher Scientific	HRP	18-4818-82

**Table 4.** Information of secondary antibodies used for Western Blotting.

### 2.1.6 Primers

Primers	Forward 5'-3'	Reverse 3'-5'
RPLP0	CTGCACTCTCGCTTTCTGGA	ACGCGCTTGTACCCATTGAT
Irf7	AGGTTCTGCAGTACAGCCAC	GGGTTCTCTCGTAAACACGGT
IL-1 $\beta$	TGCCACCTTTTGACAGTGATG	TGATGTGCTGCTGCGAGATT
IL-6	AGCCAGAGTCCTTCAGAGAGAT	GAGAGCATTGGAAATTGGGGT
IL-10	GGTGCCAAGCCTTATCGGA	TCAGCTTCTCACCCAGGGAA
Ch25h	TGCATCACCAGAACTCGTCC	GGGAAGTCATAGCCCGAGTG
TNF- $\alpha$	GACGTGGAAGTGGCAGAAGA	ACTGATGAGAGGGAGGCCAT
Klf4	GCCACCCACACTTGTGACTA	CTGTGTGTTTGCGGTAGTGC
IFN- $\beta$	GTCCTCAACTGCTCTCCACT	CCTGCAACCACCACTCATTC
Clec7a	CTAGGGCCCTGTGAAGCAAT	AATGGGCCTCCAAGGTGAAG
Slamf1	GAGCCTCTTATGCTTCAAACAACA	CAGCAGCATTGCCAAACAGT
Caspase1	AAGAAACATGCGCACACAGC	CCCTCAGGATCTTGTCAGCC

## MATERIALS AND METHODS

Atf3	CCAGCCACAGTCTCACTCAG	GACCTGGCCTGGATGTTGAA
Chil3	GGGCCCTTATTGAGAGGAGC	CCAGCTGGTACAGCAGACAA
Nr4a2	AGAGCGGACAAGGAGATCTGA	GGCATGGCTTCAGCAGAGTT
Rora	GCTGACCCAGGACACGG	CCTTGCAGCCTTCACACGTA
UZU cont F1	GTGGTACCCAGTCCTGCCCTCTTTATAATCT Length--31	
Neo16c	TCGTGCTTTACGGTATCGCCGCTCCCGATTTC Length--31	
R813 long	AGTAGATCCAAGCTCCCGGCTAAGTTCGTAC Length--31	

**Table 5. Information of primers used for PCR and qRT-PCR.** Primers were designed by the NCBI Primer-BLAST tool and purchased from Eurofins Genomics. UZU cont F1, Neo16c and R813 long were specific for Irf7 KO mice genotyping.

### 2.1.7 Miscellaneous

4', 6-diamidino-2-phenylindole (DAPI)	Vector Laboratories, Burlingame, USA
70µm-sterile EASYstrainer	Greiner Bio-One, KrEMmünster, Austria
Cell culture plate (6/12/24 well)	Sarsted, Nuembrecht, Germany
Collagenase A	Roche, München, Germany
Centrifugal Filter-10K	Merck Millipore, Burlington, USA
epT.I.P.S Standard/Bulk 0.1-5mL	Eppendorf AG, Hamburg, Germany
FACS 5mL Tubes (75 x 12mm, PS)	Sarstedt, Nuembrecht, Germany
Fixation/Permeabilisation solution	eBioscience, San Diego, USA
Filter (0.45 µM)	BD Bioscience, Heidelberg, Germany
Ficoll-Paque PLUS gradient	GE Healthcare, Uppsala, Sweden
Falcon tube (15/50ml)	Sarstedt AG, Nuembrecht, Germany
Hybond ECL nitrocellulose membrane	GE Healthcare, Cambridge, UK
MACS column	Miltenyi Biotec, Bergisch Gladbach, Germany
Macrophage detachment buffer	PromoCell GmbH, Heidelberg, Germany
Neubauer counting chamber	LaborOptik, Marienfeld, Germany
Needles	BD Bioscience, Heidelberg, Germany

# MATERIALS AND METHODS

Permeabilisation washing buffer	eBioscience, San Diego, USA
Protein size markers	ThermoFisher Scientific, Waltham, USA
Pipette tip	Sarstedt AG, Nümbrecht, Germany
RBC Lysis Solution	Qiagen, Hilden, Germany
Sterile plastic ware for cell culture	Sarstedt, Nuembrecht, Germany
Syringe	B. Braun Melsungen, Melsungen, Germany
Trypan Blue Stain (0.4%)	Gibco, Darmstadt, Germany

## 2.2 METHODS

### 2.2.1 Animals

Male C57BL/6JCrI mice were bought from Charles River Laboratories (Sulzfeld, Germany) and kept under standard conditions (22°C, 12 h light/dark cycle) with pelleted food and water ad-libitum. Male Irf7 gene knock out mice (RBRC No.: RBRC01420, strain name: B6; 129P2-Irf7<sup><tm1Ttg>/TtgRbr</sup>c, background strain: C57BL/6J) were purchased from RIKEN BRC through the National Bio-Resource Project of the MEXT/AMED, Japan. Study was carried out in strict accordance with the recommendations in the Guide for the Care and Use of Laboratory Animals of the German law of animal welfare. The experiments were performed according to the guidelines of the local authority (Regierungspraesidium, Giessen, Germany) and conformed to the Code of Practice for the Care and Use of Animals for Experimental Purposes (permission No.: M\_684 for wild type mice and No.: M\_674 for Irf7<sup>-/-</sup> mice). The mice were sacrificed by isoflurane administration followed by cervical dislocation, and all efforts were made to minimize the suffering.

### 2.2.2 Bone marrow derived macrophage (BMDM) culture

Male mice C57BL/6JCrI (8-10 weeks) were sacrificed by isoflurane administration followed by cervical dislocation. After euthanizing the mice, the femur and tibia were aseptically removed and then transferred into cold DPBS containing gentamycin (50µg/mL) using 15 mL falcon tubes. The surrounding muscles from femur and tibia were carefully removed by sterile forceps and scissors, without destroying the ends of the bones. Subsequently, the end of the bones was cropped with a scissor, and then bone marrow cells were flushed with 5mL of



## MATERIALS AND METHODS

DPBS (containing gentamycin) using a 20 mL syringe with 24 G (femur)/ 30G (tibia) needles. After flushing, the bone marrow cells were filtered through 70µm-sterile strainers (Greiner Bio-One, KrEMmünster, Austria) to remove cell clumps. The bone marrow stem cells were pelleted by centrifugation at 350g for 10min at room temperature (RT). The pelleted cells were dissolved in RBC lysis buffer (Qiagen, Hilden, Germany) for 3min at RT. The RBC lysis process was terminated by adding 7mL of DPBS and centrifugation at 350g for 10min at RT. After centrifugation, the supernatants were decanted, and the cells were dissolved in 10mL BMDM culture medium (RPMI 1640 with 10% FBS, 1% penicillin-streptomycin, 1% HEPES, 1% sodium pyruvate, 1% MEM non-essential amino acid solution (100×) and freshly added 0.1% 2-mercaptoethanol). Live cells were counted using a hemocytometer and the viability of cell were determined by trypan blue staining method.

1x10<sup>6</sup>, 2x10<sup>6</sup>, and 4x10<sup>6</sup> bone marrow cells per well were seeded into 24, 12 and 6 well plates respectively. Bone marrow cells were differentiated into macrophages by treatment with M-CSF (25ng/mL) or GM-CSF (25ng/mL) for 6 days with or without addition of 25HC or corticosterone. On day 3, cells were replenished with new medium. On day 7, differentiated macrophages were stimulated with LPS (10ng/mL) for the time periods indicating in the respective figures. Following treatments, cell lysates and supernatants were collected for Western Blotting, ELISA and qRT-PCR analysis.

### 2.2.3 Flow cytometry (FC) assay

#### 2.2.3.1 Flow cytometry assay with BMDM

After treatment, cells were washed gently two times with cold DPBS and then macrophages were detached from the plates by adding macrophage detachment solution (250-300µL/cm<sup>2</sup>, PromoCell, Germany) for 30min at 4°C. Following detachment, cells were collected in a 15mL falcon tube and then centrifuged at 350g for 10min at RT. Supernatants were discarded and cells were dissolved in FACS buffer (1% BSA (w/v in DPBS) +10mM EDTA). Cell numbers were determined by hemocytometer, and equal numbers of cells were distributed into different FACS tubes. The FACS tubes were centrifuged at 350g for 7min at 4°C. After centrifugation, supernatants were discarded and cells were dissolved in 100µL FACS buffer. The dissolved cells were blocked with an Fc blocker (anti-CD32/16, BD Pharmingen, San Jose, USA) antibody for 10min at 4°C, and then incubated with the macrophage specific antibodies (**Table 2**) for 20min at 4°C in dark. After incubation, cells were washed with 1mL FCAS buffer for 2 times. Then cells were re-suspended with 300-400µL FACS buffer, and

## MATERIALS AND METHODS

flow cytometric analysis was performed using a MACSQuant Analyzer 10 flow cytometer (Miltenyi Biotec, Bergisch Gladbach, Germany). The data were analyzed with the FlowJo software version X (Tree Star, Ashland, OR, USA).

For intracellular staining, cells were stained with fixable viability dye (BD Horizon, San Jose, USA) for 30min in dark. After staining, cells were washed with FACS buffer by centrifugation at 350g for 10min at 4°C. Cells were fixed/ permeabilized by adding 1mL of freshly prepared fixation/ permeabilisation solution (eBioscience, San Diego, USA) 30min at 4°C. The cells were washed twice with 1x permeabilisation buffer (diluted with deionized water) by centrifugation at 350g for 7min at 4°C. After centrifugation, cells were stained with antibodies targeting intracellular proteins at 4°C in the dark for 30min. Cells were washed with 1× permeabilisation washing buffer and then analyzed by MACSQuant analyzer 10 flow cytometer.

### **2.2.3.2 Flow cytometry assay with samples extracted from organs**

Mice were scarified as described above and epididymis, testis, spleen, liver, lung and brain were dissected for flow cytometric analysis. Single cell suspensions were obtained by cutting organs into small pieces with a sharp scissor and enzymatically digested for 30min at 37°C in digestion buffer. The collagenase-digested cells were filtered through a 70µm cell strainer into a new 15mL tube and centrifuged at 350g for 7min at 4°C. The supernatants were discarded and the cells were treated with RBC lysis buffer for 1min at RT to get rid of RBCs. Samples were washed with 5mL DPBS and then centrifuged at 350g for 7min at 4°C. Supernatants were discarded and cell pellets were dissolved in FACS buffer. Following cells were prepared for flow cytometry as described (section 2.2.3.1).

#### **Digestion buffer (1.5mL/sample):**

1200µL RPMI1640 with 10% FBS and 1% P/S

300µL 5mg/mL collagenase A (working concentration 1mg/mL)

1.5µL DNase I (Stock 10,000U/mL)

### **2.2.4 Protein extraction from cells**

Proteins from BMDM were harvested with protein lysis buffer mixture.

#### **Lysis buffer mixture:**

## MATERIALS AND METHODS

Stock Buffer	Working Buffer Conc.	Volume for 10mL
1M Tris/HCl pH 7.4	10mM	100 $\mu$ L
5M NaCl	150mM	300 $\mu$ L
Triton X 100	1%	100 $\mu$ L
Nonidet P 40 (NP 40)	0.25%	25 $\mu$ L
0.5M EDTA	2mM	40 $\mu$ L
100mM PMF*	1mM	100 $\mu$ L
proteinase inhibitor 100x*	1x	100 $\mu$ L
phosphorylase inhibitor 100x*	1x	100 $\mu$ L
Aqua	-	9135 $\mu$ L

\* PMF, proteinase inhibitor (PI), and phosphates inhibitors were added freshly before use.

Following challenge, treated and untreated cells were washed three times with cold DPBS. Immediately, cell lysis buffer mixture was added and kept on the ice for 30min with shaking and tapping the palates by hand every 5min. Cells were scraped using a cell scraper and transferred into a new 1.5mL tube and kept on ice for 30min with vortexing every 5min for 10s. Next, cells were centrifuged at 10,000 x g for 30min at 4°C. After centrifugation, supernatants were collected into a new precooled-tube and protein concentrations were measured using BCA kit (Thermo Fisher, Waltham, USA) by following the manufacture instructions.

### 2.2.5 Enzyme-linked immunosorbent assay (ELISA) of inflammatory cytokines

Following treatments, cell culture supernatants were analyzed for the production of inflammatory cytokines such as TNF- $\alpha$  and IL-10 by ELISA following the manufacture guidelines. IL-10 and TNF- $\alpha$  ELISA kits were purchased from BD OptEIA™. 25HC concentrations from mice were measured with the 25HC ELISA kit (MyBioSource, San Diego, USA).

### 2.2.6 Cell viability analyzed by MTT assay

The MTT assay is a colorimetric assay to determine the metabolic activity of a cell. Under defined conditions, NAD(P)H-dependent cellular oxidoreductase enzymes can reflect the number of viable cells present. Cells were cultured in 96-well plates and after treatments, the condition medium was removed, and 100 $\mu$ L MTT buffer (5mg/mL) was immediately add to each well. Plates were incubated at 37°C for 1-4h. To terminate the reaction, equal volume of

## MATERIALS AND METHODS

DMSO was added to each well and thoroughly mixed. Absorbance was measured at 570nm together with the blank control containing only DMSO buffer.

### 2.2.7 cDNA synthesis and qRT-PCR assay

#### 2.2.7.1 Total mRNA isolation

Total mRNA from treated and untreated cells was isolated by using the RNeasy Micro kit (QIAGEN, Hilden, Germany) following the manufacture's instructions. The concentration and the purity of the isolated mRNA were measured by a NanoDrop 2000/2000c spectrophotometer (Thermo Fisher, Waltham, USA).

#### 2.2.7.2 DNA digestion

DNA contamination from each sample was removed by treating total mRNA with DNase I (Invitrogen, Carlsbad, USA). In each experiment, 2.5µg of total mRNA was incubated with 0.9µL of DNase I in a reaction mixture as given below.

#### Reaction mixture:

Volume	Component
X(calculate from concentration measured on Nanodrop) µL	2.5µg RNA
0.9µL	DNase I (10U/µL)
2.0uL	10x DNase I buffer/ Buffer RDD
Total to 20µL	RNase free water

Mix well and heat at 37°C for 40min and then at 72°C for 10min. Put on ice immediately for 2min and centrifuge for 3s. Samples could be stored at -80°C.

#### 2.2.7.3 cDNA synthesis

The DNase I digested RNA samples of 2.5µg RNA (20µL) was mixed with 2µL oligo-dT (10pmol/µL) in a total reaction volume of 22µL. The samples were denatured for 10min at 70°C, and immediately kept in ice for 2min.

#### Reverse Transcribed Mixture:

Volume	Component
8µL	5x M-MLV RT buffer
2µL	dNTP/NUC mix (10mM)
1µL	RNAsin (RNase inhibitor, 40U/µL)

## MATERIALS AND METHODS

6 $\mu$ L	RNase-free water
-----------	------------------

Next, 22 $\mu$ L of reverse transcription mixture was added to each tube and incubated at 42°C for 1min to pre-heat. After pre-heating, 1 $\mu$ L of reverse transcriptase was added to each tube, mixed well with pipettes and then incubated at 42°C for 60min. The reverse transcription was stopped by incubating at 72°C for 15min. The samples were immediately kept on ice for 2min and stored at -80°C for PCR analyses.

### 2.2.7.4 Polymerase chain reaction (PCR)

#### PCR mixture:

Component	Volume ( $\mu$ L)
Template (cDNA)	1
Go Taq 5x Buffer	10
MgCl <sub>2</sub> (25mM)	4
dNTP (10mM)	1
Primer mix (10pm) /Housekeeping gene (HKG)	1
Go Taq polymerase	0.5
RNA-free aqua	32.5
<b>Total</b>	<b>50</b>

Thermo-cycling condition for PCR with RPLP0 as a HKG:

Step	Temperature and time
Initial Denaturation	94°C for 4min
Extension	94°C for 30s, 60°C for 30s, and 72°C for 30s*
Repeat extension	Repeat * 30 times
Final Extension	72°C for 10min
Stop	Keep at 8°C

### 2.2.7.5 Agarose gel electrophoresis

Reverse transcribed cDNA was resolved in 2% agarose gels. Agarose was melted in 1x TAE buffer by boiling in a microwave oven. After boiling, ethidium bromide was added to the clear agarose solution and then poured into a gel casting chamber with a suitable comb size. Once the gel was solidified, the comb was removed and the gel was mounted to the electrophoresis chamber filled with 1x TAE running buffer. Sample and a suitable size marker

## MATERIALS AND METHODS

were mixed with 6x loading buffer and loaded into the respective wells. The gels were run at 100-110V for 30min. After separation, the bands were visualized with one 350nm UV transilluminator and photographed with a gel documentation system (Biochrom, Cambridge, UK).

### 2.2.7.6 Real-time reverse transcription-polymerase chain reaction (qRT-PCR)

Briefly, cDNA was diluted 1:10 with RNA-free water. Each target primer was run together with the housekeeping gene RPLP0. Samples were measured in triplicate.

#### The reaction mixture:

Component	Volume (μL)
cDNA (1:10 diluted)	3
iQ SYBR green Supermix	12.5
Primer mix (10pM/μl)	1
DNA/RNA-free water	8.5
<b>Total</b>	<b>25</b>

Different primers have different extension temperatures which require separate runs on the iCycler iQ® System.

The qRT-PCR program runs as follows:

Action		Light Cycler
Initial Melting		95°C, 10 min
45 cycles	Melting	95°C, 20 sec
	Annealing	60°C (depending on optimal temperature of primer) 30 sec
	Extension	72°C, 30 sec
Melting point		50°C, 10 sec
Cool to		4°C

Melt curve examination was used to confirm the specificity and efficiency of the PCR products.

qRT-PCR results were analyzed with the delta threshold cycle method using RPLP0 as an internal standard to normalize the amount of cDNA. Data were analyzed by Bio-Rad CFX

## MATERIALS AND METHODS

Manager 3.1 software and presented as relative expression (RE). CT values of each sample were the mean of triplicated values.  $\Delta CT = CT \text{ (target primer)} - CT \text{ (housekeeping gene)}$ , and untreated sample were used as a control group, while treated samples were calculated as  $\Delta\Delta CT = \Delta CT - \Delta CT \text{ (control)}$ . The relative fold change was calculated as power (2,  $\Delta\Delta CT$ ). The final relative expression was always shown as the control group for value 1.

### 2.2.7.7 Genotyping of Irf7 knockout mice

In the Irf7 knock out mice (RBRC No. was RBRC01420. Strain name was B6; 129P2-Irf7<sup><tm1Ttg>/TtgRbr</sup>c), exon 2 and 3 of the Irf7 gene were replaced with a PGK-beta-geo cassette. For verification of Irf7 knockout, three specific primers were used:

Primer	Primer_name	Primer_seq	length
1	UZU cont F1	GTGGTACCCAGTCCTGCCCTCTTTATAATCT	31
2	Neo16c	TCGTGCTTTACGGTATCGCCGCTCCCGATTC	31
3	R813 long	AGTAGATCCAAGCTCCCGGCTAAGTTCGTAC	31

### The PCR products explanation:

Primer_set	Product_size	Product source
Primer 2 + Primer 3	220bp	KO
Primer 1 + Primer 3	300bp	WT

Templates were isolated from tails of the mice and PCR set-up was conducted following the protocol from the MyTaq Extract-PCR kit as follows:

### PCR set-up

Template	1μl
Primers (100pmol/μl)	1μl (3 primers together)
MyTaq HS Red Mix, 2x	12.5μl
RNA-free water	Up to 25μl

### PCR cycling conditions:

Step	Temp. (°C)	Time (s)	note
Initial denaturation	94	180	

## MATERIALS AND METHODS

Denaturation	94	30	*
Annealing	60	30	*
Extension	72	60	*Repeat for 35 cycles
Extension	72	300	

PCR products were run on 1.5% agarose gel in 1 X TAE buffer (100 V, 30min).

### 2.2.8 Mouse testicular macrophage (mTM) isolation

We isolated testicular macrophages from mice using a combination of mechanical separation, percoll gradient centrifugation and MicroBeads magnetic selection linked to specific antibodies. The protocol excluded enzymatic decomposition.

#### 2.2.8.1 Reagent and instrument

RPMI 1640+ 10% FCS+ 1% P/S; TM buffer: 0.5% BSA or FCS in PBS+ 5mM EDTA

Stock Percoll (SP): 9:1=percoll: 10x PBS

70% percoll: 7mL SP + 2mL 1x PBS; 37% percoll: 3.7mL SP + 5.3 mL 1x PBS

30% percoll: 3mL SP + 6mL 1x PBS

MS Columns; MiniMACS separator; instruments, syringe, 26G needles, 70µm strainers, FACS tubes

#### 2.2.8.2 Preparation of single cell suspension using a percoll gradient

Testes were retrieved after sacrificing the mice and put into a Petri dish containing cold DPBS on ice. The tunica albuginea was carefully removed and the testis parenchyma was transferred into 2mL tubes with 1mL RPMI+ 10% FCS+ 1% P/S. A testicular single cell suspension was obtained by cutting the testes into small pieces with a sharp scissor following the dispersion of the minced tissue 4-5 times using a 5mL syringe with 20G needles. The dispersed tissue were transferred into 50mL tubes with 20mL RPMI+ 10% FCS+ 1% P/S, and incubated into a shaking a water bath at 37°C for 20min. The cells were filtered through 70µm strainers into a new 50mL tube and centrifuged at 300g for 7min at 4°C. After centrifugation, cells were re-suspended in 4mL of 37% Percoll. The mixture was transferred into a new 15mL tube and slowly underlayered with 4mL 70% Percoll, and overlayed with 4mL 30% Percoll. Finally 2mL DPBS was added on top and centrifuged for 40min at 300g RT without break. The interface between 37% and 70% Percoll layers which contains TM was transferred into a new 15mL tube (around 2-3mL). The Percoll contamination was removed by with DPBS by



## MATERIALS AND METHODS

centrifugation at 300g 4°C for 7min twice. Finally, cells were re-suspended in DPBS and cell numbers were counted by a hemocytometer.

### 2.2.8.3 MicroBead selection

Magnetic acquisition was carried out according to the manual from Biolegend MicroBeads with CD11b or F4/80 binded microbeads. Magnetic separation was done in the provided separator. Separated cells were collected and used for further experiments, for instance FC, IF, PCR and ELISA.

### 2.2.9 Immunofluorescence (IF)

BMDM or TM were cultured on glass slides in 12 or 24-well plates for time points indicated in the respective figures. After the treatments, cells were washed three times with cold DPBS. The cells were then fixed with 4% PFA 15-20 min at RT or with pre-cooled methanol for 10-15min at -20°C. Cells were washed two times with DPBS and unspecific binding was blocked with 10% goat serum for 1h at RT. Next, cells were incubated with primary antibodies overnight at 4°C, and then washed three times with 1X TBST buffer. The cells were incubated with a fluorescent conjugated secondary antibody for 1h at RT, and then washed three times with 1X TBST buffer. Nuclei were counterstained with DAPI (Vector Laboratories, Burlingame, USA) and images were taken either by the Fluorescence Microscope Axioplan 2 imaging system (Carl Zeiss, Göttingen, Germany) or by TCSSP2 confocal laser-scanning microscope (Leica, Wetzlar, Germany).

### 2.2.10 Isolation of peritoneal macrophages

To isolate peritoneal macrophages (PM), adult mice were euthanized and the abdominal skin was carefully removed by avoiding an incision in the peritoneal wall. 1mL cold DPBS was injected slowly into the intraperitoneal cavity of the mice using a 2mL syringe with 26G needles. The mouse abdominal wall was gently massaged, and after 5min, fluid was retrieved from the peritoneal cavity using the syringe.

The retrieved peritoneal lavage was then transferred into a sterile 15mL falcon tube. The cell pellet was collected by centrifugation at 350g for 7min at RT. The pelleted cells were washed once again with DPBS and RBCs were lysed using RBC lysis buffer for 3min at RT. Next, cells were washed by centrifugation at 350g for 7min at RT. The supernatants were decanted and pelleted cells were suspended with RPMI 1640 medium and  $5 \times 10^5$  live cells were seeded into the wells of 24-well plates for 30min. Non-adherent cells were removed by extensive

## MATERIALS AND METHODS

washing with DPBS. PM were cultured at 37°C 5% CO<sub>2</sub> in culture medium containing 10% FCS and 1% P/S for further experiments. The purity of PM was ( $\approx$  90-95%) determined by using CD11b and F4/80 antibodies by flow cytometry.

### 2.2.11 Immunoblotting

#### 2.2.11.1 Buffers and solutions

##### 10 × phosphate buffered saline (PBS)

KCl: 4g      KH<sub>2</sub>PO<sub>4</sub>: 4g      NaCl: 160g  
Na<sub>2</sub>HPO<sub>4</sub> · H<sub>2</sub>O: 23g      H<sub>2</sub>O: up to 1L

Adjust pH to 7.4 with HCl

##### 10 × Tris buffered saline (TBS)

Tris base: 24.2g      NaCl: 80g  
H<sub>2</sub>O: up to 1L      adjust pH to 7.4 with HCl

##### Washing buffer TBS/T (1L)

1 × TBS: 100mL      Tween-20: 1mL  
H<sub>2</sub>O: 899mL

##### Blocking buffer

1 × TBST: 100mL      non-fat dry milk: 5g

##### 10 × Electrophoresis buffer (pH 8.3)

Tris base: 30.3g      Glycine: 144g  
SDS: 10g      H<sub>2</sub>O: up to 1L

Adjust pH to 8.3 with HCl.

##### Stripping buffer (100ml)

1 M Tris-HCl (pH 6.8): 6.25mL      10% SDS: 2mL

β-mercaptoethanol\*: 700μL      \* added freshly just before stripping of membrane

## MATERIALS AND METHODS

H<sub>2</sub>O: up to 100mL

### 1x Semi-dry transfer buffer

Tris-base: 5.76g

glycine: 2.95g

Methanol: 200mL

H<sub>2</sub>O: up to 1L

### Cathode buffer

Tris base: 30.03g

6-amino-hexanoic acid: 3.25g

Methanol: 100mL

H<sub>2</sub>O: 400mL

### **Separating gel:**

	<b>7.5%*</b>	<b>10%*</b>	<b>12.5%*</b>	<b>15%*</b>
Water (mL)	4.85	4.01	3.17	2.35
1.5 M Tris-HCl pH 8.8 (mL)	2.5	2.5	2.5	2.5
10% (w/v) SDS (μL)	100	100	100	100
Acrylamid (mL)	2.5	3.34	4.17	5
10% (w/v) APS** (μL)	50	50	50	50
TEMED (μL)	5	5	5	5
Total (mL)	10	10	10	10

\* Separating gels with different percentages were used according to the molecular weight of target proteins (based on 37.5:1 acrylamide/bisacrylamide ratio). 7.5% gel: 250~120kDa; 10% gel: 120~40kDa; 12.5% gel: 40~15kDa; 15% gel: < 20kDa.

### **Stacking gel:**

	<b>4%*</b>
Water	3mL
0.5 M Tris-HCl pH 6.8	1.25mL
10% (w/v) SDS	50μL
Acrylamide	0.65mL
10% (w/v) APS**	25μL
TEMED	5μL
Total	5mL

\*\* Ammoniumpersulfate (APS) was prepared freshly before each experiment.

## MATERIALS AND METHODS

### 2.2.11.2 Western blotting (WB)

Cells were treated as described in the figures and figure legends. Cells from experiments were washed twice with cold DPBS and lysed with freshly prepared RIPA lysis buffer (**section 2.2.4**). Next, protein concentrations were determined for each sample by the Pierce BCA Protein Assay kit. Twenty µg protein of each sample were boiled at 95°C for 10min and then denaturated samples were separated on 10-15% SDS-polyacrylamide gels. The separated proteins were electrophoretically transferred onto a 0.2µm Hybond ECL nitrocellulose membrane (GE Healthcare, Cambridge, UK) by using a PerfectBlue™ semidry electroblotter. The efficiency of protein transfer in each experiment was examined by Ponceau S staining. The membranes were washed three times with 1xTBST buffer and then blocked in a blocking buffer (5% non-fat milk in 1xTBST buffer) for 1h at RT. The primary antibodies were diluted in 5% BSA/TBST buffer and membranes were probed overnight at 4°C. Next, membranes were washed 3x10min with 1xTBST, and incubated with HRP-conjugated secondary antibodies for 1h at RT. Subsequently, the membranes were rinsed again for 3x10min with 1xTBST. The blots were developed by enhanced chemiluminescence (ECL) reagents (Thermo Fisher Scientific) and visualized by using the Fusion Imaging system (PEQLAB, Erlangen, Germany). For loading control, we used anti-mouse β-actin during each independent experiment.

### 2.2.12 Immunohistochemistry (IHC)

#### Citrate buffer, pH6.0

7mL stock A + 41mL stock B add Aqua to 500mL

Stock solution A: 4.2g citric acid ( $C_6H_8O_7 \cdot H_2O$ ) in 200mL aqua dest

Stock solution B: 29.41g sodium citrate in 1L aqua dest

#### Washing buffer

Washing buffer: 1xTBST                      Antibody buffer: 1%BSA in 1xTBST

Blocking buffer: 5%BSA in TBST or 5% milk in 1xTBST

Paraffin-fixed tissues were cut into 10µm thick slices and de-paraffinized in a descending alcohol series: 10min xylene I, 10min xylene II, 5min 100% ethanol, 5min 90% ethanol, 5min 80% ethanol, 5min 70% ethanol, 5min 50% ethanol, 5min aqua dest. For antigen retrieval, slides were placed in a cuvette with citrate buffer and boiled in a microwave oven for 15min. Pre-warm buffer was refilled every 5min. Slides were washed for 5min in washing buffer and

## MATERIALS AND METHODS

incubated with 3% H<sub>2</sub>O<sub>2</sub> in washing buffer for 15min with gentle shaking followed by washing 3x5min again. Sections were marked using a Dako Pen. Subsequently tissue was incubated with 5% BSA in 1xTBST in a dark-wet chamber for at least 1h at RT to block unspecific binding sites.

Diluted primary antibodies were added onto the sections and kept in the dark at 4°C overnight followed by 3x5min washing. Sections were incubated with conjugated secondary antibodies for 1h at RT in the dark and washed 3x5min. The AEC detection kit was used according the introductions. Intensity of staining was checked under a microscope every 5min to avoid over-staining. When the staining was sufficient, the AEC solution was removed by washing 3x5min with aqua dest. Nuclei was counterstained with hematoxylin and washed in aqua dest before cover in Kaiser's glycerol gelatine. Images were taken with a Leica DM750 microscope (Leica, Wetzlar, Germany).

### **2.2.13 Hematoxylin and Eosin (HE) Staining**

Paraffin-fixed tissues were cut into 10µm thick sections and de-paraffinized as described in the IHC protocol (see 2.2.12).

Nuclear staining/ Hematoxylin staining: Sections were stained with 1% Hematoxylin for 10min and washed with water for a further 10min followed by a wash with water for 10min. Cytoplasm staining/ Eosin staining: Sections were stained with 1% Eosin for 2-5min and washed in the Aqua dest until the water was colorless. Dehydration of sections in an ascending alcohol series: 50% ethanol for 10sec; 70% and 80% ethanol for 3min; 90% ethanol for 10sec; 100% ethanol for 2min; Xylol II for 5min; Xylol I for 5min. Slides were then covered with Vectashield® mounting medium containing DAPI. Images were taken with Leica DM750 microscope (Leica, Wetzlar, Germany).

### **2.3 Statistical methods**

Each experiment was repeated individually. One way ANOVA, Mann-Whitney tests, and unpaired t tests (with a 95% confidence) were performed using Prism 8.0 (GraphPad Software). All p-values are two-tailed. \*p < 0.05, \*\*p < 0.01, \*\*\*p < 0.005 and \*\*\*\*p < 0.001.

## RESULTS

### 3. RESULTS

#### 3.1 Testicular macrophages show specific immunosuppressive characteristics

##### 3.1.1 TM isolation by microbeads

In this study, the TM isolation protocol was modified (see chapter 2.2.8) to prevent the activation of macrophages by enzymatic digestion and high voltage pressure using FACS. To isolate pure macrophages, positive selection of TM with F4/80 MicroBeads was performed. The purity of isolated TM was determined by flow cytometry using F4/80 and CD11b antibodies. In three independent isolation experiments, the purity of TM was determined by flow cytometry (**Figure 2**).

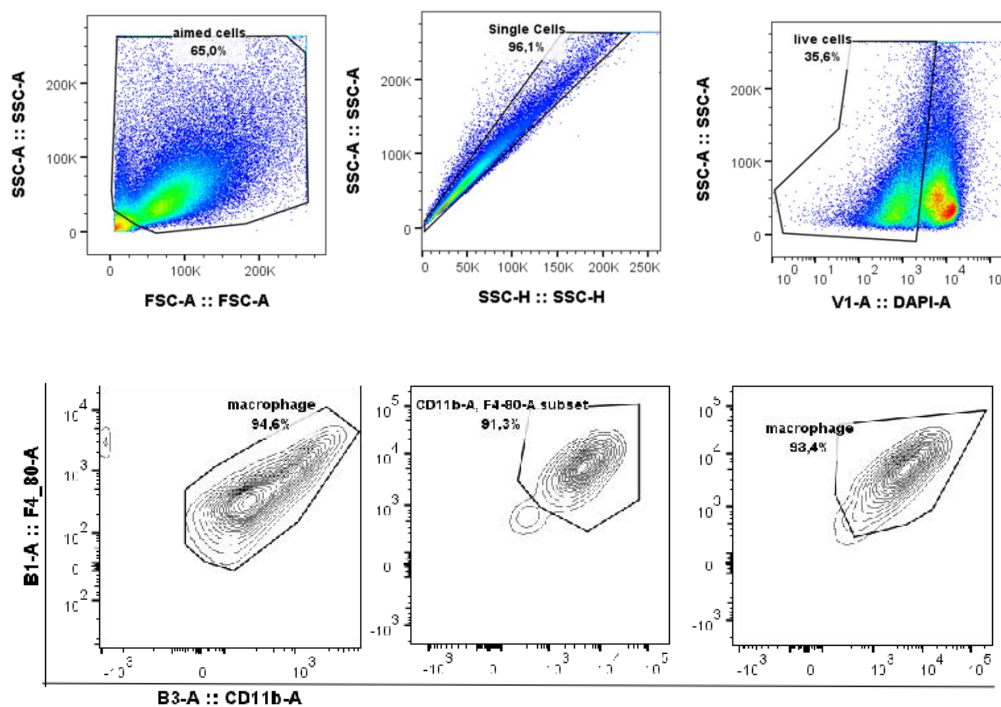


**Figure 2. TM isolation using MicroBead selection combined with Percoll gradient centrifugation.** TM isolation was done using 2 mice and a method combined Percoll gradient centrifugation with MicroBead magnetic selection. 10 $\mu$ L of F4/80 MicroBead were used for less than 10<sup>6</sup> cells. After TM isolation, anti-mouse F4/80 and CD11b antibodies were used to characterize the isolated cells by flow cytometry.

The purity of isolated TM was further confirmed by immunofluorescence (IF) analysis using pan macrophage specific F4/80 antibody (**Figure 3**). The results obtained confirmed that the purity of the isolated TM was > 90% using the new established method.

## RESULTS

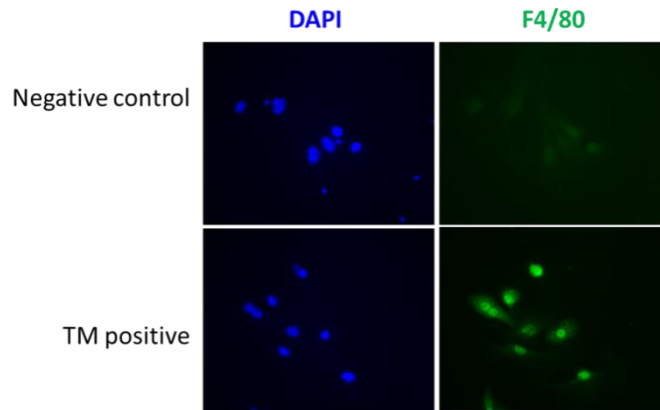


**Figure 3. IF staining of TM.** TM were isolated as described above with Percoll and MicroBeads, and cells were seeded into culture slides for IF staining with F4/80 anti-mouse antibody (x10). DAPI was used to stain cell nuclei.

### 3.1.2 TM show specific profiles compared to peritoneal macrophages

In order to confirm that the different environmental niche could influence the phenotypes of resident macrophages, we compared the expression of inflammatory genes in two different resident macrophages, i.e. TM and peritoneal macrophages (PM). PM were isolated as described in the method section 2.2.8 and IF analysis with CD68 antibody was performed to determine the purity of PM (**Figure 4**).

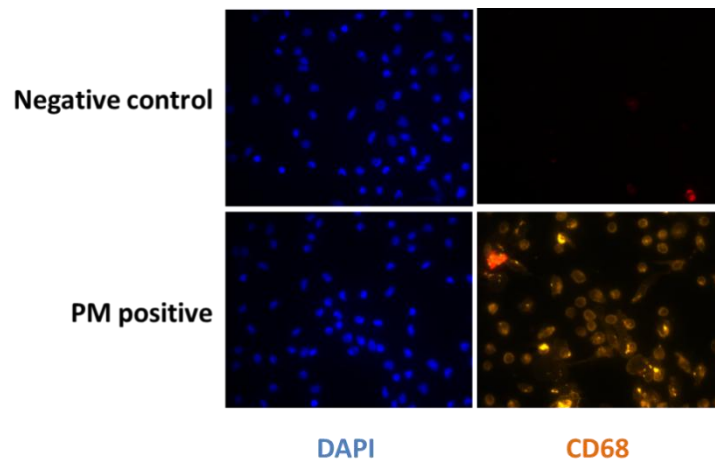


**Figure 4. IF staining of PM.** PM were isolated as mentioned above and cells were seeded into culture slides for IF staining using CD68 anti-mouse antibody (x10). DAPI was used to stain cell nuclei.

Next, the expression of pro-/anti-inflammatory genes and IFN- $\beta$  were compared between TM and PM by qRT-PCR. The expression of *Ccr7*, an important factor to balance immunity and tolerance<sup>139,140</sup> and *Cxcl10*, involved in macrophage maturation and inflammation termination<sup>154</sup>, were higher in TM than PM (**Figure 5A**). Of note, expression of *Ifn- $\beta$*  was much higher in TM than PM both at basal level and LPS-stimulated level (**Figure 5B**).

## RESULTS

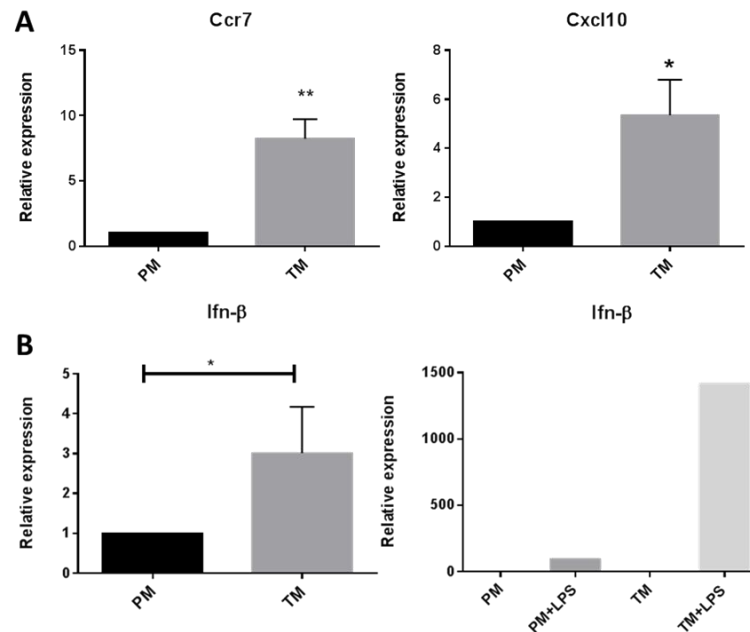
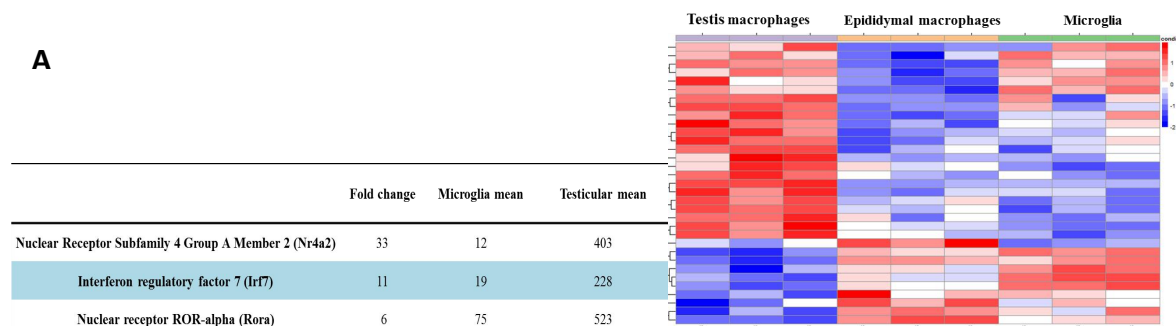


**Figure 5. TM display distinct expression profile compared to PM.** TM and PM were harvested as mentioned above. Isolated TM and PM were treated with LPS (10ng/mL) for 3h and total mRNA was isolated and analyzed for the expression levels of indicated genes. **A)** The relative expression levels of anti-inflammatory genes, *Ccr7* and *Cxcl10*. **B)** Different expression levels of *Ifn-β* in TM or PM, with or without LPS stimulation. Values are presented as mean  $\pm$  SEM of 3 independent experiments. Student t-test was employed for statistical analysis. \* $p < 0.05$ , \*\*  $p < 0.01$

### 3.1.3 TM display a significantly different gene expression profile compared to microglia

In order to characterize the specific expression profile, TM were compared to microglia by RNA-seq, and we found that immuno-related transcription factors showed dramatic difference, like *Irf7* which is closely associated with immune balance regulation of macrophages<sup>126-127</sup> (**Figure 6A**). To verify the RNA-seq data, CD45<sup>+</sup>F4/80<sup>+</sup>CD11b<sup>+</sup> TM and microglia were sorted from wild type mice. The purities were  $>95\%$  (**Figure 6B**). Relative expression of *Irf7* was higher in TM as shown by qRT-PCR (**Figure 6C**).





# RESULTS

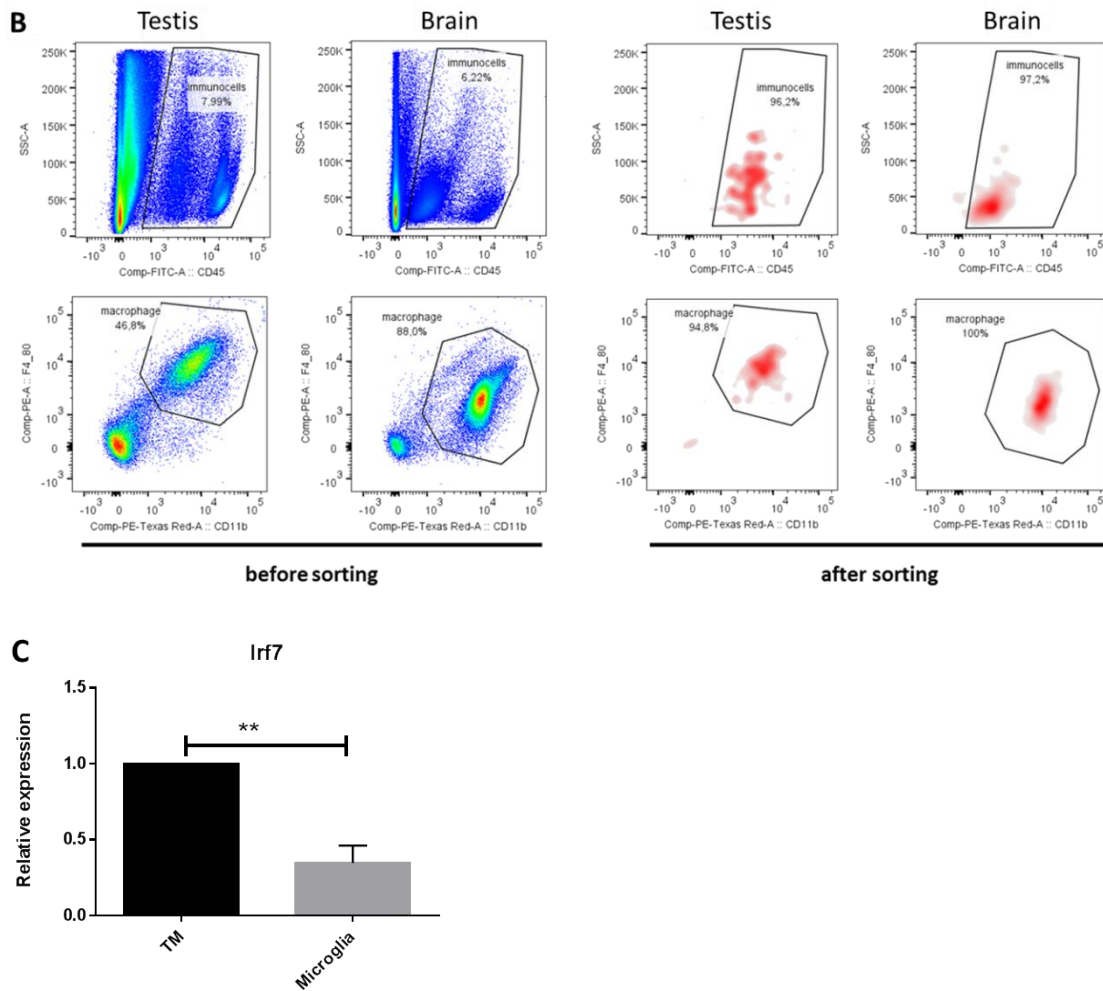


**Figure 6. TM show specific gene expression profiles. A)** RNA-Seq heat map of resident macrophages from testis, brain and epididymis. In the table, 3 of the top 10 TFs are listed which were highly expressed in TM. **B)** CD45<sup>+</sup>F4/80<sup>+</sup>CD11b<sup>+</sup> TM and microglia were sorted from mouse and the purities were around 95%. **C)** Relative expression of *Irf7* in TM and microglia. Values are presented as mean  $\pm$  SEM of 4 independent experiments. Student t-test was employed for statistical analysis. \*\*p<0.01

## 3.2 25HC displays anti-inflammatory functions to a similar extent as corticosterone

### 3.2.1 Optimization of the culture system of bone marrow derived macrophages

To investigate if testicular microenvironmental factors contribute to the phenotype of TM, BMDM were used as a surrogate macrophage model. Bone marrow macrophages were cultured as described in the methods (section 2.2.2). The degree of differentiation of bone marrow cells into macrophages was determined by flow cytometry using F4/80 and CD11b antibodies. Flow cytometry data revealed that around 97% of the cells differentiated into F4/80<sup>+</sup>CD11b<sup>+</sup> macrophages (**Figure 7**).

## RESULTS

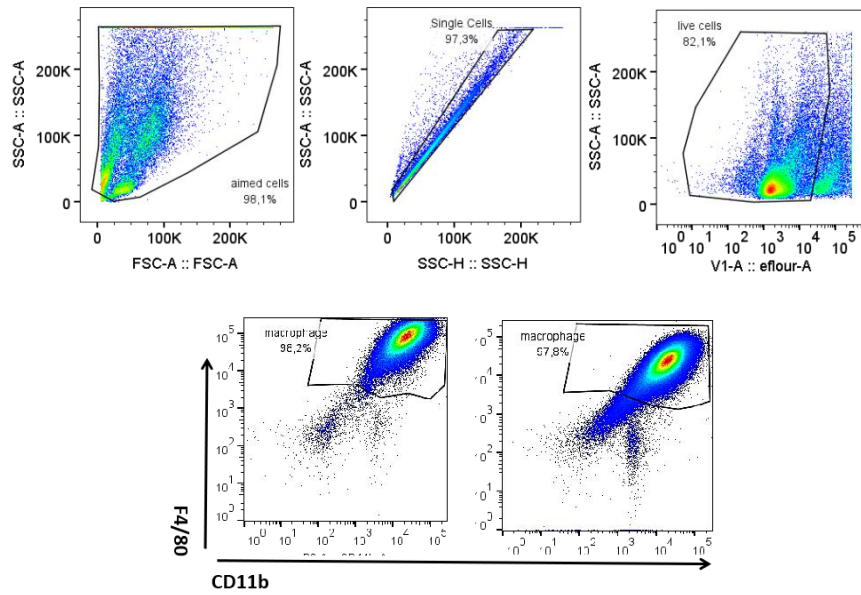
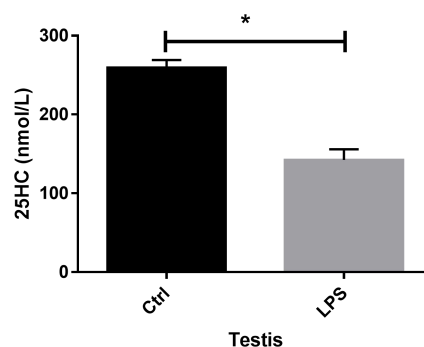


**Figure 7. Flow cytometry analysis to determine the characteristics of BMDM.** SSC-A and FSC-A gating was used to exclude small size debris; SSC-A and SSC-H gating to select single cell; SSC-A and effluent gating to select live cells without nuclear staining; SSC-A and CD45 gating for immune cells; F4/80 and CD11b gating for the CD11b<sup>+</sup>F4/80<sup>+</sup> population of macrophages. Data show that after 7 days of culture, bone marrow cells matured to macrophages with 98.2% and 97.8% of live cells expressing the macrophage markers CD11b and F4/80.

### 3.2.2 High amounts of 25HC are produced in the testis

Macrophage phenotypes and transcriptional profiles are governed by the tissue microenvironment<sup>45-48</sup>. Studies indicate that 25HC could shape the phenotypes of macrophage<sup>87-88</sup>. Thereby, to examine whether 25HC could influence the phenotypes of testicular macrophages, the concentrations of 25HC were measured in normal testis from mice. ELISA analyses revealed that the testis contains substantial amounts of 25HC ( $260 \pm 11$  nM). Next whether inflammation could inhibit or increase the testicular levels of 25HC was examined. Interestingly, stimulation with LPS significantly decreased testicular 25HC, in contrast to a previous study where inflammation induces 25HC in macrophages<sup>99</sup>.



## RESULTS

**Figure 8. Concentrations of 25HC in the testis from mouse.** The capsules of mouse testes were removed and the tissues were cut into small pieces and the cells were filtered through a 70µm strainer. Cells in RPMI 1640 medium were treated with LPS (10ng/mL) for 6h. Concentrations of 25HC were measured by ELISA. Untreated cells had around 260nM of 25HC, but after LPS treatment, 25HC decreased to a mean of 142nM. Values are presented as mean ± SEM of 3 independent experiments. Student t-test was employed for statistical analysis. \*p<0.05

### 3.2.3 25HC was cytotoxic to BMDM in a dose and time depend manner

The physiological level of 25HC in mouse serum is around 65nM which is substantially lower than in mouse testis (~260nM **Figure 8**), which indicates that the high concentration of intra-testicular 25HC could influence the phenotype of TM. To check this possibility, BMDM were treated with 25HC for 6 days followed by treatment with LPS for indicate time points in the respective figures. First, the cell viability after treatment with different dosage (100nM, 250nM, 500nM and 1000nM) of 25HC was determined by MTT assay. All dosages, except 100nM reduced the viability of cells (**Figure 9A**). However, When BMDM (after 3 days of isolation) were treated with 25HC for 3 days, only 1000nM significantly reduced the viability of cells (**Figure 9B**). When BMDM (after 6 days of isolation) were treated with 25HC, viability of cells showed no obvious change at all tested dosages (**Figure 9C**). A dose of 100nM 25HC was selected to be used from day 0 in the BMDM culture system to emulate the physiological conditions while considering the physiological level of 25HC in mouse serum and testis.

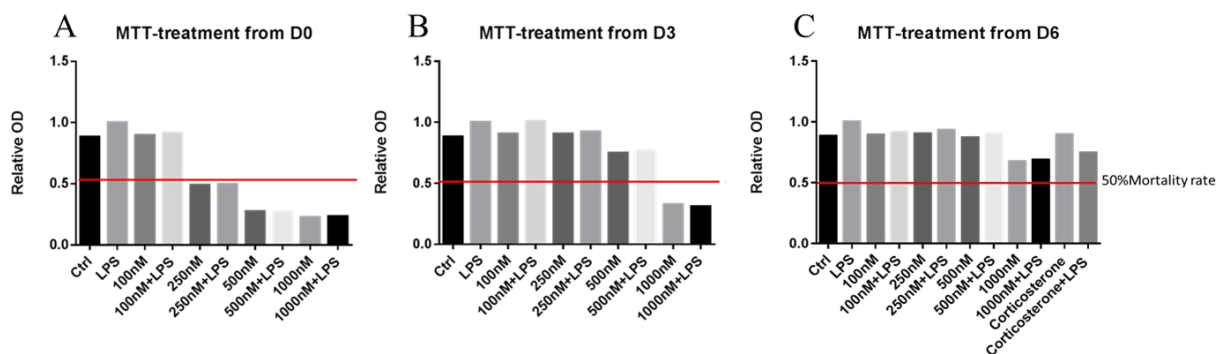


**Figure 9. Cytotoxicity assay of 25HC in BMDM.** 25HC with different concentrations were added to BMDM (cultured in triplicates with 25ng/mL M-CSF in 96-well plate) on day 0, 3 and 6 as mentioned. On day 7, BMDM were treated with LPS (10ng/mL) for 24h. MTT assay was carried out as method described as an indicator to compare cell viabilities among different groups. **A)** BMDMs treated with 25HC from D0 for 7 days. **B)** BMDMs treated with 25HC from D3 for 3 days. **C)** BMDMs treated with 25HC from D6 for 24h. Each value was the mean of triplicated values.

## RESULTS

### 3.2.4 25HC has anti-inflammatory effects on BMDM at the protein levels

The above-mentioned results (**Figure 8**) show that 25HC is produced in copious amounts in the testis. To examine if 25HC could modulate the production of inflammatory cytokines, isolated bone marrow cells were treated with M-CSF with or without 25HC for 6 days followed by LPS treatment for the indicated time points as shown in figure 10. After treatments, the production of inflammatory cytokines in cell supernatants was examined. At all times points, LPS significantly induced the production of IL-10 and TNF- $\alpha$ , however, 25HC pre-treated cells enhanced the production of IL-10 and had no effect on TNF- $\alpha$  production (**Figure 10**).

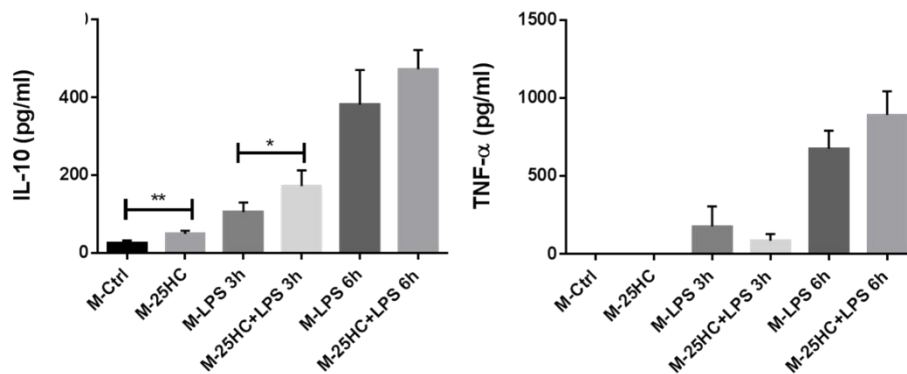


**Figure 10. Production of IL-10 and TNF- $\alpha$  by BMDM.** BMDM were cultured with 25ng/mL M-CSF and 100nM 25HC for 7 days. On day 7, cells were treated with 10ng/mL LPS for 3h and 6h. Supernatants were collected and centrifuged to remove cell debris. Production of IL-10 and TNF- $\alpha$  was measured by ELISA. Values are presented as mean  $\pm$  SEM of 3 independent experiments. One-way ANOVA test was employed for statistical analysis. \* $p < 0.05$ , \*\* $p < 0.01$

### 3.2.5 25HC shows anti-inflammatory effects at the gene expression level

To further figure out the functions of 25HC, the pro-/ anti-inflammatory gene expressions were measured. Results showed that most of the pro-inflammatory genes such as *Il-1 $\beta$* , *Il-6*, *iNos*, and *Tnf- $\alpha$*  were suppressed by 25HC and corticosterone, both at basal levels and LPS-induced levels (**Figure 11A-D**). At the same time, the expression of some classical anti-inflammatory genes were checked by qRT-PCR. Figure 11E and F show that 25HC could induce higher basal levels of *Klf4* and *Il-10*. However, 25HC showed opposite regulations of these genes upon LPS stimulation. Additional, 25HC had no effect on other M2 genes such as *Arg1* and *Chil3* (data not showed).

## RESULTS

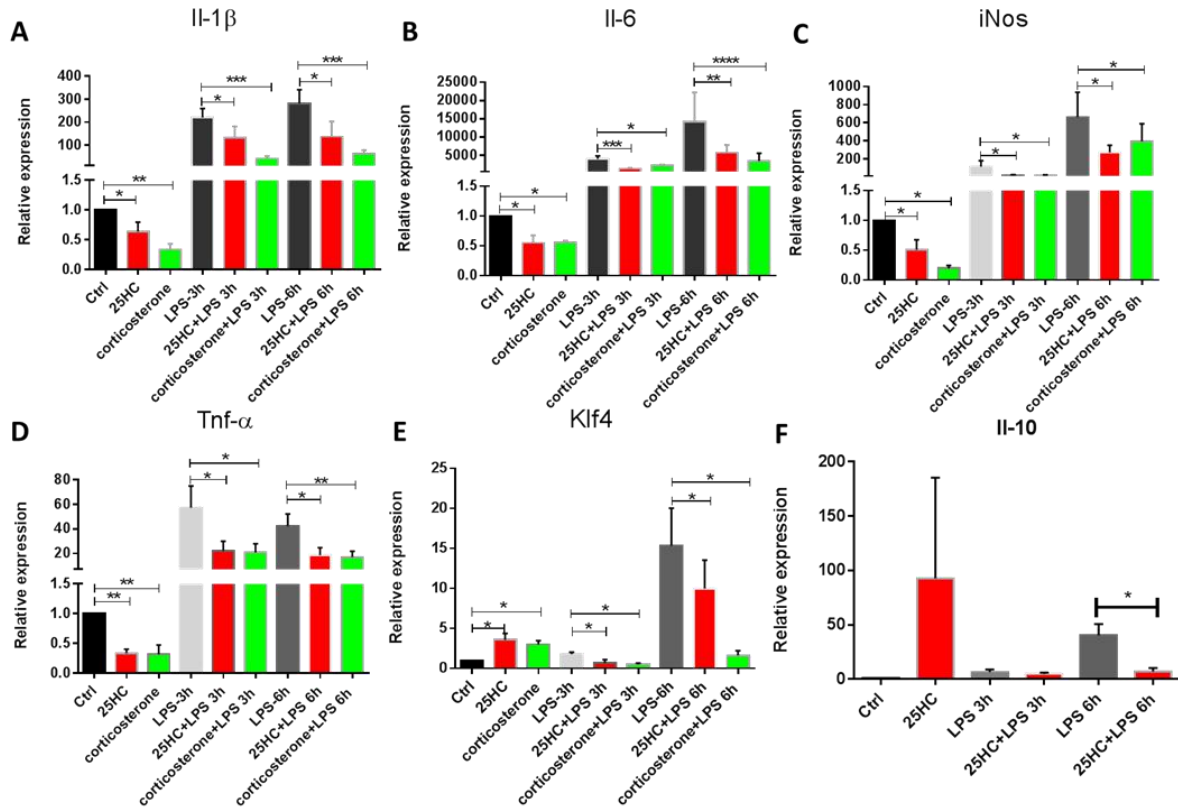


**Figure 11. Relative expression of pro-/ anti-inflammatory genes in BMDM.** BMDM were cultured with 25ng/mL M-CSF and 100nM 25HC for 7 days. 100ng/mL corticosterone was added on day 6 for 24h. On day 7, BMDM were treated with 10ng/mL LPS for 3h and 6h. Cells were harvested for total mRNA isolation and cDNA synthesis. Samples were analyzed by qRT-PCR using different primers specific for pro- and anti-inflammatory. **A)-D)** Pro-inflammatory genes, *Il-1β* (**A**), *Il-6* (**B**), *iNos* (**C**) and *Tnf-α* (**D**) were measured by qRT-PCR. **E) and F)** anti-inflammatory genes *Klf4* (**E**) and *Il-10* (**F**) were measured by qRT-PCR. Values are presented as mean  $\pm$  SEM of 6 independent experiments. One-way ANOVA test was employed for statistical analysis. \*p<0.05; \*\*p<0.01; \*\*\*p<0.005; \*\*\*\*p<0.001

### 3.2.6 Inhibition of 25HC has no obvious effects on macrophage phenotypes

LY295427 (LY) is regarded as a novel inhibitor of 25HC<sup>156</sup>. To examine whether observed immune-modulatory effect was due to 25HC, BMDM were pretreated with LY for 2h and then treated with 500nM 25HC for 3days. 25HC at this concentration had obvious cytotoxic effect on BMDM. Live cells were checked by FC. Results showed that LY alone had no cytotoxic effects on BMDM, and LY could reduce the cytotoxicity of 25HC on BMDM.

## RESULTS

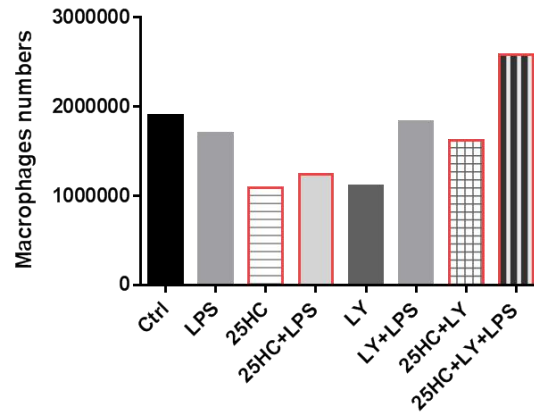


**Figure 12. Cell numbers of BMDM measured by FC.** BMDM were cultured with 25ng/mL M-CSF for 3 days. After that, fresh medium was added followed by addition of 25HC (500nM), or pretreatment with LY (20μM) for 2h and then followed by addition of 500nM of 25HC. On day 7, LPS (10ng/mL) was applied to BMDM for 24h and harvested BMDM were analyzed by FC using CD11b and F4/80 antibodies to count the cells numbers among the different groups.

Next, whether the blocking of 25HC by LY could influence the phenotype of macrophages was examined. FC data revealed no apparent influence of the blocking effect of LY on the phenotype of F4/80<sup>+</sup>CD11b<sup>+</sup> macrophages.

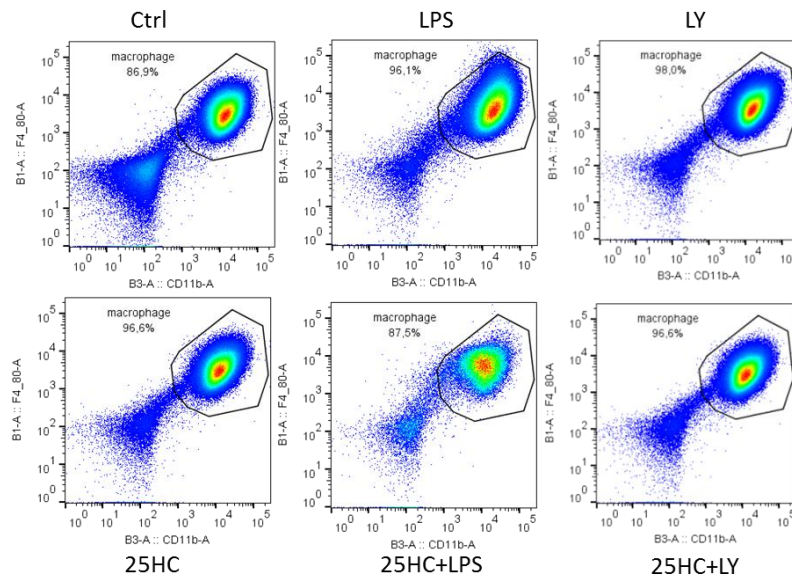


**Figure13. Examining the purities of macrophages treated with 25HC and its inhibitor.** BMDM were cultured with 25ng/mL M-CSF for 3 days. After that, fresh medium was added followed by addition of 25HC (500nM), or pretreated with LY (20μM) for 2h and then followed by addition of 500nM of 25HC. On day 7, LPS (10ng/mL) was applied to BMDM for 24h and harvested BMDM were analyzed by FC. Macrophages were gated as CD45<sup>+</sup>CD11b<sup>+</sup>F4/80<sup>+</sup>. Data showed that all samples with different treatments had similar purity ~95-98%.

In addition, I did not observe changes in the expressions of macrophage subtype markers, such as CX3CR1, CD206 (**Figure 14**) and MerTK (data not shown).



## RESULTS

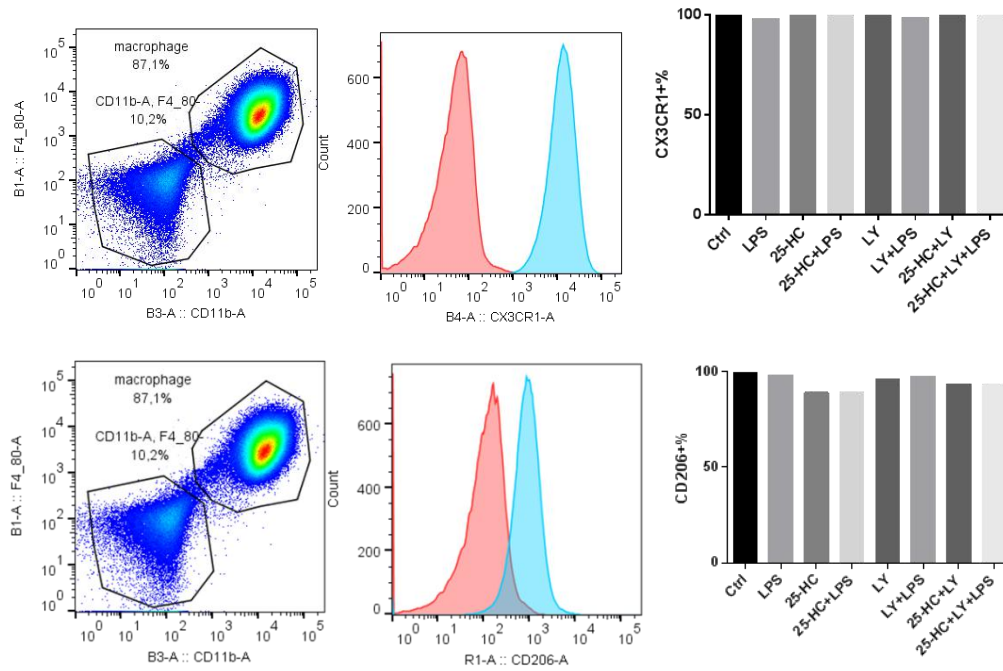


**Figure 14. Expression of specific macrophage markers by BMDM.** BMDM were cultured with 25ng/mL M-CSF for 3 days. After that, fresh medium was added followed by addition of 25HC (500nM), or pretreated with LY (20μM) for 2h and then followed by addition of 500nM of 25HC. On day 7, LPS (10ng/mL) was applied to BMDM for 24h and harvested BMDM were analyzed by FC. Markers of macrophage subtypes, CD206 and CX3CR1, were measured by using special antibodies. Percentage of CD206 or CX3CR1 was determined in CD45<sup>+</sup>CD11b<sup>+</sup>F4/80<sup>+</sup> gate.

Next, the expression of pro-inflammatory genes in BMDM was measured (**Figure 11**). 25HC induced down-regulation of pro-inflammatory genes *Tnf-α*, *Il-1β* and *iNos* and this effect was reversed back to control levels using LY.

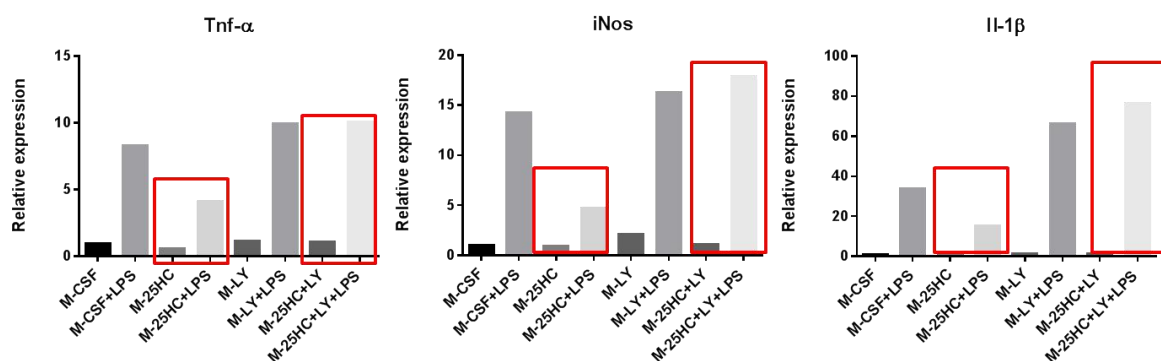


**Figure 15. Pro-inflammatory genes expressions in BMDM treated with 25HC and its inhibitor.** BMDM were cultured with 25ng/mL M-CSF for 3 days. After that, fresh medium was added followed by addition of 25HC (500nM), or pretreated with LY (20μM) for 2h and then followed by addition of 500nM of 25HC. On day 7, LPS (10ng/mL) was applied to BMDM for 24h and total mRNA was isolated for cDNA synthesis. qRT-PCR was used to assay the relative expressions of *Tnf-α*, *Il-1β* and *iNos* in different treatments.

## RESULTS

Altogether the results suggested that 25HC had no direct effect on the regulation of macrophage subtypes. In addition, 25HC displayed immune-modulatory properties by suppressing the expression of pro-inflammatory cytokines.

### 3.3 25HC down-regulates the relevant transcription factors

Similar to the RNA-seq data, qRT-PCR results revealed that *Irf7* expression was significantly higher in TM than microglia. Thus, we further examined if the high expression of *Irf7* was due to the influence of 25HC in the testicular microenvironment. qRT-PCR results revealed that 25HC and corticosterone reduced the expressions of *Irf7* and *Nr4a2* (*Nurr1*) at both the basal level and LPS-induced levels (**Figure 16**). The expression of *Rora* was not detectable in the BMDM model with different treatments (data not shown).

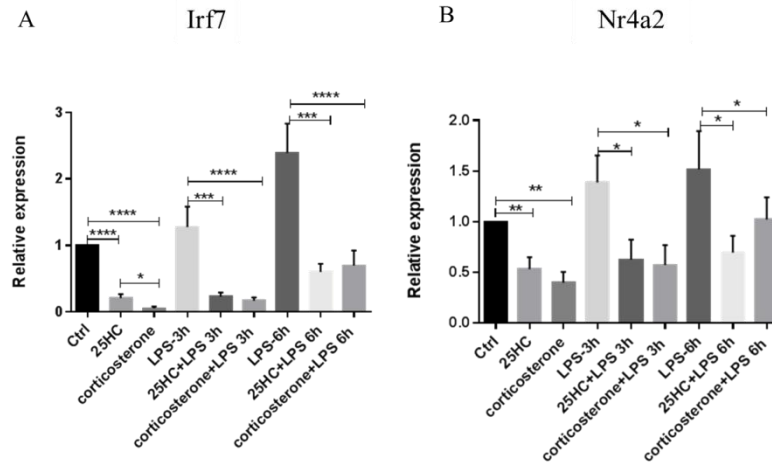


**Figure 16. Candidate TFs were repressed by 25HC and corticosterone.** BMDM were cultured with 25ng/mL M-CSF and 100nM 25HC for 7 days. 100ng/mL of corticosterone was treated on day 6 for 24h. On day 7, 10ng/mL of LPS was added to BMDM. Total mRNA was isolated for cDNA synthesis. TFs expressions, **A)** *Irf7*, **B)** *Nr4a2* and *Rora* (not shown) were measured by qRT-PCR. Values are presented as mean  $\pm$  SEM of 6 independent experiments. One-way ANOVA test was employed for statistical analysis. \* $p < 0.05$ ; \*\* $p < 0.01$ ; \*\*\* $p < 0.005$ ; \*\*\*\* $p < 0.001$

Contrary to the RNA-Seq data and TM gene expression profiles, qRT-PCR results showed that corticosterone and 25HC did not induce the expression of *Irf7* and *Nr4a2* rather there was a suppression of the expression. There might be two main reasons responsible for these opposite results. First, the bone marrow cells were differentiated into macrophages in an *in-vitro* culture condition, whereas TM were differentiated in the testicular niche. Second, besides corticosterone and 25HC, other factors could influence the phenotype and function of TM. For example, M-CSF is a well-known molecule to regulate the macrophage phenotypes. Thereby, in next experiments we examined the possibility of M-CSF in regulating the



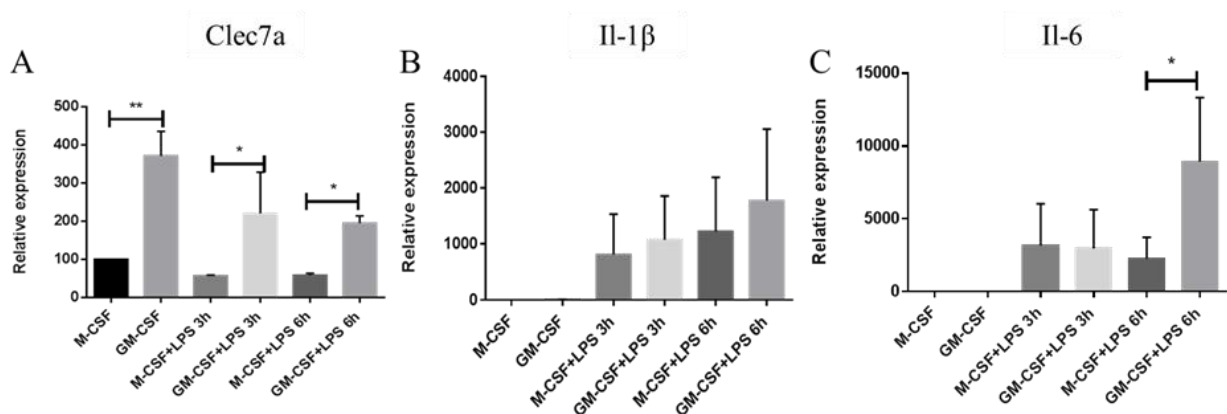
## RESULTS

phenotype of TM by comparing the expression profiles of inflammatory cytokines and transcription factors highly enriched in TM in M-CSF and GM-CSF derived BMDM.

### 3.4 BMDM show diametrically opposite inflammatory responses characteristics following M-CSF and GM-CSF stimulation

#### 3.4.1 M-CSF derived macrophages show higher expression of anti-inflammatory genes than GM-CSF derived macrophages

In order to figure out whether 25HC could display different inflammatory responses due to different CSF stimulations, and induce specific TM profiles, firstly the gene expression profiles of inflammatory genes under normal condition and after stimulation with LPS were compared. The qRT-PCR data revealed that the expression levels of M1-related genes, for instance *Il-1 $\beta$*  and *Caspase1*, showed no difference between M-CSF and GM-CSF stimulation, (**Figure 17B-D**). Of note, we found that M1-related transcription factor, *Clec7a*, was highly induced in GM-CSF derived macrophages (**Figure 17A**). Conversely, our data showed that *Tnf- $\alpha$* , *Il-6* and *iNos* (**Figure 17C, E, F**) were even highly expressed in M-CSF upon LPS stimulation. Meanwhile, the regulation of anti-inflammatory genes by M-CSF and GM-CSF upon LPS stimulations was examined. Results showed that M-CSF derived macrophages expressed higher levels of anti-inflammatory genes, such as *Il-10* and *Chil3* (**Figure 17G and H**). *Klf4* is regarded as an M2-related transcription factor<sup>37-38</sup>, but in our experiments, we found that GM-CSF but not M-CSF induced a higher expression of *Klf4* in BMDM model (**Figure 17I**), which needed further explanation.



## RESULTS

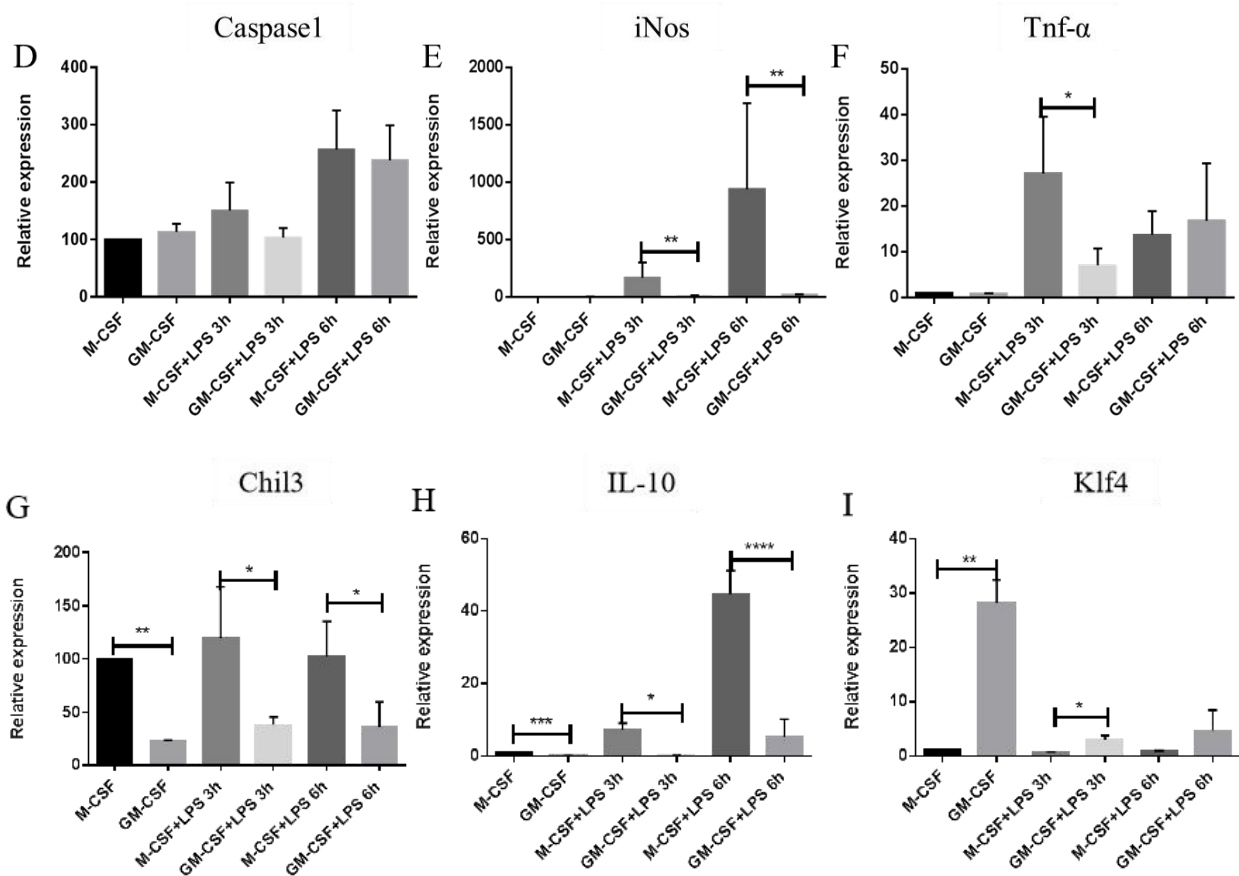


**Figure 17. BMDM derived from M-CSF and GM-CSF showed different expression profiles regarding pro- and anti-inflammatory genes.** Bone marrow cells were cultured with M-CSF (25ng/mL) or GM-CSF (25ng/mL) for 7 days and LPS (10ng/mL) was added on day 7 for 3h and 6h. Total mRNA was isolated for cDNA synthesis. Pro- and anti-inflammatory genes were measured by qRT-PCR. **A)-F)** Pro-inflammatory genes, including *Clec7a* (**A**), *Il-1β* (**B**), *Il-6* (**C**), *Caspase1* (**D**), *iNos* (**E**) and *Tnf-α* (**F**) were measured by qRT-PCR. **G)-I)** Anti-inflammatory genes, including *Chil3* (**G**), *Il-10* (**H**) and *Klf4* (**I**) were measured by qRT-PCR. Values are presented as mean ± SEM of 3 independent experiments. One-way ANOVA test was employed for statistical analysis. \*p<0.05; \*\*p<0.01; \*\*\*p<0.005; \*\*\*\*p<0.001

### 3.4.2 Production of TNF-α and IL-10 is differently regulated by CSF

To further corroborate the above results, the production of cytokines in LPS stimulated BMDM was measured. ELISA results showed that the anti-inflammatory cytokine IL-10 was produced significantly higher by M-CSF than GM-CSF derived macrophages (**Figure 18A**). Interestingly, production of TNF-α was slightly higher produced in GM-CSF derived macrophages than M-CSF, though not significantly (**Figure 18B**). Next, the activation of inflammasomes was checked by examining the production of cleaved IL-1β in cell culture supernatants by immunoblot analysis. Data showed that GM-CSF derived macrophages produced a higher amount of inflammasome IL-1β than M-CSF upon LPS stimulation (**Figure 18C**).

## RESULTS

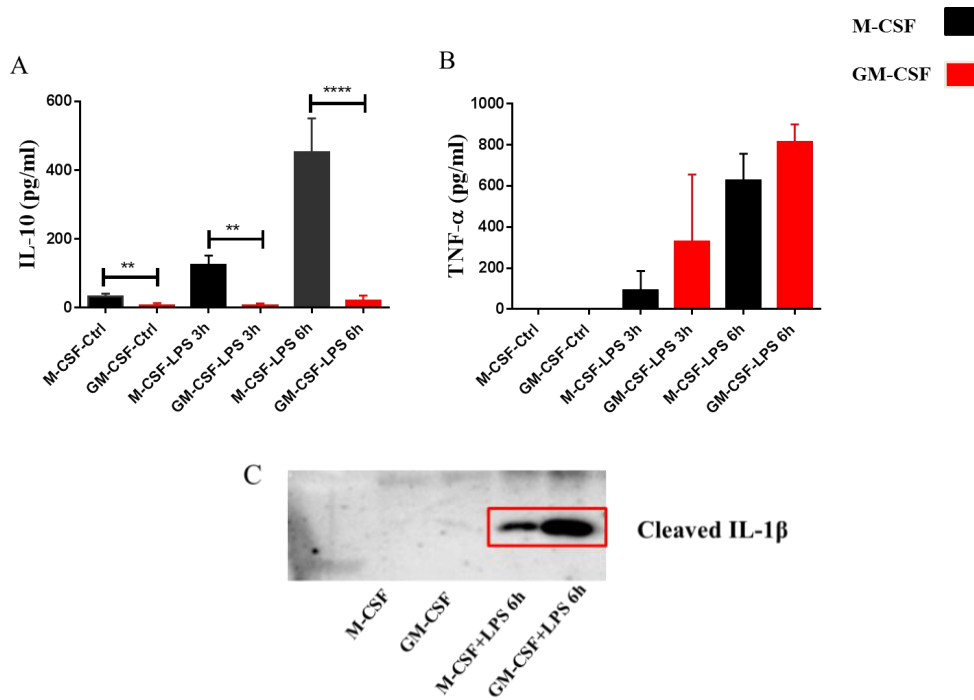


**Figure 18. Inflammatory cytokines produced by BMDM derived from different CSF showed different profiles.** Bone marrow cells were cultured with 25ng/mL M-CSF or GM-CSF. On day 7, 10ng/mL LPS was added to BMDM for 3h and 6h. **A) and B)** Production of IL-10 (**A**) and TNF- $\alpha$  (**B**) were measured by ELISA kit in supernatants. **C)** The same volume of supernatant from each group was used to compare different amount of released IL-1 $\beta$  by WB assay. Values are presented as mean  $\pm$  SEM of 3 independent experiments. One-way ANOVA test was employed for statistical analysis. \*\* $p < 0.01$ ; \*\*\*\* $p < 0.001$

### 3.4.3 M-CSF/CSF1R inhibition study

#### 3.4.3.1 Cytotoxicity of PLX-3397 (Pexidartinib) on matured BMDM

CSF1/CSF1R signaling is indispensable for the survival, development and maintenance of tissue resident macrophages<sup>58</sup>. In order to further figure out the relationship between CSF1 and the inflammatory functions of macrophages, we treated cells with PLX-3397 (PLX), a potent inhibitor of CSF1R signaling<sup>68</sup>. Till now, PLX was used experimentally mainly via oral administration to deplete resident macrophages. The cytotoxicity of the inhibitor was tested *in vitro* in BMDM using different concentrations of PLX (nM) (20, 100, 200, 300, 400 and 500) at different time points (4h, 8h, 12h and 24h). We found PLX had no significant effect on the viability of mature BMDM at all given dosages and time points (**Figure 19A**). Of note, the treatment of BMDM with 20nM PLX at 24h even increased the viability of cells (**Figure 19B**).

## RESULTS

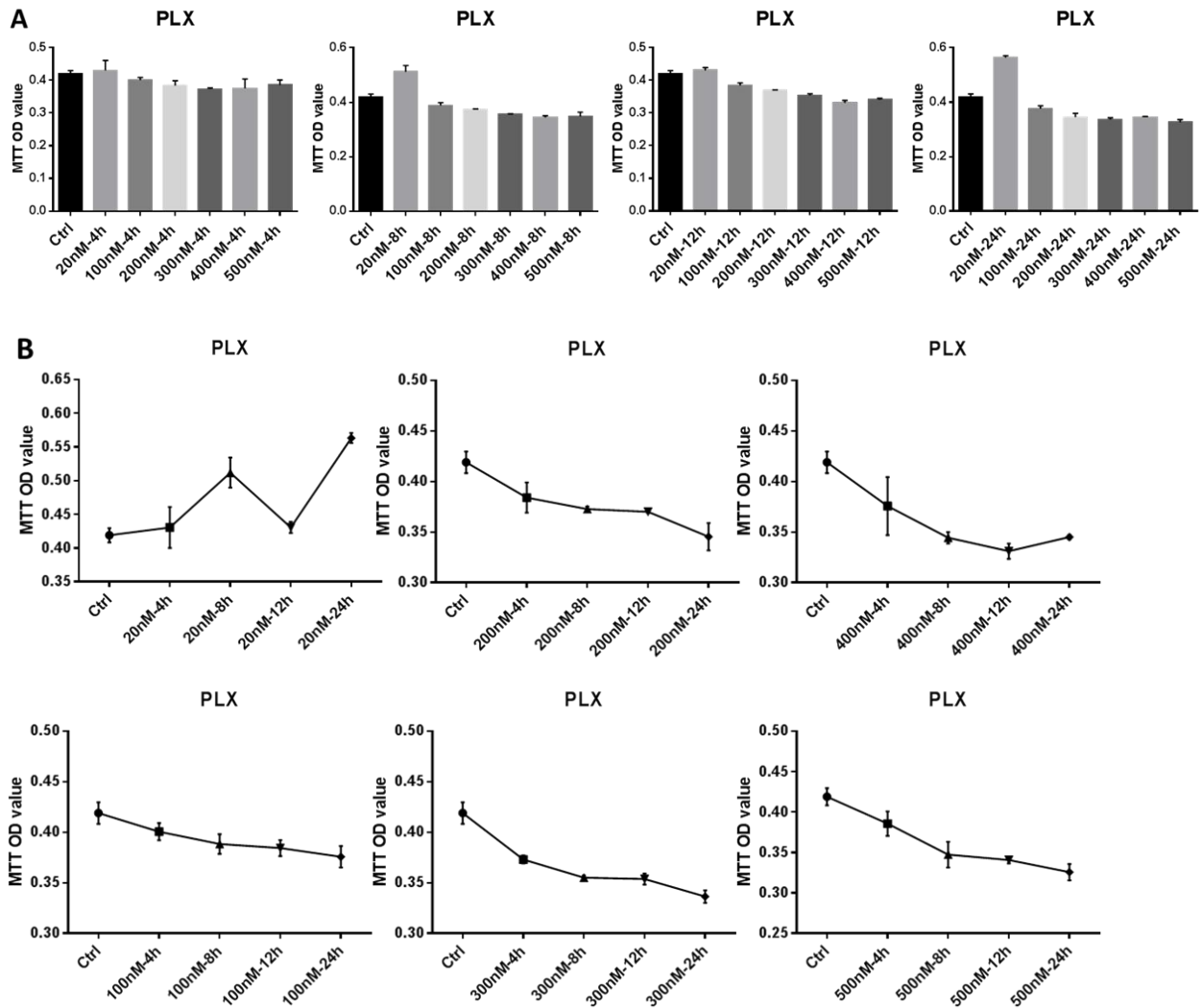


**Figure 19. The cytotoxicity of PLX, the inhibitor of CSF1R, in BMDM.** Bone marrow cells were cultured with 25ng/mL M-CSF for 7 days. On day 7, different concentrations of PLX (20nM, 100nM, 200nM, 300nM, 400nM and 500nM) were added to BMDM for 4 different time points (4h, 8h, 12h and 24h). MTT was carried out in triplicates to measure cell viability. **A)** MTT values were presented in different time points with various concentrations of PLX. **B)** MTT values were presented in the same concentration with different time points. Values are presented as mean  $\pm$  SEM of 3 independent experiments. One-way ANOVA test was employed for statistical analysis.

### 3.4.3.2 PLX blocked the activation of CSF1R targeted proteins upon LPS stimulation

To examine if CSF1/CSF1R signaling could influence the inflammatory responses of BMDM, we pretreated M-CSF derived BMDM with PLX for 2h and then subsequently stimulated with LPS for 6h. Immunoblot analyses data showed that the blockage of CSF1/CSF1R signaling using PLX attenuated the LPS-induced phosphorylation levels of Akt, STAT3 and SAPK-JNK (**Figure 20**).

## RESULTS

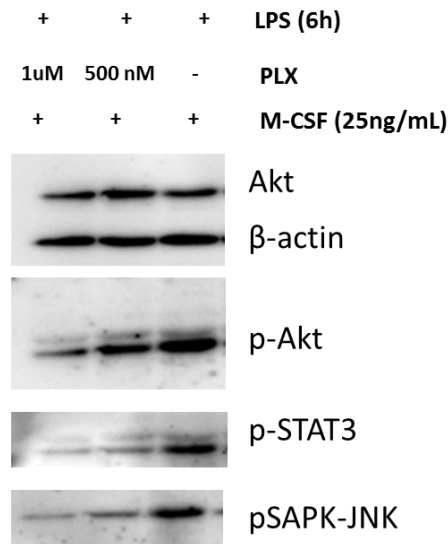


**Figure 20. Phosphorylations of Akt, STAT3 and SAPK-JNK were suppressed by PLX.** BMDM cultured with 25ng/mL M-CSF were treated with PLX (1000nM and 500nM) on day 7 for 2h. 10ng/mL of LPS was added to BMDM for 6h. Total proteins were harvested from different groups and western blotting was carried out to measure different proteins. Concentrations of Akt, p-Akt, p-STAT3 and p-SAPK-JNK were measured with specific antibodies. β-actin was used as a loading control.

### 3.4.3.3 PLX, by blocking CSF1R, suppressed the production of TNF-α

Preceding results suggested that the PLX inhibitor blocked the CSF1/CSF1R signaling. Next, if PLX inhibitor could alter the production of LPS-induced inflammatory cytokines was investigated. The blockage of CSF1/CSF1R signaling by PLX resulted in increased production of TNF-α at 3h and 6h, however, the production of IL-10 remained similar to controls (**Figure 21A-B**). Combined with the results related to production of TNF-α and IL-10 by M-CSF and GM-CSF derived BMDM, the activation of CSF1/CSF1R does not appear to be an exclusive factor in regulating inflammatory cytokines.

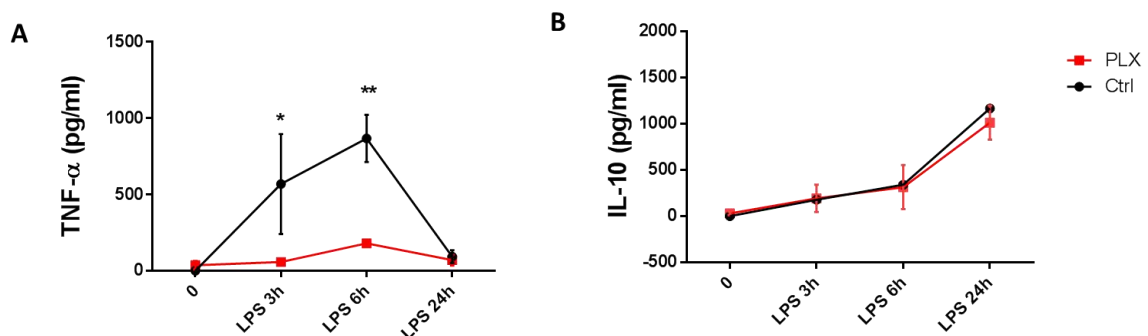


**Figure 21. Blockage of CSF1R only suppressed the production of TNF-α but not IL-10.** BMDM cultured with 25ng/mL M-CSF were treated with PLX (1000nM) on day 7 for 2h. 10ng/mL of LPS was added for 3h, 6h and 24h. **A)-B)** Supernatants were collected and the production of TNF-α (**A**) and IL-10 (**B**) were measured by ELISA. Values are presented as mean ± SEM of 3 independent experiments. One-way ANOVA test was employed for statistical analysis. \*p<0.05; \*\*p<0.01

## RESULTS

### 3.4.3.4 PLX inhibits the modulation of CSF1R-stimulated pro-/anti-inflammatory genes

Next, we measured the expressions of pro-/anti-inflammatory genes by qRT-PCR. Results showed that relative expression of pro-inflammatory genes, *Il-6*, *iNos*, and *Il-1 $\beta$*  were enhanced by PLX after LPS stimulation (**Figure 22A**). As a comparison, the expression of anti-inflammatory genes, *Atf3*, *Il-10* and *Chil3*, were suppressed by PLX (**Figure 22B**).

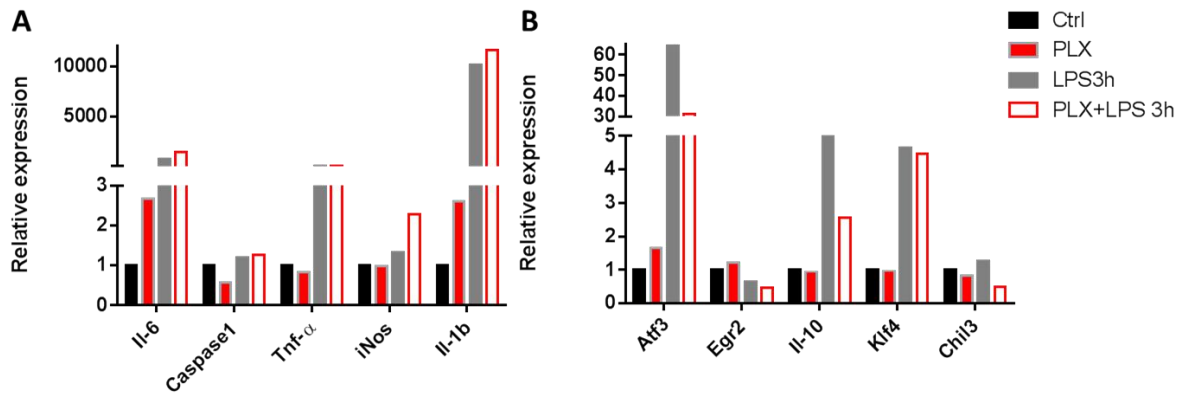


**Figure 22. Inflammatory genes regulated by M-CSF were blocked by PLX.** BMDM cultured with 25ng/mL M-CSF were treated with PLX (1000nM) on day 7 for 2h. 10ng/mL of LPS was added for 3h. Total mRNA was harvested for cDNA synthesis and qRT-PCR was used to measure the expression of pro- (A) and anti-inflammatory (B) genes (n=1).

Collectively, by comparing the inflammatory cytokines, TNF- $\alpha$  and IL-10, and pro-/anti-inflammatory gene expressions, results indicate that M-CSF display general anti-inflammatory functions, which could induce M2-like macrophage profiles. However, M-CSF or GM-CSF appear to be involved only in the initial process of macrophage polarization.

### 3.5 Inflammatory response induced by M-CSF and GM-CSF are differently modulated by 25HC

In M-CSF derived BMDM model, we showed that 25HC significantly suppressed the expression of pro-inflammatory genes and concomitantly increased the expression of anti-inflammatory genes. At protein levels, 25HC could induce the production of IL-10, but had no effect on TNF- $\alpha$ . Furthermore, the expression of *Irf7*, which was highly expressed in TM, was down regulated by 25HC. Based on these results, it was speculated that M-CSF had a stronger effect on *Irf7* regulation in the macrophage profiles than GM-CSF. We then first compared inflammatory responses of 25HC on M-CSF and GM-CSF derived macrophages.

## RESULTS

### 3.5.1 25HC suppresses TNF- $\alpha$ in GM-CSF derived macrophages

Using ELISA, we measured the production of TNF- $\alpha$  and IL-10 in GM-CSF derived BMDM treated with 25HC. Compared with M-CSF derived BMDM, Results revealed that in GM-CSF derived BMDM 25HC oppositely regulates TNF- $\alpha$  and IL-10. 25HC suppressed the production of TNF- $\alpha$  whereas the production of IL-10 remained the same in GM-CSF derived BMDM compared to control (**Figure 23**). Upon LPS stimulation, 25HC added to GM-CSF derived BMDM represses the production of TNF- $\alpha$  and has no effect on IL-10.

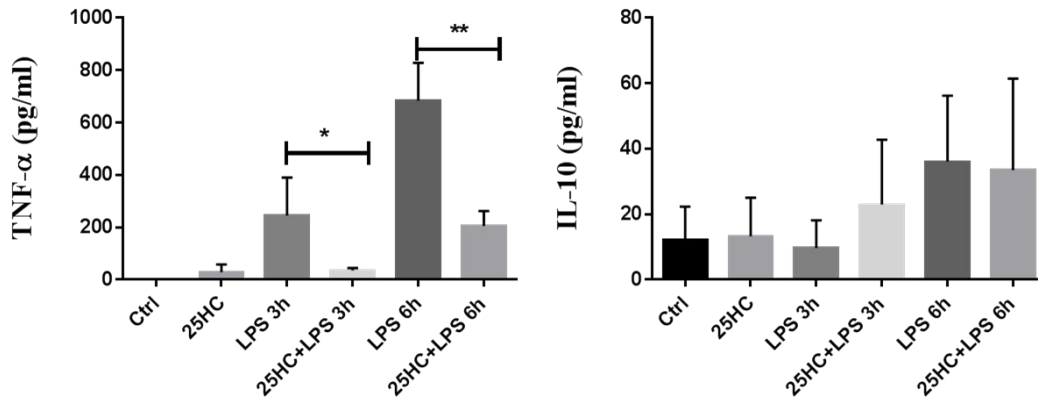


**Figure 23. Production of TNF- $\alpha$  was significantly down-regulated by 25HC in GM-CSF derived BMDM.** Bone marrow cells were cultured with 25ng/mL GM-CSF and 100nM 25HC for 7 days. On day 7, 10ng/mL of LPS was added to BMDM for 3h and 6h. Supernatants were collected and production of TNF- $\alpha$  and IL-10 were measured by ELISA. Values are presented as mean  $\pm$  SEM of 3 independent experiments. One-way ANOVA test was employed for statistical analysis. \*\* $p < 0.01$

### 3.5.2 25HC differently regulates anti-inflammatory genes in M-CSF and GM-CSF derived macrophages

*Atf3*, activating transcription factor 3, is a cyclic AMP-dependent transcription factor, which is involved in the activation transcription factor/cAMP responsive element-binding (CREB) protein<sup>39</sup>. Some studies showed *Atf3* in macrophages exerts an anti-inflammatory role by down-regulating the expression of *Ch25h*<sup>39</sup>. Our results showed that 25HC suppresses the expression of *Atf3* in M-CSF derived BMDM, but slightly enhances the expression of *Atf3* in GM-CSF derived BMDM. This regulation by 25HC is similar to that exerted on *Il-10* (**Figure 24A**).

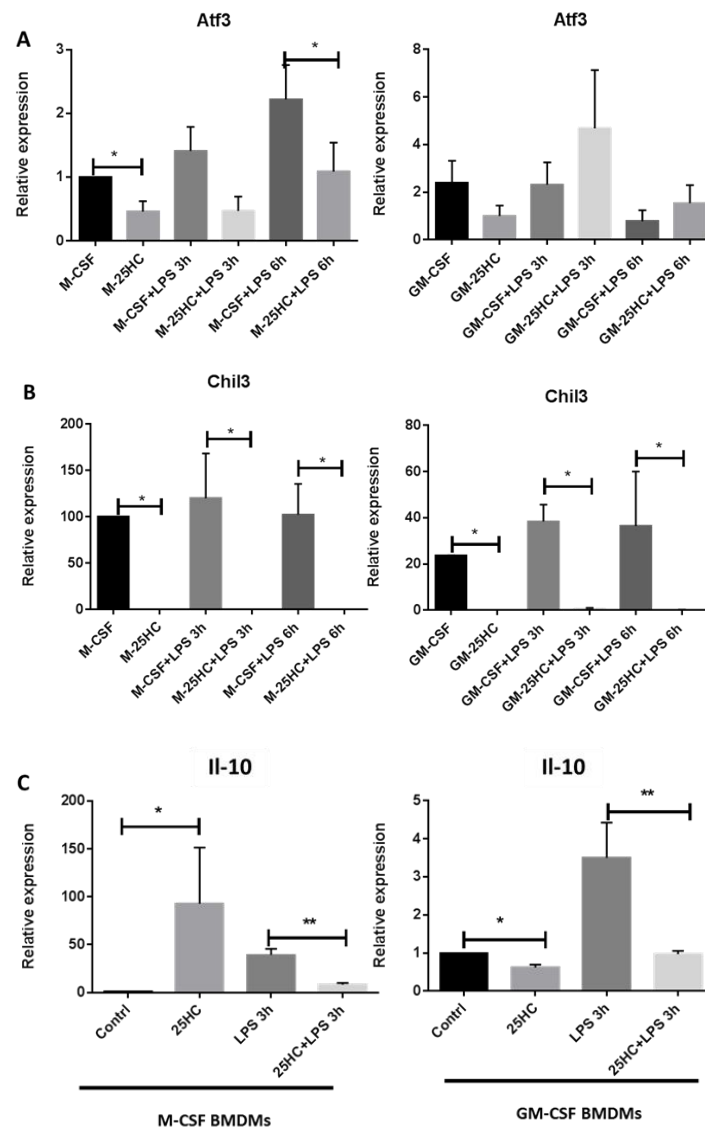
*Chil3/Ym1* is a rodent-specific AMCase (acidic mammalian chitinase), and is produced mainly by macrophages. It can be stimulated by Th2 cytokines, such as IL-4 or IL-13. *Chil3* is regarded as a classical M2a marker in macrophages<sup>35, 39</sup>. Results showed that 25HC completely abrogates the expression of *Chil3* in M-CSF and GM-CSF derived BMDM (**Figure 24B**).

## RESULTS

As we have shown, in M-CSF derived BMDM, 25HC could enhance the protein and gene expression levels of IL-10. However, in GM-CSF derived macrophages, 25HC significantly suppresses the expression of IL-10 both at basal level and LPS-induced level (**Figure 24C**).

Expression of *Klf4*, regarded as one important TF in M2 phenotype, was enhanced by 25HC in M-CSF derived BMDM at the basal level, but not in GM-CSF derived BMDM (**Figure 24D**).

Briefly, 25HC could enhance the expression of anti-inflammatory genes *Il-10* and *Klf4* only in M-CSF derived BMDM, but not in GM-CSF derived BMDM. Of note, *Atf3* and *Chil3* were suppressed by 25HC in both CSF derived BMDM.





## RESULTS

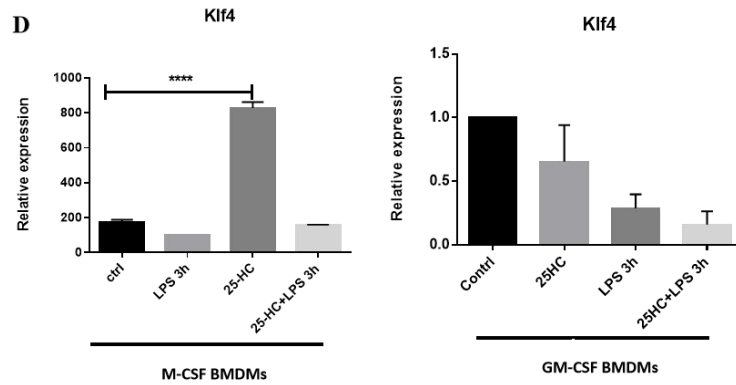
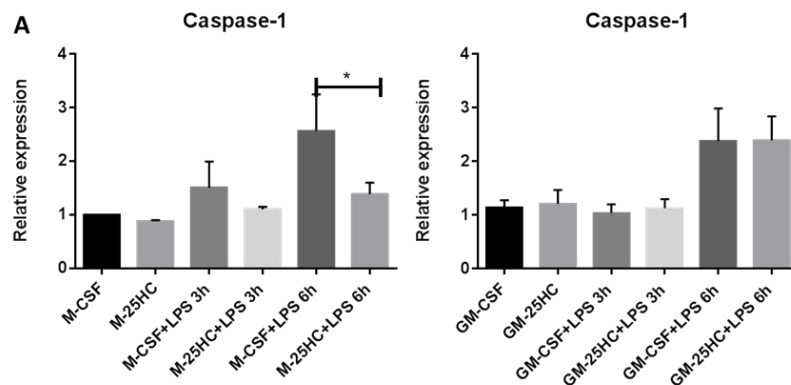


**Figure 24. Anti-inflammatory genes are differently regulated by 25HC in both CSF-derived macrophages.** Bone marrow cells were cultured with 25ng/mL M-CSF or GM-CSF and 100nM 25HC for 7 days. On day 7, 10ng/mL of LPS was added to BMDM for 3h and 6h. Total mRNA was isolated for cDNA synthesis. Expression of inflammatory genes. *Atf3* (A). *Chil3* (B). *Il-10* (C), and *Klf4* (D) were measured by qRT-PCR. Values are presented as mean  $\pm$  SEM of 3 independent experiments. One-way ANOVA test was employed for statistical analysis. \* $p < 0.05$ ; \*  $p < 0.01$ ; \*\*\*\* $p < 0.001$

### 3.5.3 Pro-inflammatory genes are mostly down-regulated by 25HC in M-CSF derived macrophages

Next, the relative expression of pro-inflammatory genes was measured by qRT-PCR. The results showed that the LPS-induced expression of pro-inflammatory genes such as *Caspase1*, *iNos*, *Tnf- $\alpha$* , and *Clec7a* were suppressed by 25HC in M-CSF derived BMDM (**Figure 25A, C, E and G**). In contrast, in GM-CSF derived BMDM, 25HC showed no obvious regulation (*Caspase1*, **Figure 25B**) or opposite regulation (**Figure 25D, F and H**).

In summary, results suggested that 25HC exerts differential inflammatory responses in M-CSF and GM-CSF derived BMDM.



## RESULTS

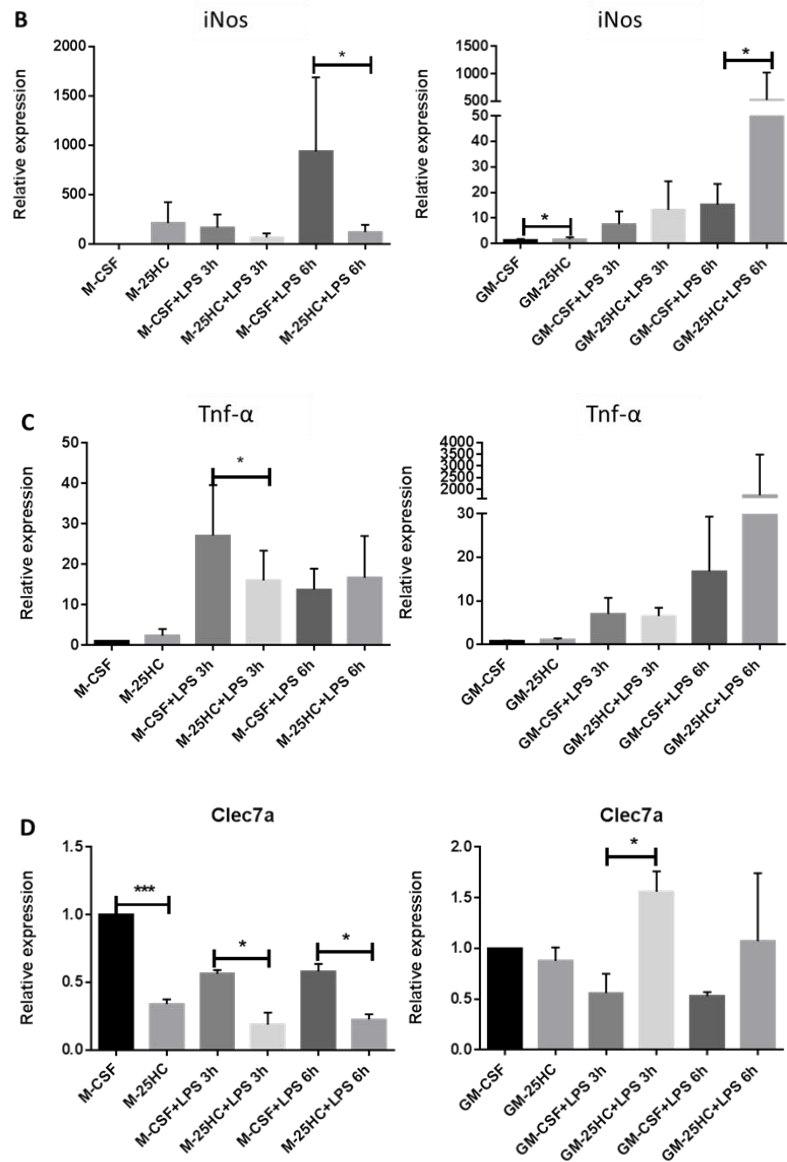


**Figure 25. 25HC differently regulates the expression of pro-inflammatory genes in M-CSF and GM-CSF derived macrophages.** Bone marrow cells were cultured with 25ng/mL M-CSF or GM-CSF and 100nM 25HC for 7 days. On day 7, 10ng/mL of LPS was added to BMDM for 3h and 6h. Total mRNA was isolated for cDNA synthesis. Expression of inflammatory genes (A) *Caspase1*, (B) *iNos*, (C) *Tnf-α*, and (D) *Clec7a* were measured by qRT-PCR. Values are presented as mean ± SEM of 3 independent experiments. One-way ANOVA test was employed for statistical analysis. \* $p < 0.05$ ; \*\* $p < 0.01$ ; \*\*\* $p < 0.005$ ; \*\*\*\* $p < 0.001$

Taken all data together, it can be concluded that in the presence of different CSF stimuli, 25HC could differentially regulate inflammatory responses in BMDM, where anti-inflammatory functions are displayed in presence of M-CSF.

### 3.5.4 IFN-β is differently regulated by 25HC and CSF

Our data showed that the expression of *Irf7* was highly expressed in TM as compared to microglia. Moreover, 25HC and IFN-β are also known to be produced in the testis by TM<sup>22, 23</sup>.

## RESULTS

However, in M-CSF derived BMDM, 25HC down-regulated *Irf7*. Here we further assessed the regulation of *Irf7* in GM-CSF derived BMDM, by 25HC as well as the enzyme, *Ch25h*, to figure out whether 25HC could regulate the expression of *Irf7* or not.

qRT-PCR results showed that 25HC could significantly suppress the expression of *Ifn-β* only in M-CSF derived BMDM (**Figure 26A-B**). Contrary to M-CSF derived BMDM, *Irf7* was not regulated by 25HC in GM-CSF derived BMDM (**Figure 16A and 26C**).

*Ch25h*, which is known to be regulated by Atf3 and IFNs, showed a negative regulation by 25HC only in M-CSF derived BMDM (**Figure 26D-E**). Taken data together, we could conclude that the activation of *Ch25h* and *Irf7* is M-CSF-related. The influence of 25HC on *Irf7* had both positive and negative feedback, which depend on 25HC concentration/activation.

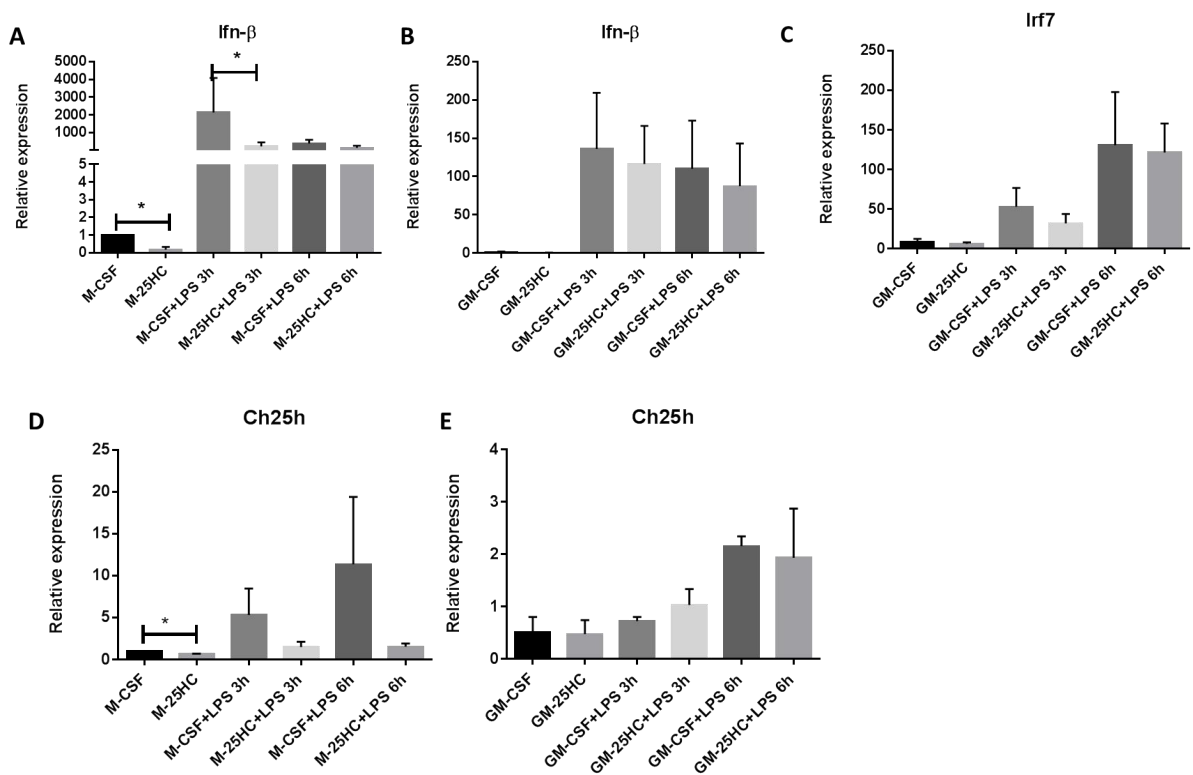


**Figure 26.** *Ifn-β*, *Irf7* and *Ch25h* were differently regulated by 25HC in BMDM derived from different CSF. Bone marrow cells were cultured with 25ng/mL M-CSF or GM-CSF and 100nM 25HC for 7 days. On day 7, 10ng/mL of LPS was added to BMDM for 3h and 6h. Total mRNA was isolated for cDNA synthesis. Expression of *Ifn-β*, *Ch25h* and *Irf7* was measured by qRT-PCR. **A)** The relative expression of *Ifn-β* in M-CSF derived BMDMs. **B)** The relative expression of *Ifn-β* in GM-CSF derived BMDMs. **C)** The relative expression of *Irf7* in GM-CSF derived BMDMs. **D) and E)** The relative expression of *Ch25h* in M-CSF (**D**) or GM-CSF (**E**) derived BMDMs. Values are presented as mean ± SEM of 3 independent experiments. One-way ANOVA test was employed for statistical analysis. \*p<0.05

## RESULTS

### 3.6 Relationship between IFN- $\beta$ , IRF7 and inflammatory response

#### 3.6.1 M-CSF induces a higher expression of *Ifn- $\beta$* than GM-CSF

Data from our group showed that in rats, TM, after LPS stimulation, could produce a higher amount of IFN- $\beta$  compared with PM. Hence, we investigated whether IFN- $\beta$  plays an immunosuppressive role as a local microenvironmental factor in the mouse testis. First, the BMDM model was used to study whether different CSF-induced macrophages had different expression of *Ifn- $\beta$* . qRT-PCR data showed no significant difference in the expression of *Ifn- $\beta$*  between M-CSF and GM-CSF derived macrophages, however the expression of *Ifn- $\beta$*  was significantly higher after LPS stimulation in M-CSF derived macrophages than GM-CSF (Figure 27A).

Our aforementioned results (Figure 16) indicated that the expression of *Irf7*, in BMDM treated with 25HC, decreased, which was contradictory with to RNA-seq results. We speculated the underlying reason would be that M-CSF may regulate the expression of *Irf7* during the differentiation of macrophages. Hence, we compared the expression of *Irf7* in two different CSF derived BMDM at basal levels and LPS induced levels. Data showed that the expression of *Irf7* was significantly higher in M-CSF derived BMDM than GM-CSF, both at basal levels and LPS-induced levels (Figure 27B).

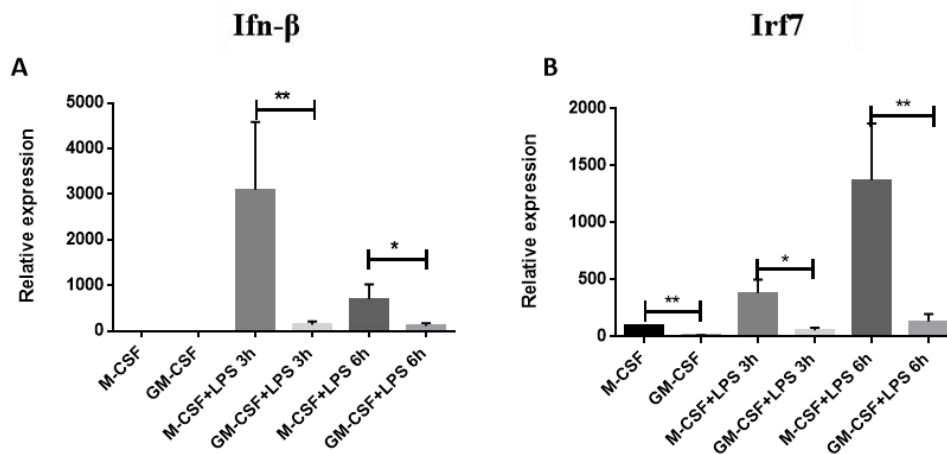


**Figure 27. IFN- $\beta$  and *Irf7* were similarly regulated by CSF.** Bone marrow cells were cultured with 25ng/mL M-CSF or GM-CSF for 7 days. On day 7, 10ng/mL of LPS was added to BMDM for 3h and 6h. Total mRNA was isolated for cDNA synthesis. Expression of *Ifn- $\beta$*  (A) and *Irf7* (B) and were measured by qRT-PCR. Values are presented as mean  $\pm$  SEM of 3 independent experiments. One-way ANOVA test was employed for statistical analysis. \* $p < 0.05$ ; \*\* $p < 0.01$

## RESULTS

### 3.6.2 IFN1R inhibitor study

#### 3.6.2.1 The IFN1R inhibitor B18R is not cytotoxic to BMDM

B18R is an IFN decoy receptor for type I IFNs, encoded by the Vaccinia virus genome and by the genomes of other orthopox viruses. B18R binds to type I IFN from multiple species and prevents IFN signaling through its receptors<sup>131</sup>. In order to figure out the roles of IFN- $\beta$  in inflammation regulation, the inhibitor of IFN1R was used to block the activation of type I interferon during inflammation responses. First, we evaluated the cytotoxicity and working concentration of B18R to BMDM models by using the MTT assay. Data obtained from MTT assay showed that concentrations increasing concentration from 1ng/mL to 500ng/mL checked at different time points had similar effects on the viability of cells (**Figure 28A-B**).

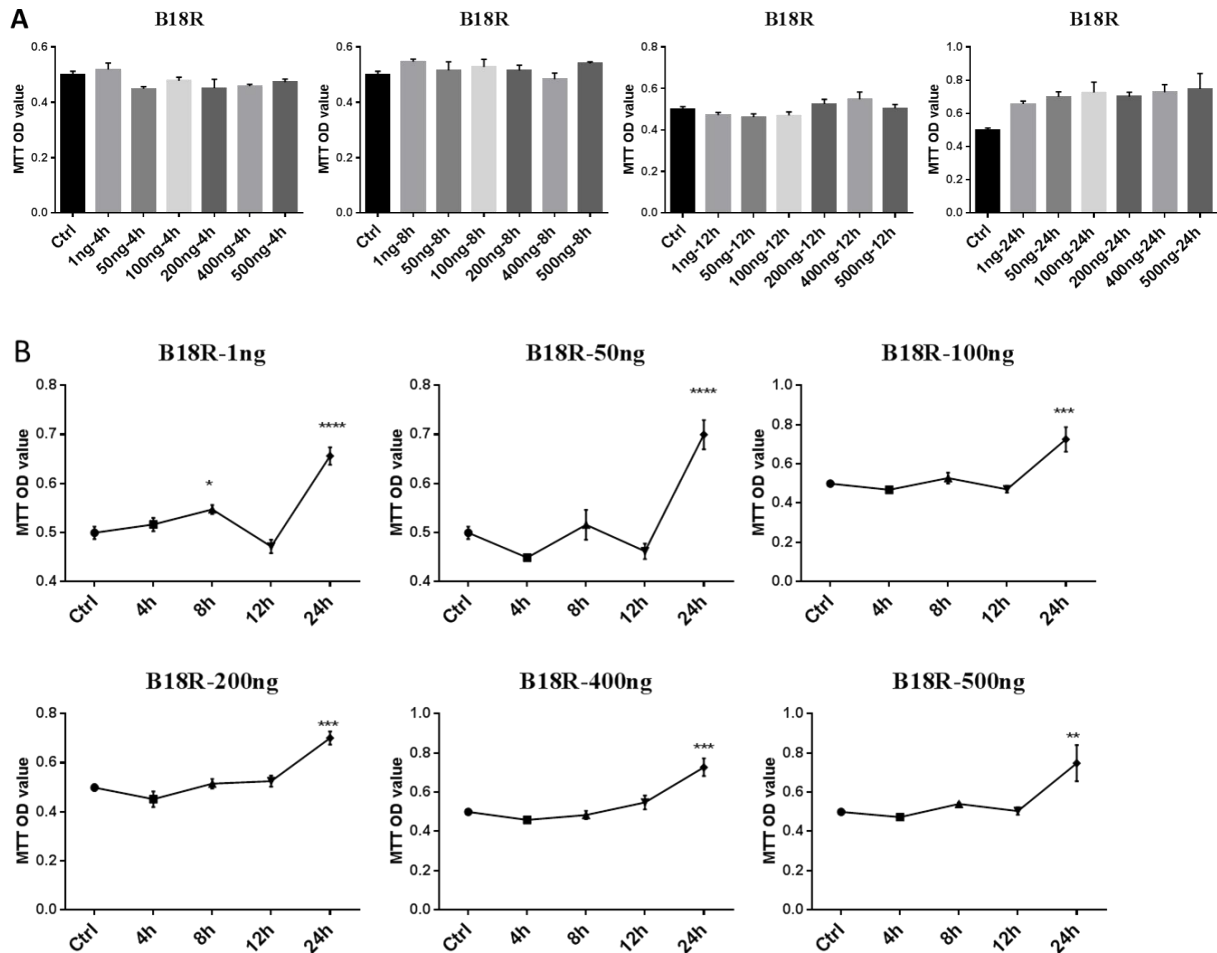


**Figure 28. The cytotoxicity of IFN1R inhibitor to BMDM.** Bone marrow cells were cultured with 25ng/mL M-CSF for 7 days. On day 7, different concentrations of B18R (1ng, 50ng, 100ng, 200ng, 400ng and 500ng) were added to BMDM for 4 different time points (4h, 8h, 12h and 24h). MTT assay was carried out in triplicates to measure cell viability. **A)** MTT values were presented in different time points with various concentrations of B18R. **B)** MTT values were presented in the same concentration with different time points. Values are presented as mean  $\pm$  SEM of 3 independent experiments. One-way ANOVA test was employed for statistical analysis. \* $p < 0.05$ ; \*\* $p < 0.01$ ; \*\*\* $p < 0.005$ ; \*\*\*\* $p < 0.001$

## RESULTS

### 3.6.2.2 B18R blocks the activation of p-STAT1

B18R works as an inhibitor of IFN- $\beta$  via competitive binding with IFN1R, which would inhibit the activation of downstream protein induced by IFN- $\beta$ <sup>132</sup>. To verify its inhibitory effect, we used WB to assay the IFN1R targeted downstream protein, notably the phosphorylation of STAT1, which is also important to inflammation regulation.

When we compared the phosphorylation of Stat1 among B18R (2h later with IFN- $\beta$ ), RPMI (negative control) and only IFN- $\beta$  treated groups, we found that the phosphorylation of Stat1 was almost totally abolished abrogated by B18R (**Figure 29**).

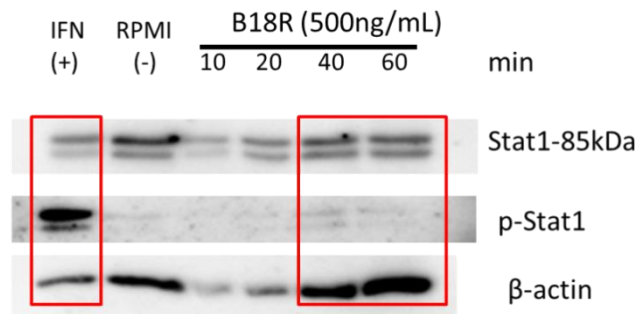


**Figure 29. Phosphorylation of Stat1 was totally abolished by B18R.** Bone marrow cells were cultured with 25ng/mL M-CSF for 7 days. B18R (500ng/mL) was added to BMDM for 2h. The positive group (+) was treated with 10ng/mL IFN- $\beta$  for 60min, and negative group (-) was treated with RPMI medium. Other groups were treated with 10ng/mL LPS for 10min, 20min, 40min and 60min. Proteins were harvested as mentioned, and Stat1 and p-Stat1 antibodies were used to detect expressions of proteins.  $\beta$ -actin was used as a loading control.

### 3.6.2.3 Blocking of IFN1R by B18R has no effect on the LPS-induced inflammatory response

Many studies have shown that IFN- $\beta$  could be induced by viruses or bacterial infections. Considering that in rodent testis, IFN- $\beta$  could be highly induced by LPS, and that M-CSF induced a high level of IFN- $\beta$ , we regarded IFN- $\beta$  as a potential factor that can induce M2 profile and regulate inflammatory responses. Hence, we used B18R to figure out whether the blockage of IFN1R could regulate inflammatory responses.

ELISA results showed that the inhibition of IFN1R had no effect on the production of IL-10 and TNF- $\alpha$  (**Figure 30A-B**). Similarly, we did not observe the changes in the activation of inflammasomes as the expressions of cleaved caspase 1 and IL-1 $\beta$  remained the same in all treated groups (**Figure 30C**).

## RESULTS

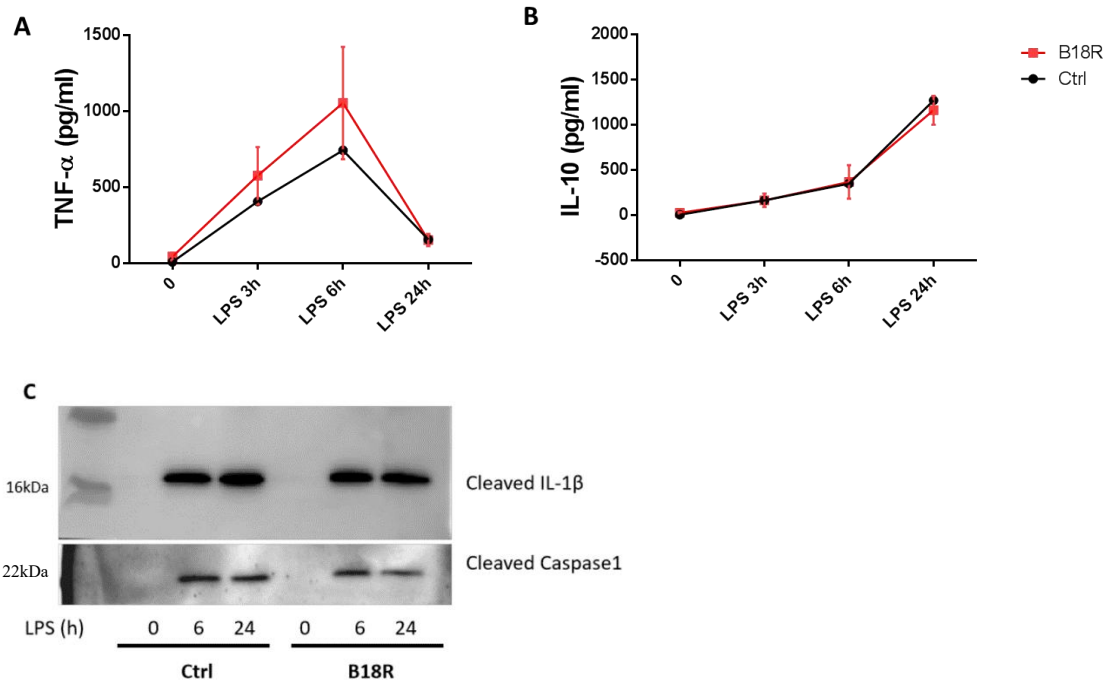


**Figure 30. Blocking of IFN1R by B18R has no effect on the LPS-induced inflammatory responses.** BMDM cultured with 25ng/mL M-CSF were treated with B18R (500ng/mL) on day 7 for 2h. 10ng/mL of LPS was added for 3h, 6h and 24h. **A)-B)** Supernatants were collected and the production of IL-10 (**A**) and TNF-α (**B**) were measured by ELISA. **C)** Supernatants were collected for WB 6h and 24h after LPS treatment. The same volume of supernatant from each group was used to analyze the released IL-1β and caspase 1. Elisa results are presented as mean ± SEM of 3 independent experiments. One-way ANOVA test was employed for statistical analysis.

As a short summary, by using the inhibitor of IFN1R, we found that IFN-β had no obvious effect on inflammatory responses. Considering the high expression of Irf7 in M-CSF and TM gene profile, we speculated that Irf7 may be the specific TF along with M-CSF and 25HC in macrophage inflammatory regulations.

### 3.7 IRF7 deficiency in mice modulates immune cells *in vivo*

Combining all the aforementioned data and results, we found out that M-CSF is regarded as an initial factor to induce immunosuppressive profiles of macrophages, and that 25HC together with M-CSF exhibit anti-inflammatory functions on macrophages. IFN-β can't regulate inflammatory cytokines secretion by macrophages. After that, we hypothesized that IRF7, which is closely governed by M-CSF, highly expressed in TM, and had intimate relationship with CH25H/25HC, is the critical factor in forming immunosuppressive macrophage profiles. Moreover, we analyzed the immune profiles of resident macrophages and BMDM in wild type (WT) and Irf7 knock out mice (KO).

## RESULTS

### 3.7.1 Verification of *Irf7* knock out by PCR

*Irf7* is highly expressed in TM and is known to induce alternative macrophage phenotype<sup>134-137</sup>. Hence, we investigated if IRF7 could influence the phenotype and functions of TM. First, to confirm the proper establishment of the purchased *Irf7* KO mice, we performed genotyping using the tail of WT and KO mice. For the verification of *Irf7* KO, specific primers were used as mentioned in the methods part. PCR results confirmed the deletion of a specific exon in *Irf7* KO mice which was sufficient to confirm the knockout.

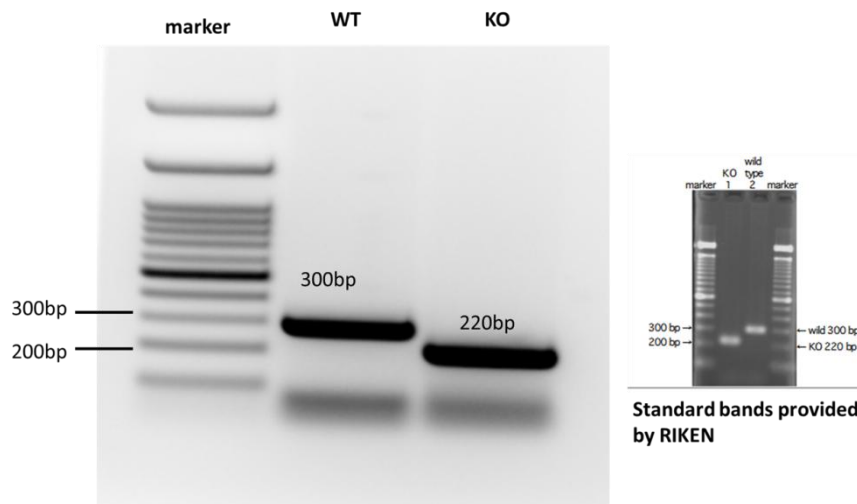


**Figure 31. Genotyping verification of *Irf7* knockout mice.** Tails from WT and KO mice were used as templates for genotyping assay by PCR with 3 different specific primers for target insert DNA sequence. Primer sets and PCR synthesis conditions were used as mentioned in the methods part. Gel was exposed to UV light and the generated image was captured in inverted color. Efficient knock out of *Irf7* showed the presence of a specific band around 220bp, while wild type was 300bp (3 individual experiments were carried out).

### 3.7.2 Mice deficient of *Irf7* show no change in the ratio of body/testis weight

We compared the body weight and testis weight of KO mice with age matched wild type male mice of C57BL/6J strain background. *Irf7* knock out mice generally had lower body weights and testes weights (**Figure 32A-C**). However, the ratio of testis/body weight had no obvious difference when compared with WT mice (**Figure 32D**).



## RESULTS

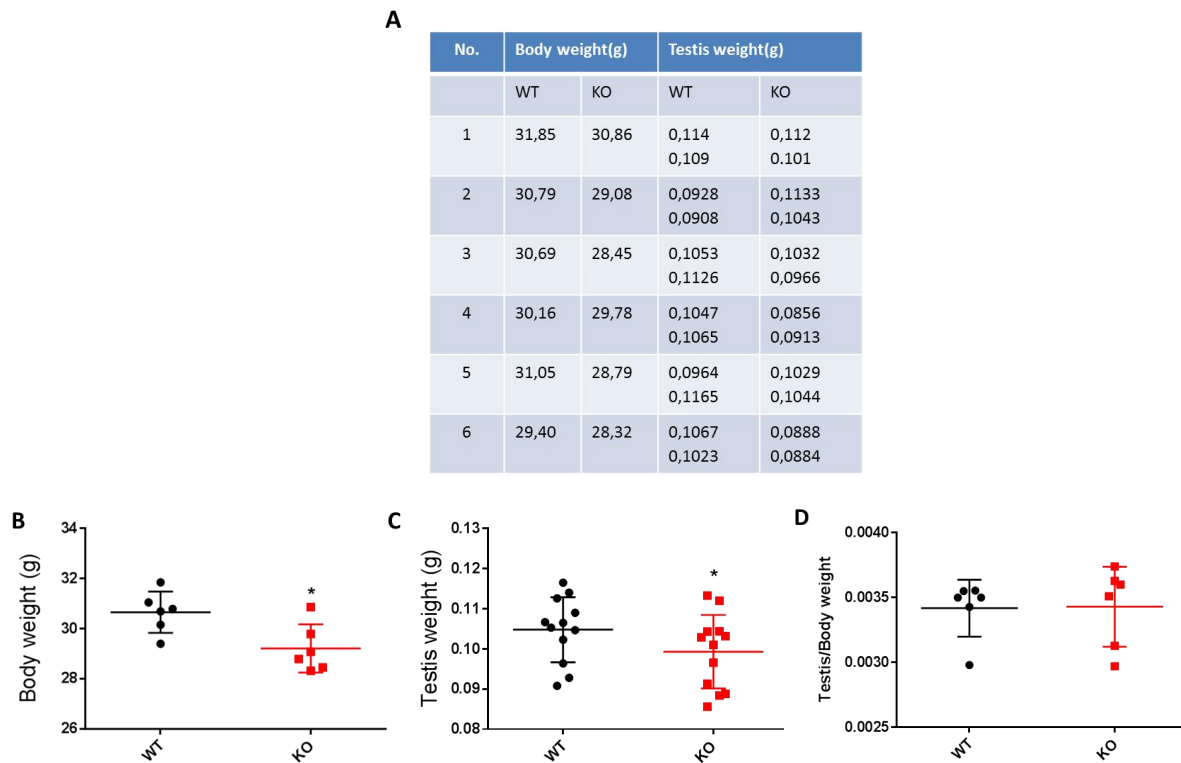


**Figure 32. The influence of *Irf7* KO on mice body weights and testes weight.** Body weights and both testes were measured in WT and KO mice (N=6). **A)** The data of body weights and testis weight from KO and WT mice. **B)** The comparison of body weight between KO and WT mice. **C)** The comparison of testis weight between KO and WT mice. **D)** The comparison of the ratio of testis/body weight between KO and WT mice. Values are presented as mean  $\pm$  SEM of 6 independent experiments. Statistical analysis was carried out using t-test. \* $p < 0.05$

### 3.7.3 IRF7 deficient mice show normal structure histology

To determine if the deficiency of *Irf7* could impair the testicular structure and spermatogenesis. HE staining was performed. The structure of the testis and spermatogenesis of *Irf7* KO mice was comparable with WT mice (**Figure 33A** KO testis, WT not shown). In addition, no significant change in the number of CD206<sup>+</sup> TM was observed between *Irf7* KO and WT mice (**Figure 33B**).

## RESULTS

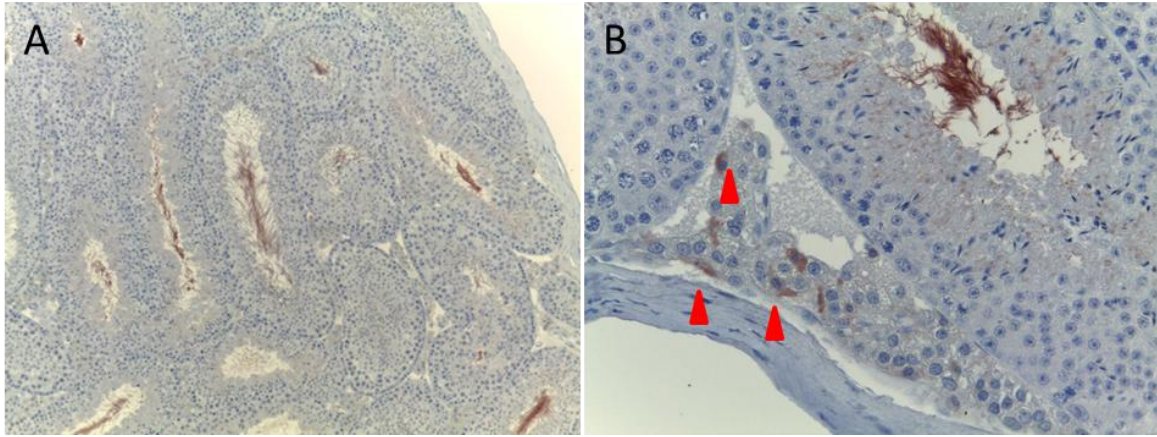


**Figure 33. HE and IHC staining of Irf7 knock out mouse testis.** Testes from Irf7 knock out and wild type mice were cut at 5 $\mu$ m thickness and stained by IHC with CD206 antibody. **A)** The general structure of KO testis showed no difference with WT (10x); **B)** KO testis with IHC staining with CD206, the red arrows mark the presence of testicular macrophages (20x).

### 3.7.4 Irf7 knock out influences leukocyte modulation *in vivo*

We then analyzed different populations of immune cells in different organs from WT and KO mice. Analysis of each KO mouse was carried out in parallel with one WT mouse for a total of 6 experiments. We detected in different organs lymphocyte (CD45<sup>+</sup>), monocyte and neutrophils (GR1<sup>+</sup>), macrophages (F4/80<sup>+</sup> and/or CD11b<sup>+</sup>), B cells (CD19<sup>+</sup>), T cells (CD3<sup>+</sup>) and subtypes of resident macrophages markers (SiglecF, CD206, CD64 and MHC II).

General gating strategy for flow cytometry analysis for different organs was carried out as mentioned below. Some resident macrophage gating was modified due to their special phenotypes (**Figure 34A**). All samples from different organs were gated with same strategy to identify immune cells (CD45<sup>+</sup>, **Figure 34B**). CD45<sup>+</sup> cells were further stratified into CD3 (T) cells, CD19 (B) cells, monocyte and neutrophils (GR1<sup>+</sup>), macrophages (F4/80<sup>+</sup> and/or CD11b<sup>+</sup>), and subtypes of resident macrophages markers (SiglecF, CD206, CD64 and MHC II).

## RESULTS

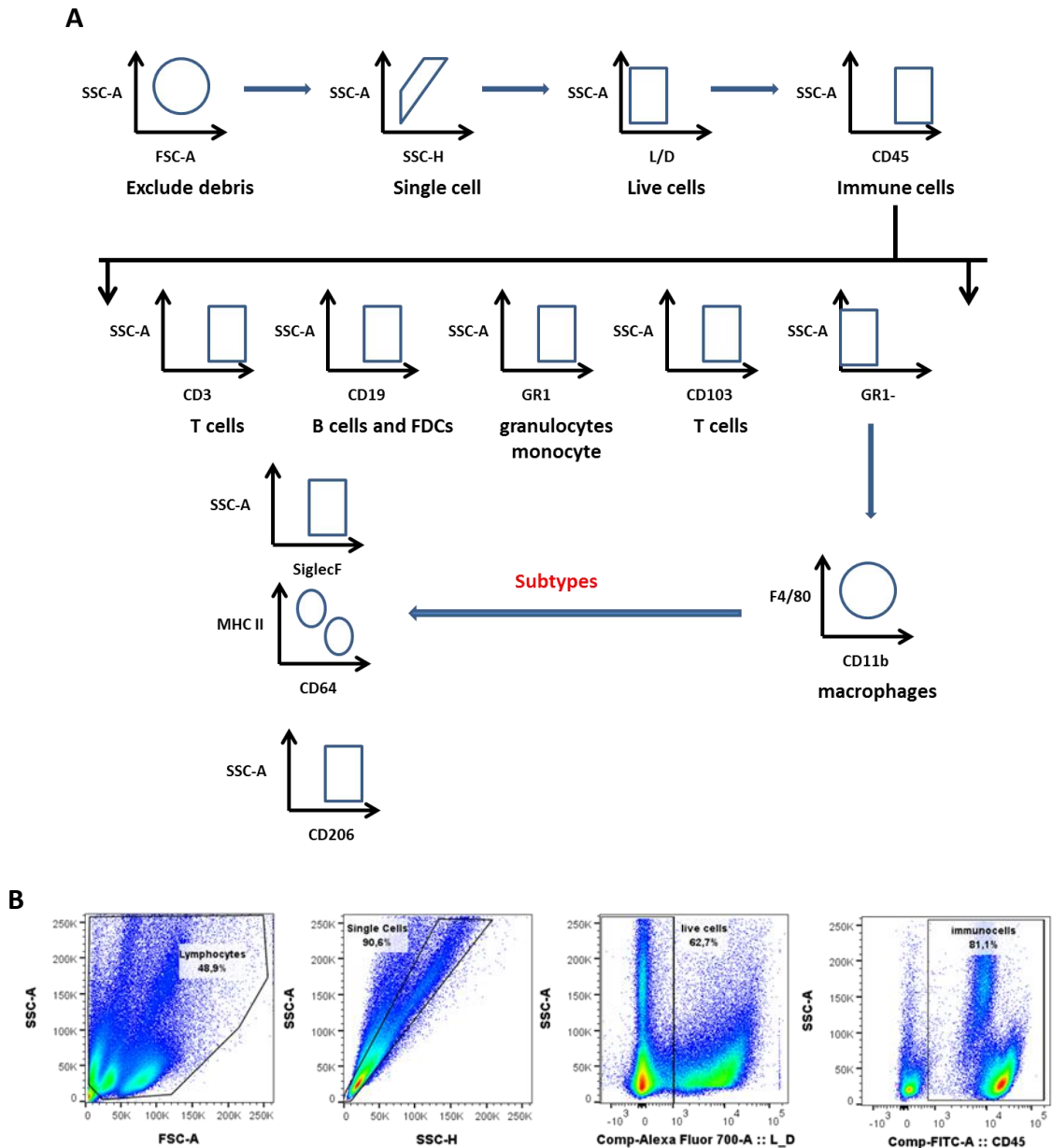


**Figure 34. General gating strategy for flow cytometry analysis from different organs.** Every sample from WT and KO mice were measured on BD Arial FACS. **A)** The whole general gating strategy for immune cells: SSC-A/FSC-A to exclude small size debris; SSC-A/SSC-H to choose single cells; SSC-A/L-D to choose live cells; CD45<sup>+</sup> to select immune cells. From CD45<sup>+</sup> population, the following populations were analyzed: CD3 (T cells), CD19 (B cells), GR1 (distinguish monocyte/GR1<sup>+</sup> from macrophage/GR1<sup>-</sup>) and CD103 (T cells). In GR1<sup>-</sup> cells, macrophages were chosen as F4/80<sup>+</sup> and/or CD11b<sup>+</sup>. Then in the macrophage population, different subtype markers were used. **B)** General gating to choose immune cells from blood sample.

**Blood.** Blood contains various kinds of immune cells, which are mainly derived from bone marrow stem cells. According to the profiles of blood immune populations, we applied a slight change in the gating method on the general gating strategy, where monocyte-derived macrophages were regarded as CD11b<sup>+</sup> (**Figure 35A**). The FC data significantly revealed more B cells (CD19<sup>+</sup>) and T cells (CD3<sup>+</sup>) in KO mice than the WT mice. The percentage of

## RESULTS

macrophages ( $\text{GR1}^-\text{CD11b}^+$ ) was the same in both mice strains. Interestingly, in  $\text{CD11b}^+$  cells, percentage of  $\text{MHC II}^+$  cells was significantly more in KO mice, which indicated that the function of antigen presentation may be enhanced in *Irf7* deficient mice (**Figure 35B**).

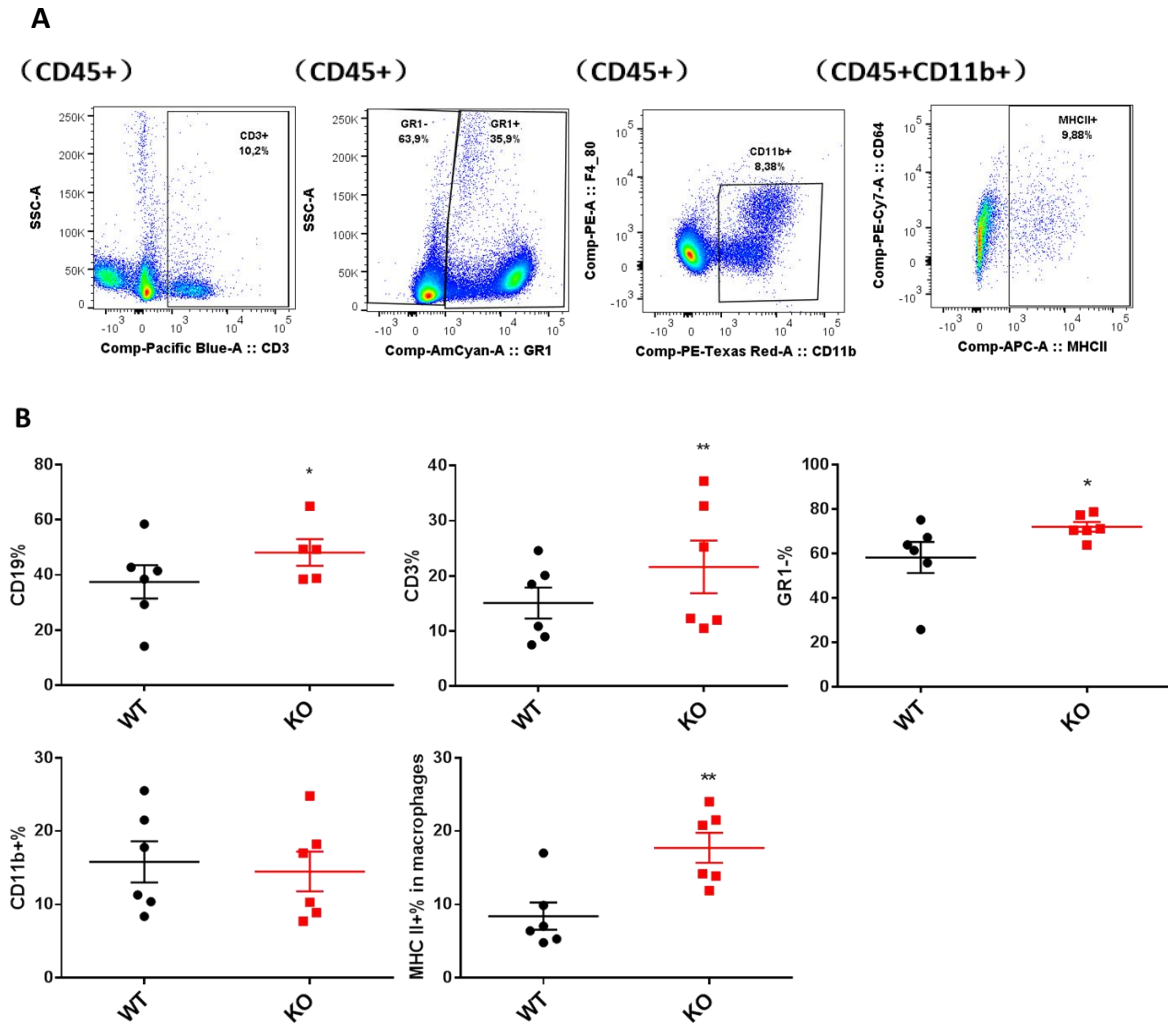
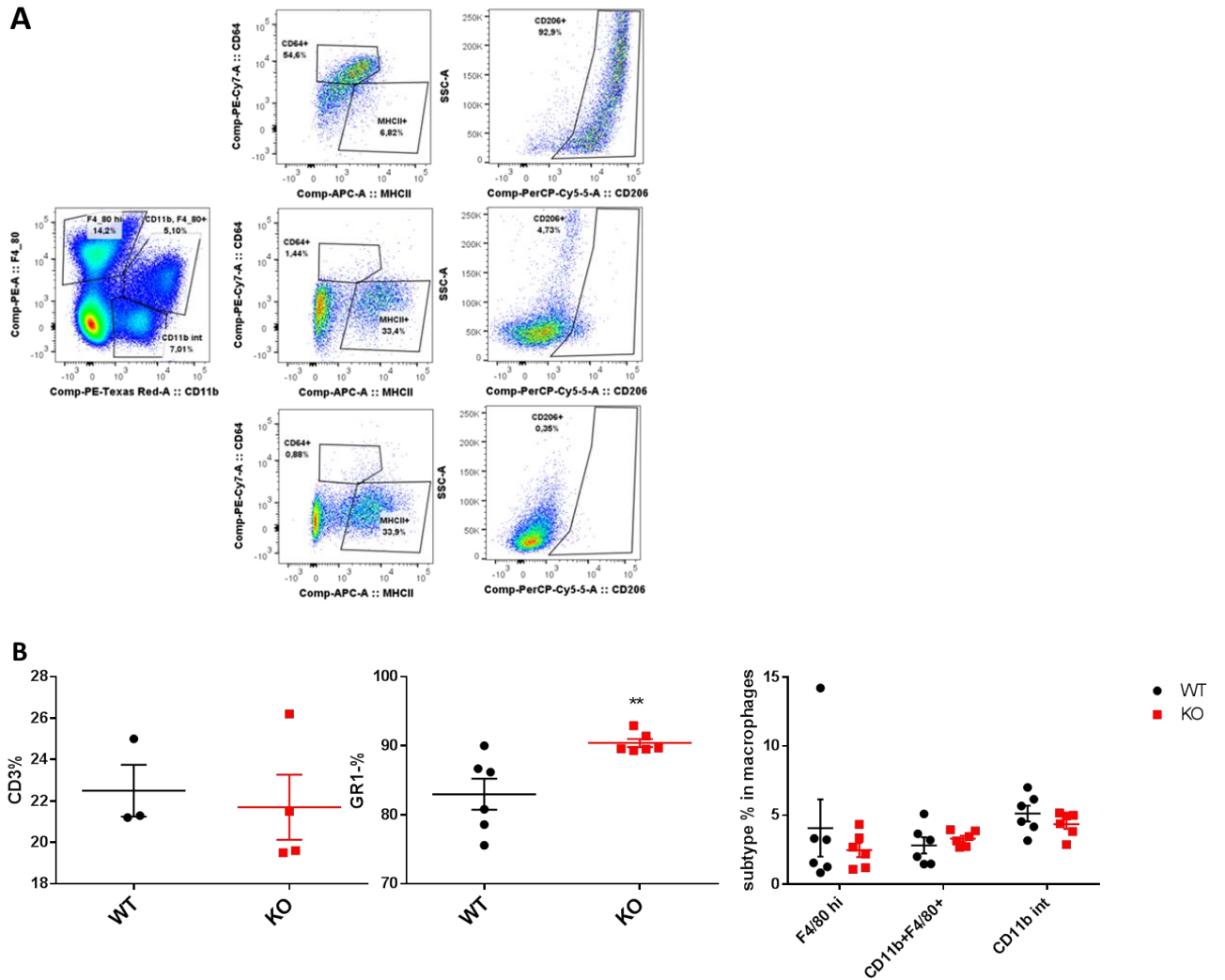


**Figure 35. Flow cytometry data from blood samples from WT and KO mice. A)** The adapted gating method according to the profiles of blood. CD3, CD19 and GR1 were directly gated from  $\text{CD45}^+$  populations. CD11b gating was based on  $\text{CD45}^+\text{GR1}^-$  populations for macrophages. MHC II gating was from  $\text{CD45}^+\text{GR1}^-\text{CD11b}^+$  populations. **B)** Different percentages of immune cell populations in blood were detected between *Irf7* KO and WT mice. Values are presented as mean  $\pm$  SEM of 6 independent experiments. Student t-test was employed for statistical analysis. \* $p < 0.05$ , \*\* $p < 0.01$

**Spleen.** Spleen is an immune organ, which also contains plenty of different kinds of immune cells as well as specific subtypes of resident macrophages. In the spleen, there existed three different populations of resident macrophages or monocyte-derived macrophages, namely  $\text{F4/80}^{\text{hi}}$ ,  $\text{CD11b}^+\text{F4/80}^+$  and  $\text{CD11b}^{\text{int}}$  respectively. We measured the expressions of CD64, MHC II and CD206 in each type of macrophages to distinguish the sub-phenotypes (**Figure 36A**). Data showed that the percentage of T cells ( $\text{CD3}^+$ ) and B cells ( $\text{CD19}^+$ ) was not

## RESULTS

different between WT and KO mice (not showed). Similar to blood, GR1<sup>+</sup> population increased significantly in KO mice. However, from the GR1<sup>+</sup> population, macrophage percentages of all three populations showed no obvious difference between KO and WT mice (**Figure 36B**). Among the three different populations of macrophages, especially F4/80<sup>+</sup>CD11b<sup>+</sup> and CD11b<sup>int</sup>, CD206<sup>+</sup> population was not different between WT and KO mice, but the expression of MHC II<sup>+</sup> significantly increased in these two populations of macrophage (**Figure 36C**).



## RESULTS

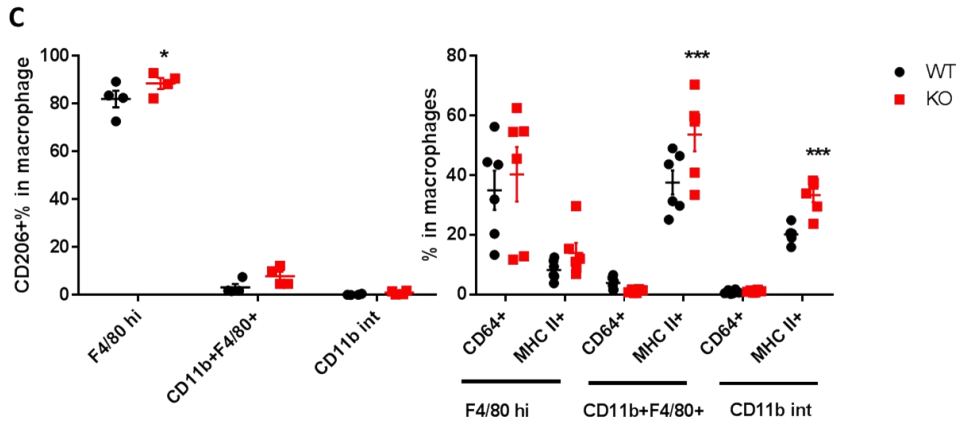


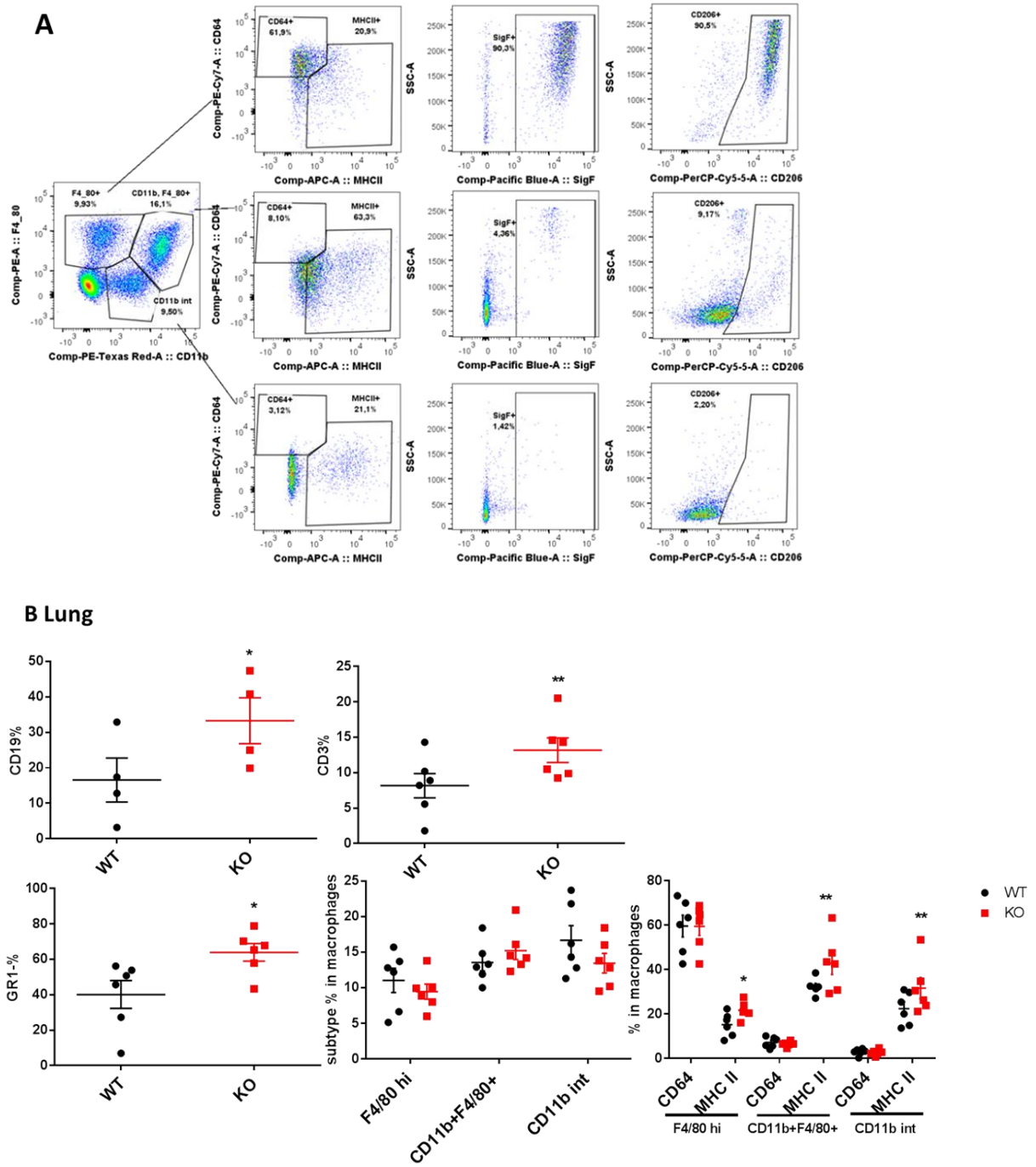
**Figure 36. FC data from spleen samples from WT and KO mice. A) General gating strategy of spleen. B) Percentage of specific subtypes of macrophages in the spleen. CD11b and F4/80 gating were based on CD45<sup>+</sup>GR1<sup>-</sup> populations. MHC II and CD64 gating were from different parts of F4/80 and CD11b gating as mentioned in data as well as CD206 gating. C) Percentages of different immune cell population and subtypes of macrophages in the spleen of Irf7 KO and WT mice. Values are presented as mean  $\pm$  SEM of 6 independent experiments. One-way ANOVA test and student t-test were employed for statistical analysis. \* $p < 0.05$ , \*\* $p < 0.01$ , \*\*\* $p < 0.005$**

**Lung and liver.** We also compared lung and liver immune cell populations of KO and WT mice. These two organs also have specific resident macrophages, namely Kupffer cells in the liver, and large and small alveolar macrophages (also known as alveolar macrophages and interstitial macrophages) in the lung<sup>37, 42</sup>. Similarly, in the lung and liver, macrophages there also had three different subtypes, namely F4/80<sup>hi</sup>, CD11b<sup>+</sup>F4/80<sup>+</sup> and CD11b<sup>int</sup> respectively (**Figure 37A, lung as example**). In the lung, a specific marker, SiglecF, can be used to distinguish different subtypes. Data showed that similar patterns of immune cell profiles (T cells (CD3<sup>+</sup>), B cells (CD19<sup>+</sup>) and monocyte (GR1<sup>+</sup>) are present as in the blood. Macrophage proportions (three populations) showed no difference between KO and WT mice, also the expressions of CD206 and SiglecF in the three populations of macrophages were not different. However, consistent with the blood and spleen, the expression of MHC II in all the three subtypes of macrophages was enhanced in KO mice (**Figure 37B**).

When we compared the immune cells in the liver between KO and WT mice, we found that there are no differences among all populations of immune cells analyzed (**Figure 37C**).



# RESULTS



## RESULTS

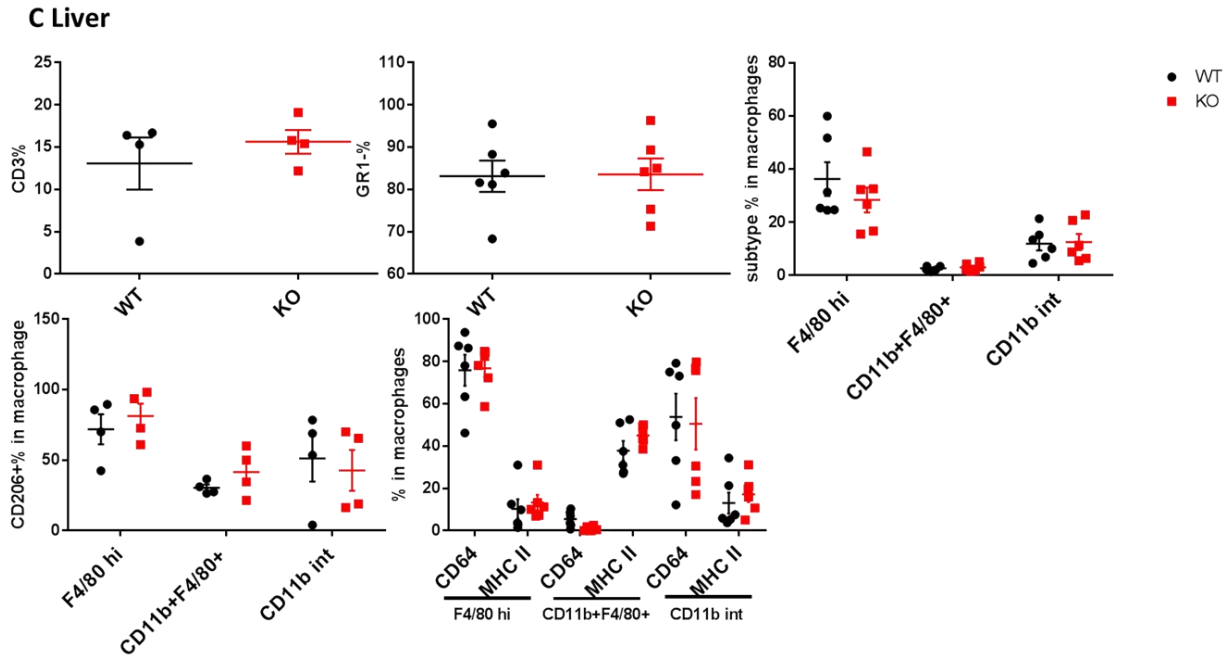


**Figure 37.** Flow cytometry data from lung and liver samples of WT and KO mice. **A)** Resident macrophages in the lung were identified using F4/80 and CD11b. In different sub-populations of macrophages, we measured expression of CD206 and SiglecF. **B) and C)** Presence of different immune populations and subtypes of macrophages in lung (**B**) and liver (**C**) between *Irf7* KO and WT mice. Values are presented as mean  $\pm$  SEM of 4-6 independent experiments. One-way ANOVA test and T-test were employed for statistical analysis. \* $p < 0.05$ , \*\* $p < 0.01$

**Male reproductive organs: seminal vesicle, prostate and vas deference.** Apart from the testis and epididymis, we compared all other male reproductive organs in *Irf7* KO and WT mice. Similar gating strategy was used as was applied in the lung.

Prostate showed no differences in CD3, CD19 and GR1 expression between KO and WT mice. In GR1<sup>+</sup> populations, expression of F4/80 and CD11b was not different, and the expression of CD64 and MHC II in three populations of macrophage also showed no difference as well between WT and *Irf7* KO mice. Interestingly, we found a significant decrease of CD206 in CD11b<sup>+</sup>F4/80<sup>+</sup> macrophage in the prostate of KO mice, which indicated that M2-like macrophages decreased in the prostate of *Irf7* KO mice (**Figure 38A**).

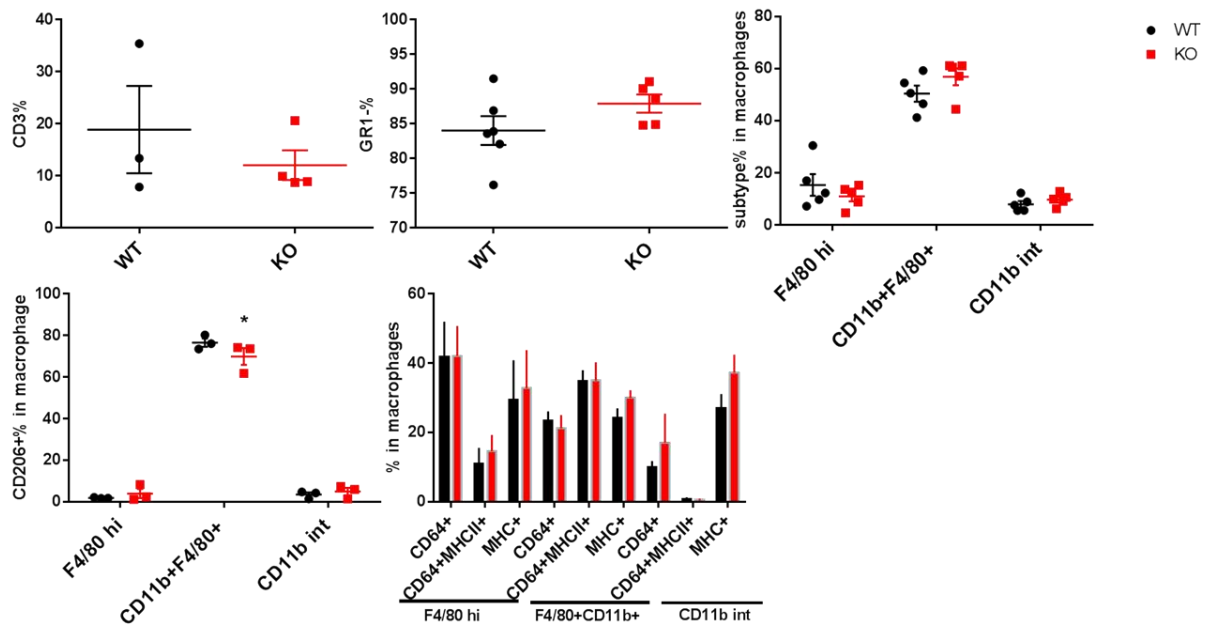
Immune cells including T cells, B cells, monocyte, macrophage, and the expressions of CD64 and MHC II in the seminal vesicle were not affected by the deficiency of *Irf7* (**Figure 38B**).

Immune cells in the vas deference were found to be slightly affected by *Irf7* deficiency where the percentage of GR1 negative increased, but different populations of resident macrophages were not affected (**Figure 38C**).

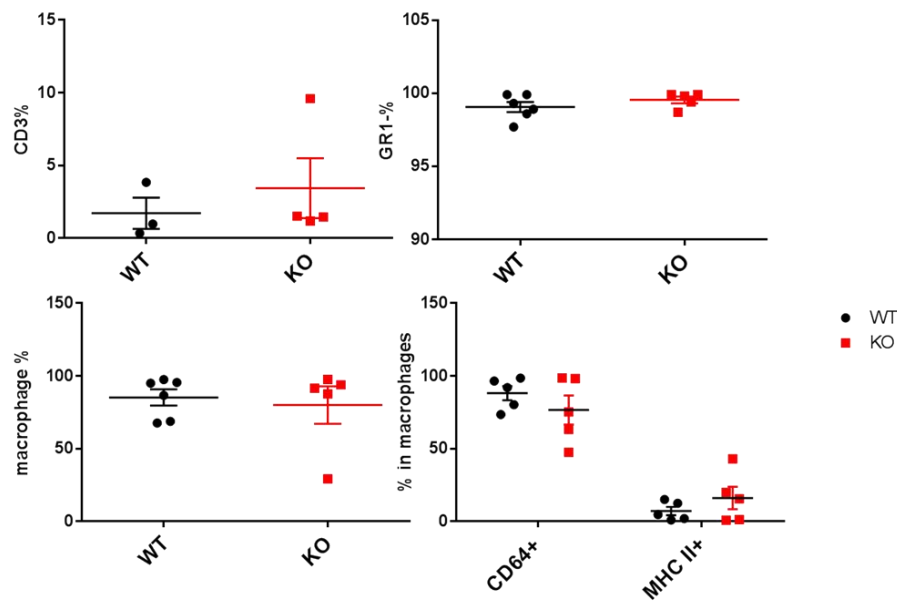


# RESULTS

## A Prostate



## B Seminal vesicle



## RESULTS

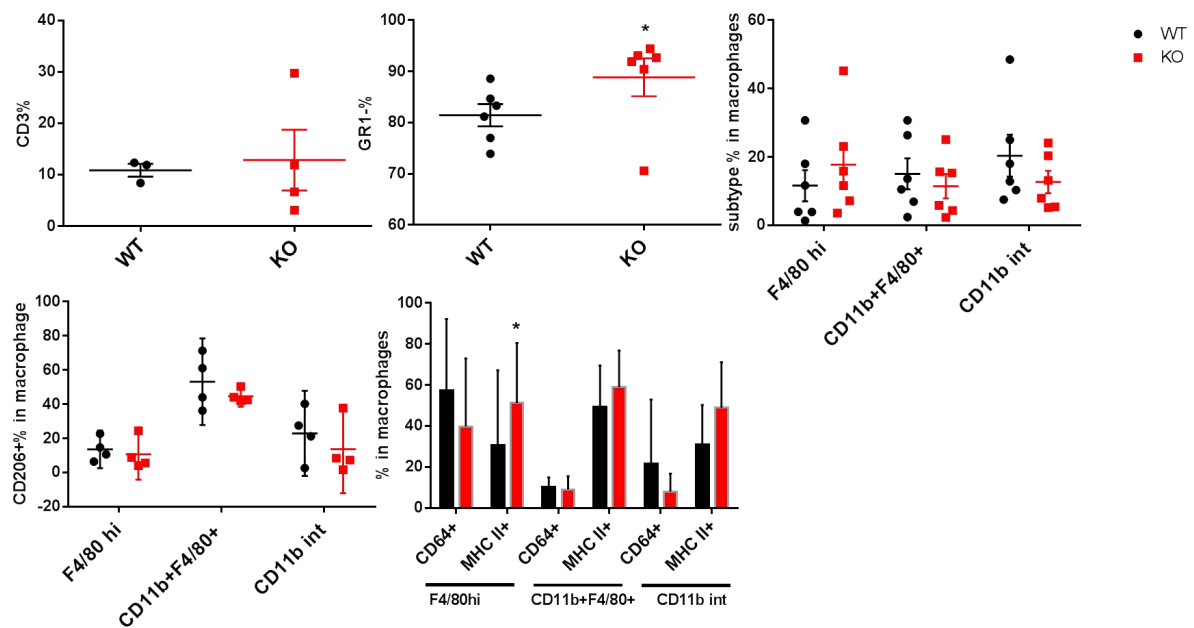


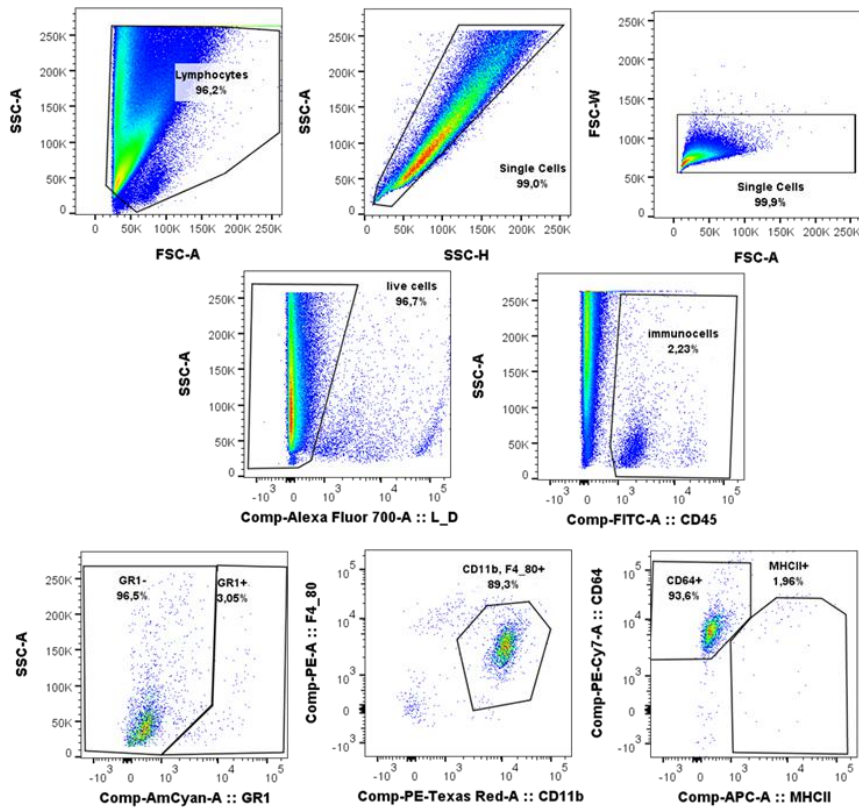
**Figure 38. Immune cell of male reproductive organs.** Three male reproductive organs, prostate, seminal vesicle and vas deferens, were compared in Ir7 KO and WT mice. Percentages of different immune cell populations and subtypes of macrophages were measured. **A)** Different immune cells in prostate between KO and WT mice. **B)** Different immune cells in seminal vesicle between KO and WT mice. **C)** Different immune cells in vas deferens between KO and WT mice. Values are presented as mean  $\pm$  SEM of 4-6 independent experiments. One-way ANOVA test and student t-test were employed for statistical analysis. \*p<0.05

***Brain, epididymis and testis.*** Microglia in the brain is one of the classical resident macrophage phenotypes, which has been shown to be mainly induced and maintained by local factors via specific TFs<sup>67</sup>. Additionally, from the RNA-seq data, we knew that *Irf7* was comparatively lower expressed in the brain. Here we compared the populations of immune cells in these three organs.

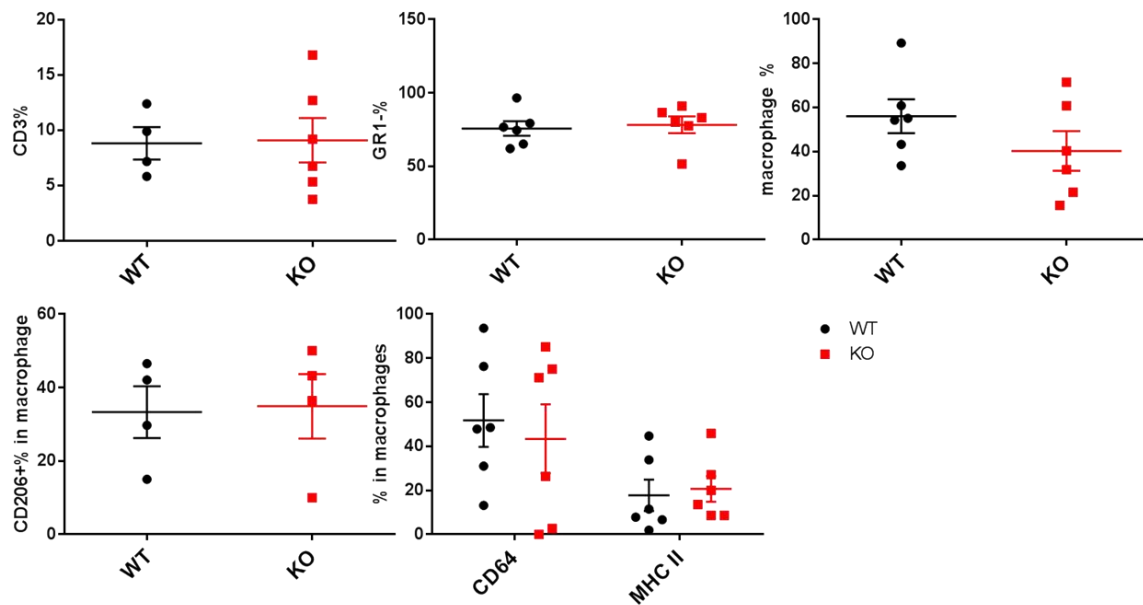
Testis and brain immune cell populations were examined in live CD45<sup>+</sup> cells. The FC data showed no change in the percentage of immune cells in the brain of Irf7 KO and WT mice (**Figure 39 A-B**). Using the same gating strategy applied in the brain, we analyzed the immune cells in the testis. We found that T cells (CD3<sup>+</sup>) increased significantly and macrophages (CD11b<sup>+</sup>F4/80<sup>+</sup>) significantly decreased in KO mice. Expression of CD206 was not different in macrophages, but the expression of CD64 and MHC II showed consistent changes observed in other organs, namely enhanced MHC II<sup>+</sup> but lower CD64<sup>+</sup> expression (**Figure 39C**). Although we observed a high expression of Irf7 in epididymal macrophages (**Figure 6A**), data revealed no change in the percentage of T cells, B cells and macrophages, as well as sub-populations of macrophages in KO mice compared to WT mice (**Figure 39D**).

# RESULTS

## A Brain

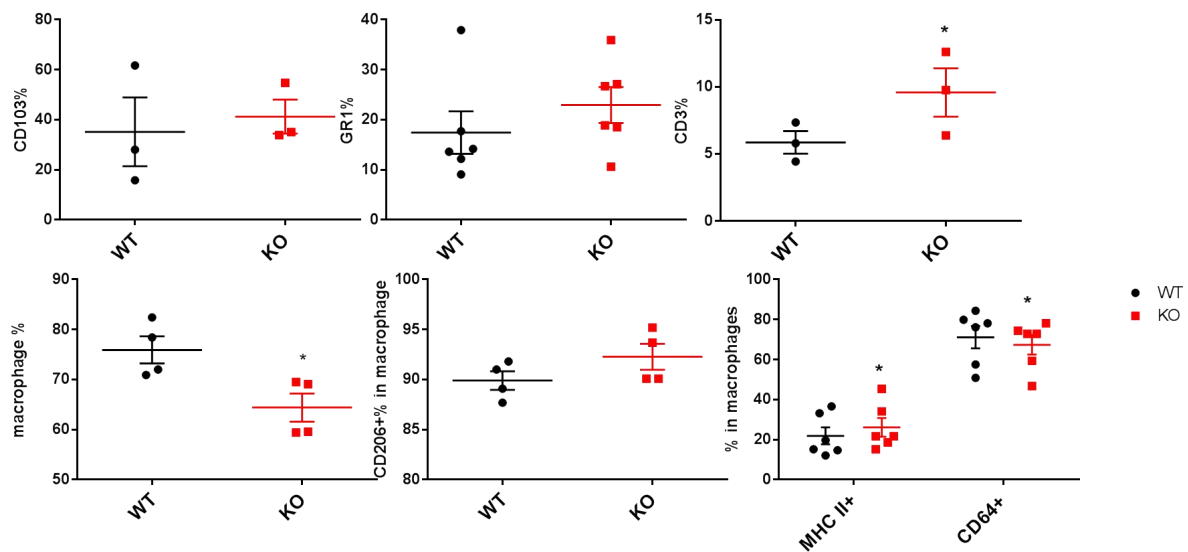


## B Brain



## RESULTS

### C Testis



### D Epididymis

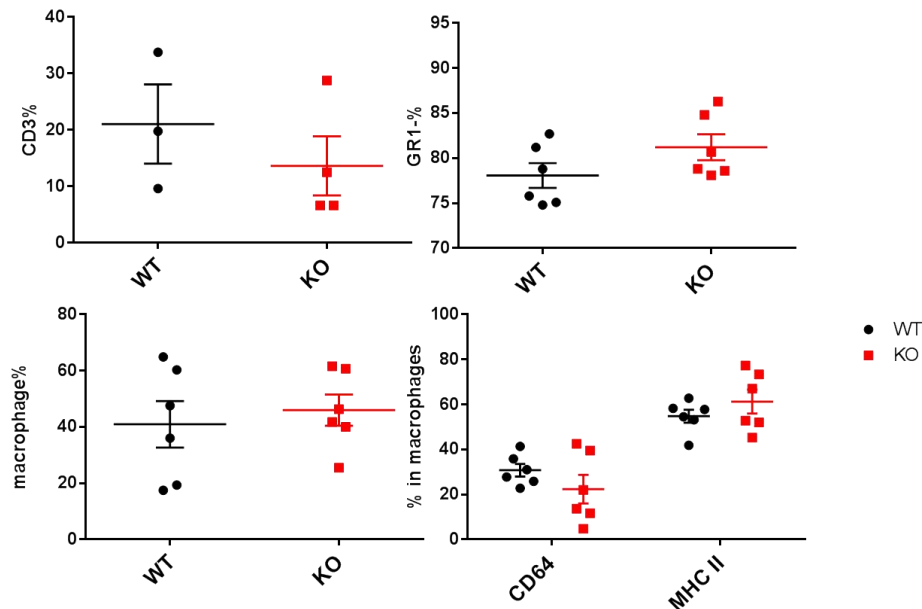


**Figure 39. Immune cell populations of brain, epididymis and testis.** A) Gating strategy for immune cells in the brain. After gating the single cells, live cell and immune cells (CD45<sup>+</sup>), GR1<sup>+</sup> cells were chosen and further gated using F4/80<sup>+</sup>CD11b<sup>+</sup> to identify microglia. following that, CD64 and MHC II markers were used to distinguish subtypes of microglia. **B-D)** Percentages of different immune cell populations and subtypes of macrophages were measured in the brain (**B**), testis (**C**) and epididymis (**D**). Values are presented as mean  $\pm$  SEM of 4-6 independent experiments. One-way ANOVA test and student t-test were employed for statistical analysis. \* $p < 0.05$

As a summary, we analyzed different immune cell populations in ten organs and tissues in *Irf7* KO and WT mice. To our knowledge, this was the first study that addressed all male reproductive organs to study the functions of *Irf7*. Results showed that in most organs, T cells

## RESULTS

and B cells increased significantly in KO mice. Only in the testis, the percentage of macrophages decreased. Of note, all resident macrophage, including TM, MHC II expression was enhanced in the Irf7 KO mice which would provide better antigen presentation responses needed to initiate inflammatory response. All data indicated that Irf7 is a critical TF to suppress MHC II expression, and especially in the testis, Irf7 was important to preserve TM to suppress MHC II expression, and especially in the testis, Irf7 also was important to TM population and ratio of subtypes.

### **3.7.5 Irf7 modulates the inflammatory response of BMDM**

Our FC data showed that the proportion of MHC<sup>+</sup> macrophages significantly increased in Irf7 KO mice. To further corroborate our results and examine the immunosuppressive role of IRF7, bone marrow cells isolated from Irf7 and WT mice were allowed to differentiate into macrophages by culturing in presence of M-CSF and GM-CSF.

#### **3.7.5.1 Inflammatory cytokines are differentially regulated by Irf7 in M-CSF and GM-CSF derived macrophages**

ELISA results showed that the production of IL-10 was significantly lower at all investigated time points in M-CSF derived BMDM from Irf7 KO mice. In contrast, IL-10 production was significantly increased at 24h in GM-CSF derived macrophages of Irf7 KO mice. Production of TNF- $\alpha$  was the same in M-CSF and GM-CSF derived BMDM from KO and WT mice (**Figure 40**).

Combined with previous results, we can conclude that M-CSF but not GM-CSF can induce the expression of Irf7. M-CSF derived BMDM expressed a higher amount of IL-10, which could be suppressed by the deficiency of Irf7. From this, we could summarize that M-CSF might play an anti-inflammatory role via Irf7. All data from WT and KO mice indicated that Irf7 had no or slight effect on TNF- $\alpha$ , and M-CSF could regulate TNF- $\alpha$  via other pathways.

## RESULTS

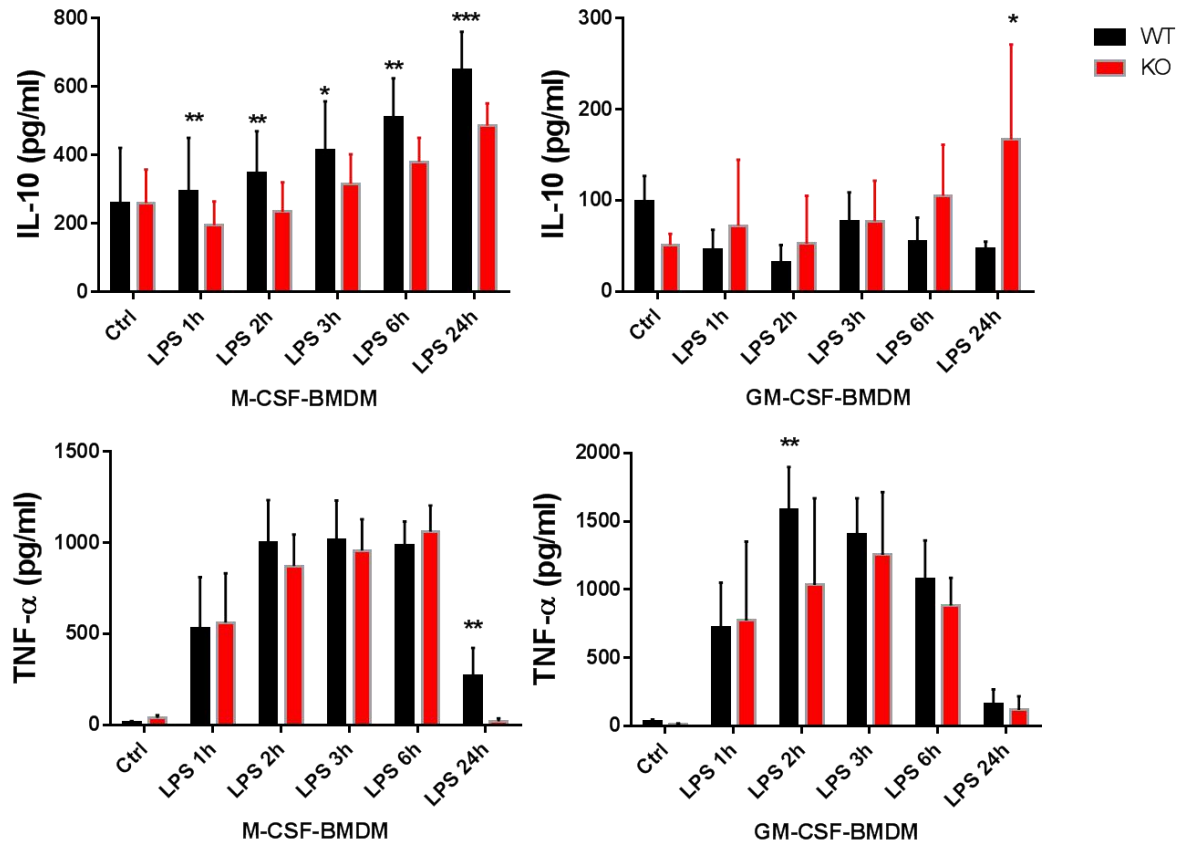


**Figure 40. Inflammatory cytokines in BMDM from WT and KO mice.** Bone marrow cells were stimulated by 25ng/mL M-CSF or GM-CSF for 7 days, followed by LPS (10ng/mL) treatment for 1 to 24 hours. Supernatants were collected and production of TNF-α and IL-10 was measured by ELISA kit. Values are presented as mean ± SEM of 6 independent experiments. One-way ANOVA test was employed for statistical analysis. \*p<0.05, \*\*p<0.01, \*\*\*p<0.005

### 3.7.5.2 Differential expression of pro-/anti-inflammatory genes in WT and Irf7 KO BMDM

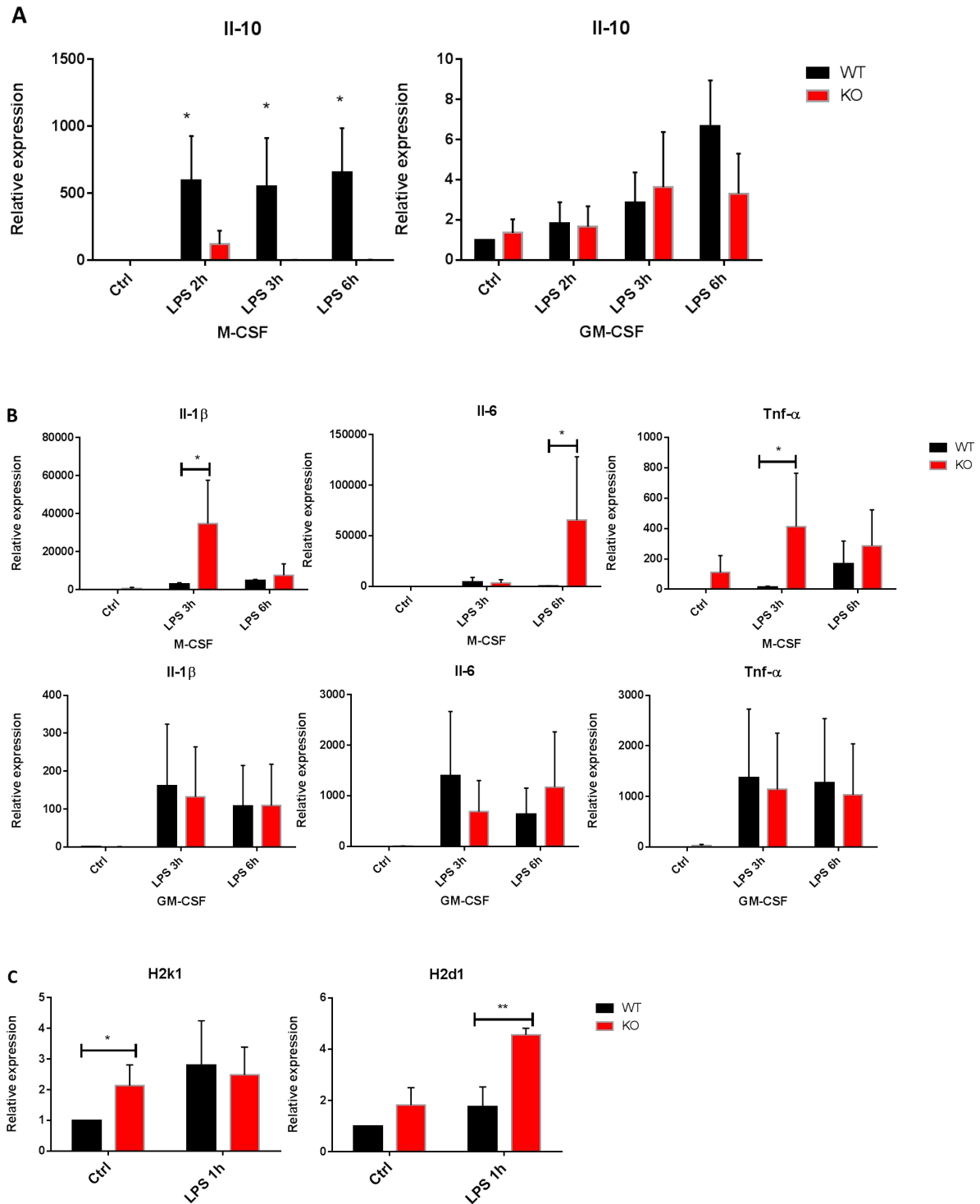
Among all anti-inflammatory genes or M2-like related genes, IL-10 showed a dramatic difference between KO and WT mice. Figure 41A shows that in Irf7 KO mice, both basal and LPS-induced expressions of IL-10 were almost abolished compared with WT mice. However, these changes only happened in M-CSF derived macrophages.

After that, we analyzed the expression of pro-inflammatory genes. We found almost all genes were enhanced in Irf7 KO mice, but this only happened in M-CSF derived macrophages. GM-CSF derived macrophages showed no obvious difference compared to WT. IN certain instances even opposite immune response regulations were reported compared to WT mice (Figure 41B).

Our data from FC showed that in Irf7 KO mice, resident macrophages expressed higher levels of MHC II. Thus, we used the BMDM model to measure the expression of two chains of

## RESULTS

MHC II, namely H2K1 and H2D1. Results showed that in GM-CSF derived macrophages there was no difference in the expression of the chains between KO and WT mice (data not shown). However, in M-CSF derived macrophages, both genes were enhanced at either basal level or LPS-induced level in *Irf7* KO BMDM, which were consistent with the FC results, indicating that *Irf7* was critical to suppress the function of MHC II (**Figure 41C**).



## RESULTS

**Figure 41. Expression of immune related genes in BMDM from WT and KO mice.** Bone marrow cells were stimulated by 25ng/mL M-CSF or GM-CSF for 7 days followed by LPS (10ng/mL) treatment for 1 to 6 hours. Total mRNA was collected for cDNA synthesis and expression of pro- and anti-inflammatory genes were measured by qRT-PCR. **A)** The relative expression of *Il-10* in BMDM model between KO and WT mice with M-CSF or GM-CSF. **B)** The relative expression of pro-inflammatory genes in BMDM model between KO and WT mice with M-CSF or GM-CSF. **C)** The relative expression of sub-chains of MHC in BMDM model between KO and WT mice. Values are presented as mean  $\pm$  SEM of 3 independent experiments. One-way ANOVA test and student t-test were employed for statistical analysis. \* $p < 0.05$ ; \*\* $p < 0.01$

### 3.7.5.3 *Irf7* influences the activation of CH25H and IFN- $\beta$

25HC is controlled by its synthetic enzyme CH25H, which is an IFN-stimulated gene. 25HC showed dual functions in inflammation that are controlled by local environments. IRF7 is the master TF in IFNs expression. Thus, we further studied the changes of 25HC and IFN- $\beta$  in *Irf7* KO mice.

Firstly, only in M-CSF derived BMDM, we found that IFN- $\beta$  expression was almost abolished in *Irf7* KO mice. Ch25h was dramatically repressed in *Irf7* KO mice in M-CSF derived BMDM (**Figure 42A**). Even though the decrease also happened in GM-CSF derived BMDM, the expression levels were thoroughly low in both KO and WT mice (data not shown), which was also shown in our previous results.

Interestingly, we measured the production of 25HC by ELISA and found that even the expression levels of Ch25h was almost abolished in *Irf7* KO mice. At basal levels, the levels of 25HC were higher in KO BMDM compared to WT (**Figure 42B**). This result indicated again that 25HC was not only governed by CH25H, but also a feedback control exists via *Irf7*.



## RESULTS

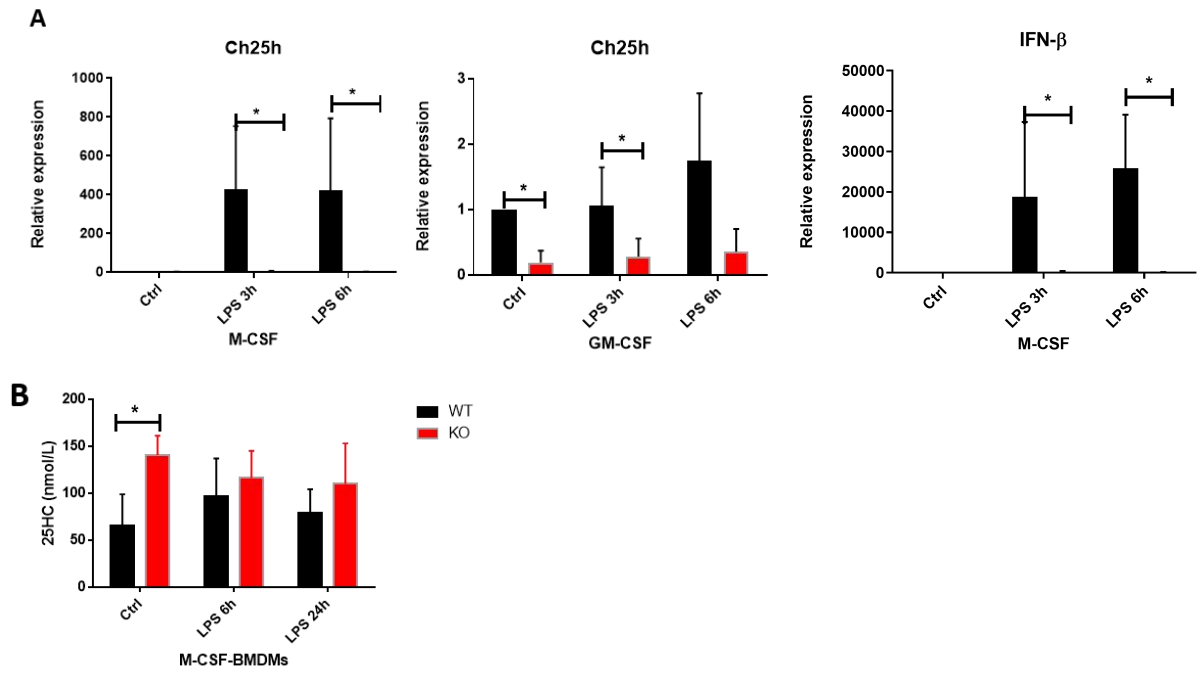


**Figure 42. *Irf7* directly influenced 25HC and IFN- $\beta$ .** Bone marrow cells were stimulated by 25ng/mL M-CSF or GM-CSF for 7 days followed by LPS (10ng/mL) treatment for 1 to 6 hours. **A)** Total mRNA was collected for cDNA synthesis and expression of *Ch25h* and *Ifn- $\beta$*  were measured by qRT-PCR. **B)** Supernatants were collected to assay the concentration of 25HC by ELISA assay. Values are presented as mean  $\pm$  SEM of 3 independent experiments. One-way ANOVA test was employed for statistical analysis. \* $p < 0.05$

## DISCUSSION

### 4. DISCUSSION

#### 4.1 Testicular macrophages show specific immune characteristics

The typical immune privilege of the testis was initially described more than 200 years ago by John Hunter and re-confirmed by Head and his colleagues much later<sup>20-21</sup>. Numerous studies pointed to a role of TM in establishing an immune privileged environment which is indispensable for spermatogenesis<sup>7-11</sup>. More recent studies were devoted to investigate the underlying mechanisms of testicular immune privilege, which pointed to multiple promising mechanisms, that include the integrity of the blood-testis-barrier, immunosuppression by local microenvironmental factors as well as the development of a systemic immune tolerance to neo-antigens on developing germ cells<sup>23-25</sup>. In agreement with other studies of resident macrophages like the microglia in the brain<sup>29-32</sup>, evidence indicated that local factors may be responsible for the phenotype of resident macrophages<sup>13,28</sup>. In 2002, Bryniarski et al. took advantage of the macrophage esterase activity, FcR<sup>+</sup> characteristic and the different densities of cells in the testis in order to isolate TM which expressed low levels of TNF- $\alpha$  and high levels of IL-10<sup>56</sup>. However, many recent studies have shown that the isolation of resident macrophages using enzymic digestion for obtain the single cell suspension may result in irreversible changes to the macrophages, especially in studies measuring inflammatory responses<sup>56-58</sup>. In this study, we utilized two different methods to isolate TM from mice for different aims. To directly compare the profiles of resident macrophage with microglia, TM and microglia were sorted using F4/80 and CD11b antibodies by FACS, and the purity was about 95% (Figure 6). In order to preserve the naive inflammatory profile of TM, we modified an isolation method using gradient centrifugation of percoll combined with positive selection with F4/80 conjugated microbeads. The purity of isolated TM was above 90% (Figure 2). As a comparison, microglia can be successfully harvested by percoll gradient centrifugation and this method has been proven not to alter the immune response of macrophages<sup>57</sup>. This new method to isolate TM from mouse avoids the activation of macrophages by enzyme during the tissue digestion procedure. However, the new method results in low yield of cell numbers as a consequence of the small size of mouse testis, the relative small population of TM and the losses in each step of the purification procedure. Thus the isolation method still needs further improvement.

TM are the major immune cell population in the testis, and are currently divided into two subtypes based on their locations and markers<sup>48-51</sup>. Mossadegh-Keller et al. further

## DISCUSSION

characterized these two populations of TM by immunofluorescence (IF) and FC, indicating that interstitial TM are M-CSFR<sup>+</sup>CD64<sup>hi</sup>MHCII<sup>-</sup> and peritubular TM are M-CSFR<sup>lo</sup>CD64<sup>lo</sup>MHCII<sup>+</sup><sup>48</sup>. Although some novel markers for phenotypical clarification of TM were described recently, such as Lyvel as an interstitial macrophage marker<sup>53</sup>, different expression levels of MHC II and CD64 serve well to differentiate the two populations of TM<sup>48</sup>. More recently, Pia Rantakari et al. Further showed that the two populations of TM are both mainly derived from embryonic precursors with distinctive expressions of CD64, CD11b and F4/80 and so on<sup>157</sup>. In this study, we further confirmed that TM exclusively expressed M-CSFR (Figure 3) and are IL-34-independent<sup>160</sup>. Furthermore, according to the different origins of TM, expression of MHC II and CD64 were also evident in the TM examined from *Irf7* KO mice in this study (Figure 39).

Wang et al. compared TM with PM from rats, and found that the NF-κB signaling pathway was obviously blocked in TM resulting in an immunosuppressive profile<sup>13</sup>. In this study, by comparing with PM from mouse, TM were found to express significantly higher levels of the immune tolerance genes *Ccr7* and *Cxcl10*, and can induce 10 times higher expression of *Ifn-β* than PM upon LPS stimulation (Figure 5). Furthermore, our preliminary RNA-seq data from TM and microglia showed that these two types of immunosuppressive resident macrophages express distinctly different TFs, of which *Irf7*, *Rora* and *Nr4a2* are shown to relate the inflammatory response<sup>134-136</sup>(Figure 6). In agreement with our RNA-seq data, TM isolated by FACS also displayed significant higher level of *Irf7* than microglia (Figure 6). However, *Rora* and *Nr4a2* were undetectable in the BMDM model with or without specific treatment of 25HC, although they are shown to regulate inflammatory response of macrophages in some other studies<sup>146-147</sup>. In the early 2000s, RORA was found to play critical roles in normal circadian rhythms, and shows important functions in regulating the function of Th17 cells<sup>148</sup>. Whether high levels of RORA and NR4A2 in the TM detected by RNA-Seq can regulate the functions of macrophages in different conditions needs further study.

### 4.2 25HC displays dual functions in inflammation

25HC exerts a stronger negative feedback of cholesterol metabolism other than cholesterol itself<sup>90</sup>. Under physiological conditions, the CH25H enzyme and its product 25HC are at low or undetectable levels, but both can be rapidly induced in the heart, brain, muscle, kidney, lung, and most notably, liver upon *in vivo* exposure to a TLR4 agonist<sup>88-91</sup>. Many studies also have shown that macrophages and DCs are prominent sources of 25HC production<sup>92-93</sup>. 25HC, as a derivate of cholesterol, was demonstrated in many studies to display important anti-viral

## DISCUSSION

functions, and in some other papers was shown to repress bacterial-induced inflammatory responses<sup>95-98</sup>. However, when studying foam cell formation in atherosclerosis, 25HC exhibited a multiple function on macrophages, for instance, by acting as an amplifier of inflammation via AP-1 and on the other hand repressing phagocytosis<sup>103-104</sup>. The importance of 25HC in inflammatory regulation is stressed by its intimate relationship with IFNs<sup>95, 102</sup>. In 2010, Park and Scott reported that CH25H expression is TLR- and IFN-dependent<sup>96</sup>. Numerous studies have then shown that IFNAR-JAK-STAT signaling is the principle pathway through which ISG are induced in antiviral responses<sup>96-98</sup>. Bauman and colleagues pointed out that 25HC produced by macrophages in response to TLR activation displays a negative regulation on B cells, suppression of the production of immunoglobulin A, a mechanism for local and systemic negative regulation of the adaptive immune response by the innate immune system<sup>100</sup>.

25HC is mainly produced by macrophages and is regarded important in the testis in assisting sex hormone production by LC<sup>110</sup>. In this study, the concentration of 25HC in the testis was measured with or without LPS stimulation. Results showed that, in the testis, the concentration of 25HC is as high as 260nM (Figure 8), which is much higher than serum concentrations of 65nM as shown in the result part<sup>99</sup>. After LPS stimulation, the concentration of 25HC decreased substantially to around 140nM (Figure 8), in contrast to what other studies showed in different settings<sup>88-93</sup>. High concentrations of 25HC in the testis and the reducing levels following inflammatory stimulation lead us to further investigate 25HC function in the BMDM model.

Studies using the Vero cells, the 174x CEM cell line and other cell types have shown that 10-100μM of 25HC are not cytotoxic<sup>93, 149</sup>. However, in the BMDM model of our study, 25HC shows significant cytotoxicity to cells which is time- and concentration-dependent (Figure 9). One μM of 25HC for a short time (24h) shows no cytotoxicity to BMDM, but displays significant cytotoxicity to BMDM for a longer period or at higher concentrations (Figure 9). To imitate the physiological condition of a chronic exposure of 25HC, lower concentrations of 25HC (100nM, 250nM and 500nM) were added to BMDM for prolonged periods (3 days and 7 days) to measure the cytotoxicity. Results show that 100nM of 25HC displays no cytotoxicity to BMDM for 7 days incubation, while other higher concentrations of 25HC show more obvious cytotoxicity to BMDM (Figure 9). Comparing our data with previous studies, we can conclude that 25HC shows different effects on cell viabilities and even functions to different types of cells or with different concentrations. Additionally, it should be

## DISCUSSION

also noted that studies with opposite results were conducted using different concentrations of 25HC, from 10nM to 100 $\mu$ M<sup>100, 108</sup>. Previous investigations found that under normal conditions, levels of CH25H and its product 25HC are low or undetectable, but can be rapidly induced to a TLR4 agonist<sup>88-91</sup>. However, in this study, we found that high concentrations of 25HC (500nM-1000nM) were extremely cytotoxic to BMDM. But the level of 25HC in the testis is rather high at a concentration around 250nM. All these results indicate that 25HC is produced at high levels in some specific organs and can display divergent roles at different concentrations. Whether the low level of 25HC in peripheral blood system and high level of 25HC in organs are balanced by some exchange mechanisms is unclear as is whether different levels of 25HC are the key factor for the macrophage differentiation from peripheral blood system to resident macrophages.

Our data show that 25HC can significantly repress the expression of pro-inflammatory genes (*Il-1 $\beta$* , *Il-6*, *Tnf- $\alpha$*  and *iNos*), while enhancing the expression of anti-inflammatory genes (*Klf4*, *Il-10*, Figure 11) in M-CSF-derived macrophages, but not in GM-CSF-derived macrophages. The changes exerted by 25HC on inflammatory genes and the cytotoxicity to BMDM can be reversed by using an inhibitor of 25HC, namely LY295427 (Figure 12 and 15). However, further data show that 25HC does not affect the production of TNF- $\alpha$  after LPS treatment, while significantly enhancing the production of IL-10 at both basal and LPS-induced levels (Figure 10), which is in contrast to previous results<sup>97-98</sup>. Interestingly, these changes of inflammatory proteins only happen in M-CSF-derived macrophages, but not in GM-CSF-derived macrophages, which are similar with gene regulations by different CSF. For example, one study, which focused on the formation of foam cells in atherosclerosis, found that 25HC acted as an amplifier for inflammation via AP-1<sup>103</sup>. Furthermore, BMDM cultured with 25HC for 7 days with or without the inhibitor LY295427 shows no difference in the expression of sub-phenotype markers, eg. CX3CR1, MHC II, CD64, MERTK and CD206 (Figure 14). All these data indicate that 25HC does not directly alter the phenotype of macrophages, but can show anti-inflammatory functions on macrophages stimulated by M-CSF.

Next, the inflammatory responses were further compared between GM-CSF and M-CSF derived macrophages. Interestingly, the challenge with 25HC in GM-CSF derived macrophages showed a dramatic difference to that of M-CSF stimulated cells. The addition of 25HC to GM-CSF derived macrophages did not alter the expressions of pro- and anti-inflammatory genes. However, the production of TNF- $\alpha$  in GM-CSF derived macrophages was significantly decreased by 25HC, while IL-10 production was not affected (Figure 23), an

## DISCUSSION

obvious opposite result in M-CSF derived macrophages. These distinct results exerted by 25HC were not reported in previous studies. As one reason, these studies used only one macrophage stimulation factor in their *in vitro* models when they investigated the function of macrophages, and the use of different CSFs might be the reason why opposite results sometimes were documented among different studies<sup>97-98, 103-104</sup>.

Furthermore, we also compared the regulation of pro- and anti-inflammatory gene expressions by 25HC using GM-CSF or M-CSF stimulated BMDM. *Atf3*, *Il-10* and *Klf4*, which are important M2 markers display higher levels of expression by 25HC in M-CSF conditions, and show no change when stimulated by GM-CSF (Figure 24). On the other hand, some classic pro-inflammatory genes, eg. *Caspase1*, *iNos*, *Tnf-α* and *Clec7a* are repressed by 25HC when pretreated with M-CSF, but not affected when GM-CSF is used (Figure 25). In line with the respective protein regulation, changes of the anti- and pro-inflammatory genes both indicate that the obvious anti-inflammatory functions on macrophages exerted by 25HC are M-CSF-dependent. However, among the anti-inflammatory genes *Chil3* shows interesting changes by 25HC. High expression of *Chil3* has been linked to diseases like inflammatory bowel disease, autoimmune neuro-inflammation, rheumatoid arthritis and asthma<sup>138, 140-141</sup>. Clinic evidence also showed that patients with autoimmune diseases have abnormal cholesterol regulation, especially in hepatic steatosis patients, which highlights the relationship between cholesterol regulation and *Chil3*<sup>142</sup>. In this regarding, Starossom and colleagues found that silencing *Chil3/Chi3l3* can aggravate the severity of experimental autoimmune encephalomyelitis<sup>141</sup>. *Chil3* was shown to display critical functions in tissue repair, immunosuppression and anti-inflammation<sup>138-141</sup>. Both in M-CSF and GM-CSF derived macrophages, 25HC can almost abolished the expression of *Chil3* (Figure 24), which is shown as a key factor in forming the M2 phenotype<sup>138-139</sup>. The strong inhibition occurs in presence of both studied CSFs and the inflammatory challenge. In this study, 25HC at both high and low levels abolished the expression of *Chil3* at basal and LPS-induced conditions (Figure 24). Osborne et al. found that virus-helminth co-infection in the intestine can undermine antiviral immunity and is related with the alternative activation of macrophages<sup>144</sup>. During an impaired antiviral response, *Chil3* is considered critical to restore the antiviral activity<sup>143-144</sup>. However, in our study, 25HC, as the key compound in macrophages for antiviral immunity, strongly repressed the expression of *Chil3g*. This unexpected results indicate that the anti-viral function of 25HC is conducted by macrophages via different pathways in different settings involving *Chil3*. The exact regulatory mechanism of *Chil3* is still unknown and the connection between 25HC and *Chil3* needs further investigation.

## DISCUSSION

According to the findings in this study, we can clearly see that 25HC exerts obvious anti-inflammatory functions in the presence of M-CSF, but not in GM-CSF derived macrophages, which indicates that 25HC can differently regulate inflammatory responses which are controlled by different environmental factors, such as CSF. As 25HC does not induce an M2 polarization of macrophages individually, then what is the mechanism by which 25HC enhances the anti-inflammatory function of macrophages and is only M-CSF-dependent? Our data point to a role of M-CSF in the mediation or upstream in the sequence cascade of 25HC. As a small part shown in the Figure 43, the immunosuppressive function of 25HC is related with M-CSF. Next, we will discuss the role of CSF and the potential TF between CSF and 25HC.

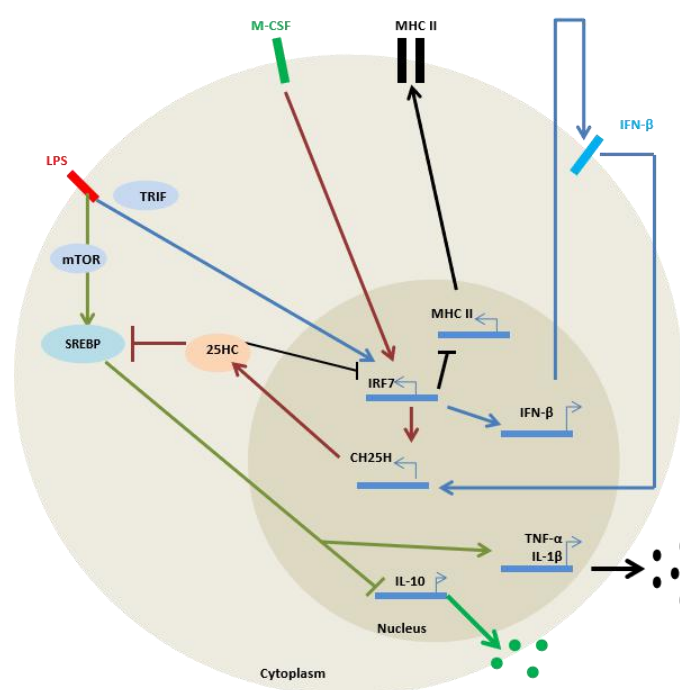


**Figure 43.** The mechanism of IRF7, M-CSF and 25HC in regulating the testicular macrophage profile.

### 4.3 M-CSF induces an immunosuppressive environment in the testis

During the last decades, studies have documented that M-CSF and GM-CSF derived macrophages exhibit different inflammatory profiles<sup>72-73</sup>. Studies have shown that M-CSF derived macrophages have a profile similar to an M2 anti-inflammatory macrophage phenotype, while GM-CSF derived macrophages show a greater tendency to induce inflammation as the M1 pro-inflammatory phenotype macrophage<sup>72-73</sup>. Of note, M-CSF-induced macrophages are flexible to adjust the phenotypes according to different environmental switch, while GM-CSF-derived macrophages are recalcitrant due to their impaired mitochondrial function<sup>49</sup>. As we have discussed above, 25HC shows distinct

## DISCUSSION

functions in different CSF conditions. So we further investigate the roles of M-CSF and GM-CSF in regulating macrophage inflammatory profiles. We first compared the different inflammatory profiles of BMDM cultured with M-CSF and GM-CSF. In accordance with previous studies, macrophages derived from M-CSF showed generally a classic M2 profile with high levels of *Il-10* and *Chil3*, while GM-CSF induced M1 macrophages with high levels of *Clec7a* and *Il-6* (Figure 17 and 18). It is interesting to note that the inflammatory production of TNF- $\alpha$  shows no difference in the presence of M-CSF or GM-CSF, while IL-10 has significant higher levels in M-CSF derived macrophages (Figure 18). Meanwhile, the production of IL-1 $\beta$  is lower in M-CSF cultured macrophages than GM-CSF cultured. However, our results demonstrated that M-CSF alone could not fully induce an M2 profile. For example, *iNos* was significantly induced in M-CSF derived macrophages, which is a typical M1 marker, while *Klf4* was enhanced under GM-CSF conditions (Figure 17). By using the CSF1R inhibitor PLX, the changes of regulated genes were reversed, indicating that M-CSF alone can directly affect some of the inflammatory response of macrophages (Figure 22).

Referring to the data from the 25HC stimulation experiments, we find that TNF- $\alpha$  and IL-10 are oppositely regulated in M-CSF and GM-CSF derived macrophages with or without addition of 25HC (Figure 10 and 23). These data indicate that the inflammatory response of macrophages is regulated by 25HC and M-CSF via a common pathway, especially the production of IL-10. Previous studies showed that the LPS/TLR4 pathway can activate TRAM/TRIF and continually trigger the activation of p38 and the NF- $\kappa$ B proteins, p65 and p105<sup>143-144</sup>. Phosphorylated p38 together with p105 that phosphorylates CREB is leading to the production of IL-10<sup>144</sup>. At the same time, phosphorylated p65 and p50, the degradation products of p105, can form a heterodimer, which modulates the transcription of IL-12, a process negatively impacted by the mechanism that produces IL-10 and positively induces the production of TNF- $\alpha$ <sup>144</sup>. In this study, results showed that the blockage of CSF1R only reduces the production of TNF- $\alpha$  but not IL-10 (Figure 21), which indicates that LPS/TLR4 activation can induce specific downstream pathways linking M-CSF/CSF1R with p65 and p50/MEK/ERK/RSK pathways, not by activating p38/CREB/IL-10 pathway. When 25HC is added, the production of TNF- $\alpha$  is not affected, but IL-10 is significantly enhanced by 25HC following M-CSF stimulation. This change indicates that M-CSF can activate the p38/CREB/IL-10 pathway to modulate the downstream roles of 25HC, which is different from the pathway activated by M-CSF alone. These results indicate that M-CSF is important factor or even acting as an upstream factor in macrophage polarization. Inspired by the fact that microglia in the brain are maintained by IL-34 and in addition to the data discussed above,



## DISCUSSION

we assume that M-CSF is also the key factor in the testis responsible for maintaining the M2 resident TM. In our *in vitro* model, we find that CSF alone can not totally induce M1 or M2 phenotype. 25HC displays different functions in the presence of M-CSF or GM-CSF. All these data indicate that M-CSF creates an immunosuppressive environment and 25HC exerts as an immunosuppressive factor in an M-CSF-dependent manner.

The differences in the regulation between M-CSF and GM-CSF derived macrophages were found to be mainly IFN-dependent<sup>74-75</sup>. Thus, we compared the expression of *Ifn-β* and related ISG, *Ch25h* in M-CSF and GM-CSF conditions with or without the additional treatment of 25HC. Our previous data of TM sorted by FACS from RNA-seq and qRT-PCR show high levels of *Irf7* (Figure 6). Data also demonstrated that M-CSF can induce high expression levels of *Ch25h*, *Ifn-β* and *Irf7* (Figure 26). However, in BMDM, GM-CSF could barely induce the expression of *Irf7* and *Ifn-β* (Figure 27). Combining previous studies<sup>74-75</sup> with our data, high levels of *Irf7* in TM and BMDM are closely related to the upper stimulation of M-CSF. Next, we investigated the relationship between 25HC and *Irf7*, and whether *Irf7* alone is responsible in the inflammatory response of TM or by activating downstream of IFN-β. Data show that 25HC differently regulates the expressions of *Irf7* in the M-CSF or GM-CSF cultured cells (Figure 26). 25HC significantly represses the expression of *Irf7* in M-CSF derived macrophages, while in GM-CSF derived macrophages the expression of *Irf7* is not affected (Figure 16 and 26). Interestingly, *Ch25h* as one gene of ISG, shows no effect in GM-CSF condition at both basal and LPS-induced levels (Figure 26). 25HC also displays a strong negative feedback on the expression of *Ch25h* in M-CSF condition, but not under GM-CSF conditions (Figure 26). Here in my study, all data point to a close connection of high levels of *Irf7* in associate with M-CSF and 25HC. 25HC, in this study, shows obvious immunosuppressive function only under M-CSF conditions. Thus a high expression of *Irf7* can be significantly induced by M-CSF but not GM-CSF. All these results gave us an indication that M-CSF could be a key upstream factor expressing for the modulation of high levels of *Irf7*, *Ifn-β*, *Ch25h* and thus producing high concentrations of 25HC in the testis. All these factors together are all required in order to create the immunosuppressive environment in the testis. However, the underlying mechanism of how M-CSF modulates the inflammatory functions of 25HC and whether *Chil3* is also involved still require further investigation. In additional, we also point out the two different pathways of the p38/CREB/IL-10 and p50/MEK/ERK/RSK in the inflammatory responses, which are modulated by M-CSF alone or together with 25HC due to the distinct regulations of TNF-α and IL-10 by both M-CSF/GM-CSF and 25HC. As showed in Figure 43, in the TM, M-CSF

## DISCUSSION

acts as an upstream factor to activate the IRF7 and IFN- $\beta$ , and then 25HC is highly activated by the stimulation of CH25H enzyme.

### 4.4 IRF7 causes a tolerant immune phenotype in macrophages

The TLR signaling pathway is mediated via four adaptor molecules: MyD88, TIRAP/MAL, TRIF/TICAM1 and TRAM<sup>120-121</sup>. Stimulation of TLR3, TLR4, TLR7, and TLR9 with the respective ligands can induce type I IFN production<sup>121</sup>. Even in MyD88<sup>-/-</sup> cells, TRIF activation can lead to IFN- $\beta$ -inducible gene expression, such as interferon regulatory factors (IRF)<sup>121</sup>. Reboldi et al. has shown that IFN- $\beta$  can regulate inflammatory responses via CH25H/25HC<sup>128</sup>. Other studies showed that pre-treatment of macrophages from mice or human with IFN can suppress the production of pro- and mature IL-1 $\beta$  and enhances the production of IL-10<sup>125</sup>. As we have discussed above, M-CSF and 25HC together display strong anti-inflammatory functions in macrophages, and this regulation is closely associated to IFN and IRF. Results also reveal that 25HC and IFN- $\beta$  are regulated in a similar manner by M-CSF (Figure 26). Firstly, the roles of IFN- $\beta$  were investigated in regulating macrophage functions. When the IFN1R inhibitor was added to IFN- $\beta$ -treated BMDM, the productions of TNF- $\alpha$  and IL-10 did not change upon LPS stimulation compared to control (Figure 30), indicating that the inflammatory response of macrophages is not directly governed by IFN- $\beta$  upon LPS stimulations. Moreover, our data showed that the addition of IFN1R inhibitor also did not affect the productions of IL-1 $\beta$  and caspase1 compared to control (Figure 30), which is also contrast to the conclusion that IFN- $\beta$  could decrease the production of pro-inflammatory cytokine IL-1 $\beta$  as mentioned previously<sup>125</sup>. IRF7/3 are shown to be indispensable in the inflammatory regulation and blockage of IFN1R may be insufficient to alter the downstream pathways<sup>125-126</sup>. In addition, type I IFN can be activated by TLR3, TLR4, TLR7, and TLR9 ligands, and the downstream pathways are either MyD88-independent or dependent<sup>121</sup>. Here in this study, we exclusively applied LPS as a TLR4 ligand to induce inflammatory responses. Even though the direct inhibition of IFN1R has no effect on the inflammatory response of BMDM, the close connection among IFN- $\beta$  with 25HC and IRF7 is worth further study. In BMDM as a different cell type, data show that IFN- $\beta$  is regulated similarly with IRF7 by these two factors, M-CSF and 25HC, and that IRF7 is closely governed by IFN- $\beta$ . Whether the function of IFN- $\beta$  is condition-dependent is unknown yet. Here in this study, results indicate that the LPS-induced inflammation is IFN- $\beta$ -independent under M-CSF and 25HC conditions.

## DISCUSSION

IRFs are transcriptional mediators, which can be induced by bacterial or viral infection<sup>129</sup>. IRF7 is essential for the differentiation of monocytes to macrophages where cells would acquire CD11b and CD11c marker expression<sup>130</sup>. IRF7 is regarded as the master regulator of type I IFN-dependent immune responses<sup>130</sup>. However, the antiviral response by IFN needs timely termination via negative regulation to minimize inflammatory damage<sup>130-131</sup>. In this regards, it was shown that, IRF7 together with FOXO3 acts as a negative regulator in IFN responses<sup>134</sup>. Our RNA-Seq data showed that the expression of *Irf7* is significantly higher in TM than microglia (Figure 6). Owens et al. have found the DC from *Irf7*<sup>-/-</sup> mice displayed enhanced inflammatory responses<sup>135</sup>. Similarly, other studies showed that IRF7 acts as an important negative regulator of IFN and displays immunosuppressive functions<sup>131-134</sup>. As discussed above, *Irf7* and *Ifn-β* are similarly regulated by M-CSF and 25HC (Figure 27), and the inhibition of IFN-β has no effect on inflammation. We then further studied the role of IRF7 in inflammatory responses. Here, M-CSF can induce the expression of *Irf7*, whereas 25HC shows an obvious repression of *Irf7* under M-CSF condition. This opposite regulation of *Irf7* indicates that *Irf7* is directly activated by M-CSF, negatively regulated by 25HC in different settings. This conclusion is also supported by the finding that *Irf7* is highly expressed in the testis with a high concentration of 25HC, and that LPS stimulation increases the expression of *Irf7* while inducing a reduction of 25HC (Figure 8). Thus, we further show that M-CSF acts as a trigger in the testis to induce a high expression of *Irf7* and a high concentration of 25HC. Next, we compared BMDM from wild type (WT) mice with *Irf7* knock out (KO) mice to further verify the roles of IRF7. Consistent with the Owens study, our results showed that BMDM from *Irf7* KO mice produced significantly lower levels of IL-10 upon LPS stimulation than those from WT mice (Figure 41). Taken these data together, our data suggest that the production of IL-10 is governed by IRF7, while IRF7 is directly activated by M-CSF. Under this condition, 25HC displays both positive and negative regulations of IRF7 according to the concentrations of 25HC. Moreover, our study indicates that the production of TNF-α is not directly affected by IRF7 and 25HC under M-CSF condition.

Cohen et al. pointed that the switch from a pro- to an anti-inflammatory (M1-to-M2) phenotype in macrophage is controlled by IRF7<sup>137</sup>. IRF7 in the brain is down-regulated by TGFβ1, and this inhibition can be reversed by IFN-β<sup>137</sup>. Similar with our RNA-Seq data, *Irf7* is expressed at low levels in the mouse brain (Figure 6). Microglia sorted by FACS demonstrated a lower expression level of *Irf7* than TM confirmed by qRT-PCR analysis (Figure 6). As was discussed above, deficiency of *Irf7* KO leads to stronger inflammatory

## DISCUSSION

response than WT, and other studies also pointed out that IRF7 is critical for governing macrophage phenotype. This leads to a further comparison of immune populations, including resident macrophages from different organs in *Irf7* KO and WT mice (Figure 32-39). In the brain, *Irf7* deficiency induces no obvious changes in immune cell, especially the macrophage phenotypes (Figure 39). These results provide further evidence that IRF7 can barely influence the immune profile of microglia in the brain. Using this KO model, we found that the deficiency of *Irf7* has no effect on the structure of testis and spermatogenesis (Figure 33). In contrast, *Irf7* KO mice have lower body and testis weights, whilst the ratio of testis/body between KO and WT mice are similar (Figure 32). This interesting change of weights points to the potential function of IRF7 in metabolism.

Interestingly, out of the ten studied organs, *Irf7* deficiency decreases the percentage of resident macrophages exclusively in the testis (Figure 39). As discussed above, *Irf7* is highly expressed in the TM (Figure 6) and the survival of macrophages is known to be CSF-dependent<sup>58-60</sup>. Our study showed that *Irf7* deficiency can lead to a reduction in TM number, a point not discussed before. The data from our study indicate a tight connection between M-CSF and high expression level of IRF7 in the testis, which might be the underlying mechanism that IRF7 creates an immunosuppressive environment via M-CSF. Meanwhile, M-CSF in the testis regulates TM survival and function through IRF7. Recently, Sieweke et al. detailed the characteristics of the two populations of TM by indicating that interstitial TM are M-CSFR<sup>+</sup>CD64<sup>hi</sup>MHCII<sup>-</sup> and peritubular TM are M-CSFR<sup>lo</sup>CD64<sup>lo</sup>MHCII<sup>+</sup> cells<sup>48</sup>. To further investigate the role of *Irf7*, the levels of MHC II and CD64 in the TM population were measured by FC. We found that the percentage of MHC II positive TM increased while CD64 high TM decreased (Figure 39). Considering the new findings about the origins of testicular resident macrophages<sup>48,157</sup>, this result suggests that *Irf7* deficiency reduces the portion of yolk sac-derived interstitial TM and increases the percentage of fetal liver-derived and bone marrow-derived peritubular TM<sup>48-51</sup>. Of note, our data also show that most of the organs have higher portion of MHC II positive in the resident macrophage population in *Irf7* KO mice compared to WT mice, although the resident macrophages between KO and WT demonstrated no obvious difference (Figure 36-39). These interesting changes indicate that most of the resident macrophages in *Irf7* KO mice have a stronger ability to present antigens to trigger inflammatory responses. This could point to the hypothesis that the high expression level of *Irf7* in the testis can blunt the immune responses of TM due to the low expression of MHC II. As indicated in the Figure 43, M-CSF in the testis could activate the high expression of IRF7, and the downstream production 25HC. IRF7 in the TM displays strong repression of MHC II.

## DISCUSSION

The testis and epididymis are two closely connected organs, and both need to protect sperms from autoimmune responses by the systemic tolerance and the immunosuppressive environment<sup>145</sup>. However, the epididymis has a distinct immune profile compared to the testis<sup>145</sup>. In this regard, our data from the RNA-Seq analysis shows that *Irf7* is also highly expressed in EM (Figure 6). Nevertheless, resident macrophages and other immune cell populations demonstrate no difference in the *Irf7* KO epididymis compared to WT (Figure 39). Three parts of epididymis, namely caput, corpus and cauda, have distinct immune profiles and immune cell populations<sup>145, 150-151</sup>. Our study investigate the whole epididymis instead of individual part and whether the high expression of IRF7 exist in different part and exert different functions is unknown.

By utilizing *Irf7*<sup>-/-</sup> mice, it was previously showed that IRF7 is the master regulator of type I interferons in TLR9/virus infection via activation of DC-MyD88-independent pathway and CD8<sup>+</sup> T cell-MyD88-dependent activation<sup>136</sup>. However, in our study, we found that *Irf7* deficiency induced a higher percentage of T cells and B cells, not a reduction (Figure 35-39). In a lymphocytic choriomeningitis virus infection study, IRF7 was found to be required for the activation of CD4<sup>+</sup> T cells, not CD8<sup>+</sup> T cells<sup>152</sup>. However, our results show that the percentage of CD3<sup>+</sup> native T cells is much higher in *Irf7* KO mice in the blood, lung and testis than in WT mice (Figure 35-39). CD3 is the critical T cell co-receptor in activating the innate immune responses of cytotoxic T cell and T helper cells<sup>153</sup>, and this regulation of CD3 is consistent with the change of MHC II expression to enhance the extent of inflammatory responses in *Irf7* KO mice. As discussed above, most organs in *Irf7* KO mice showed a consistent enhanced expression of MHC II (Figure 35-39), indicating that *Irf7* has a suppressive role on the function of antigen presentation in macrophages under normal conditions. To further confirm this role of *Irf7*, we found that BMDM from *Irf7* KO mice also express higher levels of two chains of MHC, namely *H2k1* and *H2d1* than those in WT mice (Figure 41).

CH25H is one of the important ISG in IFN-related inflammation<sup>89</sup>. By comparing the LPS-induced expression of *Ch25h* between *Irf7* KO and WT mice, we saw that IRF7 is indispensable for the activation of *Ch25h* both under M-CSF and GM-CSF stimulations (Figure 42). However, the concentration of 25HC in *Irf7* KO BMDM is much higher than WT BMDM under M-CSF stimulation (Figure 42). Considering that 25HC is the efficient negative feedback of CH25H, thus we hypothesize that the production of high levels of 25HC is activated by IRF7 and maintained its concentration by small loop of CH25H activity.

## DISCUSSION

In this study, three local environmental factors in the testis are identified to closely interact in inducing the distinct TM immunosuppressive phenotype. TM as the only cells in the testis producing M-CSF can induce high levels of IRF7 and 25HC, and all these three factors combined together create an immunosuppressive local environment for testicular macrophages. Our data also indicate that the survival of TM is affected by IRF7. 25HC shows multiple functions in inflammatory responses depend on the concentrations applied. As Figure 43 shows, in the testis, M-CSF conjugated on the receptor of TM surface can induce a high expression of IRF7 and production of 25HC. High levels of 25HC can repress the inflammatory responses by enhancing the IL-10 production and IRF7 under normal condition can repress the expression of MHC II, which together creates an immunosuppressive environment in the testis.

## SUMMARY

### 5. SUMARRY

Testicular macrophages (TM) are the most prevalent immune cell population of the testis. TM are characterized by a unique ability to balance an activation of the innate immune response against microbes with immune tolerance to neo-antigens of developing spermatozoa. TM are heterogeneous and display an immunosuppressive phenotype that is governed by the testicular microenvironment. The testis contains numerous immuno-modulatory molecules such as corticosterone, testosterone, prostaglandins, 25HC and activins, that all could putatively influence the TM phenotype by inducing a unique set of transcription factors. To date, the testis-derived signals that control the special phenotype of TM and function by inducing a specific transcription factor that enables these cells to fulfill their function in testicular immune privilege are still elusive. Therefore, we sought to identify factors that could trigger a specific transcription factor which in turn shapes the phenotype of TM. Using comparative RNA Seq whole genome expression analysis, IRF7 was identified as such candidate transcription factor for TM. Amongst the immunosuppressive molecules prevalent in testicular tissue, 25HC was tested on M-CSF- and GM-CSF-derived bone marrow macrophages for its capacity to induce a TM signature set of genes. In this regard, 25HC displays anti-inflammatory properties in M-CSF-derived macrophages in comparison to GM-CSF-derived macrophages. Of note, in contrast to GM-CSF-derived macrophages, M-CSF-derived macrophages express higher levels of IRF7 and 25HC. Because TM itself can produce M-CSF, this factor can act in an autocrine manner to trigger a cascade that via M-CSF stimulation results in the expression of IRF7. Using *Irf7*<sup>-/-</sup> mice, it was demonstrated that IRF7 is important to repress MHC II expression in macrophages in most of the organs examined. Of note, in *Irf7*<sup>-/-</sup> mice, the number of testicular macrophages was reduced compared to macrophages in all other organs tested. Moreover, the expression of *Ifn-β* and the 25HC producing enzyme Ch25h is abolished in M-CSF-treated BMDM from *Irf7*<sup>-/-</sup> mice. In conclusion, this study links the cholesterol metabolism to the regulation of inflammation in the male gonad. In this regard, M-CSF in the testis seems to constitute an upstream factor to induce high levels of 25HC and finally IRF7. IRF7 as a transcription factor can then regulate gene expression towards an anti-inflammatory profile characteristic for TM.

# ZUSAMMENFASSUNG

## 6. ZUSAMMENFASSUNG

Testikuläre Makrophagen (TM) stellen die häufigste Immunzellpopulation im Hoden dar. Diese Zellen sind charakterisiert durch ihre besondere Fähigkeit zu einer adäquaten Immunantwort gegenüber inflammatorischen Stimuli bei gleichzeitiger Immunsuppression bzw. Toleranz gegenüber den Neoantigenen auf männlichen Keimzellen. Der Phänotyp der heterogenen TM Population wird durch intrinsische Signale aus dem Hodengewebe erzeugt. Der Hoden enthält zahlreiche anti-inflammatorisch wirksame Moleküle, wie z.B. Corticosteron, Testosteron, Prostaglandine, 25HC, IL-10 sowie Activin, die allesamt potentielle Kandidaten darstellen Schlüsseltranskriptionsfaktoren zu induzieren, die dann die Expression von TM Gensignaturen steuern. Für TM konnten bisher, im Gegensatz zu einigen anderen Gewebsmakrophagen, noch keine Schlüsseltranskriptionsfaktoren identifiziert werden. Ziel dieser Arbeit war die Identifikation von Schlüsseltranskriptionsfaktoren und den Gewebemolekülen, die für ihre Induktion in TM verantwortlich sind. Mittels vergleichender RNA Seq Sequenzanalyse konnte der Transkriptionsfaktor IRF7 als ein solcher Kandidat in TM identifiziert werden. Aufgrund der hohen Mengen im Hoden wurde unter den immunsupprimierenden Faktoren 25HC ausgewählt und in M-CSF und GM-CSF stimulierten BMDM (bone marrow derived macrophages) auf seine Kapazität untersucht TM Signaturgene zu induzieren. Hierbei konnte gezeigt werden, dass 25HC einen anti-inflammatorischen Phänotyp in M-CSF, aber nicht in GM-CSF stimulierten Makrophagen induziert. Wichtig ist die Beobachtung, dass M-CSF-behandelte Makrophagen deutliche höhere Level an IRF7 Transkripten und 25HC im Überstand aufweisen. Da 25HC von TM selber produziert wird, ist ein autokriner Loop denkbar, bei dem durch M-CSF-Einfluss die Produktion von 25HC in TM stimuliert wird, was wiederum die Expression von IRF7 auslöst. In IRF7<sup>-/-</sup> Mäusen wurde in TM eine reduzierte Expression von MHCII und eine spezifisch geringere Anzahl an TM im Gegensatz zu residenten Makrophagen in anderen Organen gefunden. Zudem war in M-CSF stimulierten BMDM, die aus Irf7<sup>-/-</sup> Mäusen isoliert wurden, die Expression der Transkripte von *Ifn-β* und dem 25HC Synthesecoenzym Ch25h inhibiert. Zusammenfassend kann man schlussfolgern, dass in dieser Studie ein Zusammenhang zwischen dem Cholesterolverstoffwechsel und der Regulation des inflammatorischen Phänotyps in Immunzellen des Hodens gezeigt werden konnte. Hierbei stellt M-CSF einen Initialfaktor dar, der in TM über hohe Level an 25HC den Transkriptionsfaktor IRF7 induziert, der wesentlich für die Aufrechterhaltung des anti-inflammatorischen Phänotyps der TM ist.



# REFERENCE

## 7. REFERENCE

1. O'Shaughnessy P. (2015). Chapter 14 - Testicular Development. In T. M. Plant & A. J. B.T.-K. and N. P. of R. (Fourth E. Zeleznik (Eds.) (pp. 567–594). San Diego: Academic Press. <https://doi.org/10.1016/B978-0-12-397175-3.00014-4>.
2. Jégou B. (1991). Spermatids are regulators of Sertoli cell function. *Annals of the New York Academy of Sciences*, 637, 340–353. <https://doi.org/10.1111/j.1749-6632.1991.tb27321.x>.
3. Eberhard N., Hermann M. B., Susan N. (2010). *Andrology: Male Reproductive Health and Dysfunction*. Springer-Verlag Berlin Heidelberg, doi: 10.1007/978-3-540-78355-8.
4. Skinner M. K., McLachlan R. I., & Bremner W. J. (1989). Stimulation of Sertoli cell inhibin secretion by the testicular paracrine factor PModS. *Molecular and Cellular Endocrinology*, 66(2), 239–249. [https://doi.org/10.1016/0303-7207\(89\)90036-1](https://doi.org/10.1016/0303-7207(89)90036-1).
5. Mayerhofer A. (2013). Human testicular peritubular cells: more than meets the eye. *Reproduction* (Cambridge, England), 145(5), R107-16. <https://doi.org/10.1530/REP-12-0497>.
6. Meineke V., Frungieri M. B., Jessberger B., Vogt, H., & Mayerhofer A. (2000). Human testicular mast cells contain tryptase: increased mast cell number and altered distribution in the testes of infertile men. *Fertility and Sterility*, 74(2), 239–244. [https://doi.org/10.1016/s0015-0282\(00\)00626-9](https://doi.org/10.1016/s0015-0282(00)00626-9).
7. Hutson J. C. (1992). Development of cytoplasmic digitations between Leydig cells and testicular macrophages of the rat. *Cell and Tissue Research*, 267(2), 385–389. <https://doi.org/10.1007/BF00302977>.
8. Wiktor-Jedrzejczak W. W., Ahmed A., Szczylik C., & Skelly R. R. (1982). Hematological characterization of congenital osteopetrosis in op/op mouse. Possible mechanism for abnormal macrophage differentiation. *Journal of Experimental Medicine*, 156(5), 1516–1527. <https://doi.org/10.1084/jem.156.5.1516>.
9. Wiktor-Jedrzejczak W., Bartocci A., Ferrante A. W. J., Ahmed-Ansari A., Sell K. W., Pollard J. W., & Stanley E. R. (1990). Total absence of colony-stimulating factor 1 in the macrophage-deficient osteopetrotic (op/op) mouse. *Proceedings of the National Academy of Sciences of the United States of America*, 87(12), 4828–4832. <https://doi.org/10.1073/pnas.87.12.4828>.
10. Hedger M. P. (2002). Macrophages and the immune responsiveness of the testis. *Journal of Reproductive Immunology*, 57(1–2), 19–34. [https://doi.org/10.1016/s0165-0378\(02\)00016-5](https://doi.org/10.1016/s0165-0378(02)00016-5).
11. Stanley A., & Akbarsha M. A. (1994). Ultrastructural changes in the Leydig cell on treatment with vincristine. *Cytobios*, 79(316), 51–58..
12. Rettew J. A., Huet-Hudson Y. M., & Marriott I. (2008). Testosterone reduces macrophage expression in the mouse of toll-like receptor 4, a trigger for inflammation and innate immunity. *Biology of Reproduction*, 78(3), 432–437. <https://doi.org/10.1095/biolreprod.107.063545>.
13. Wang M., Fijak M., Hossain H., Markmann M., Nüsing R. M., Lochnit G., Bhushan S. (2017). Characterization of the Micro-Environment of the Testis that Shapes the Phenotype and Function of Testicular Macrophages. *The Journal of Immunology*, 1700162. <https://doi.org/10.4049/jimmunol.1700162>.
14. Wang J., Wreford N. G., Lan H. Y., Atkins R. & Hedger M. P. (1994). Leukocyte populations of the adult rat testis following removal of the Leydig cells by treatment with ethane dimethane sulfonate and subcutaneous testosterone implants. *Biology of Reproduction*, 51(3), 551–561. <https://doi.org/10.1095/biolreprod51.3.551>.

# REFERENCE

15. Gaytan, F., Bellido, C., Romero, J. L., Morales, C., Reymundo, C., & Aguilar, E. (1994). Decreased number and size and the defective function of testicular macrophages in long-term hypophysectomized rats are reversed by treatment with human gonadotrophins. *The Journal of Endocrinology*, 140(3), 399–407. <https://doi.org/10.1677/joe.0.1400399>.
16. Duckett, R. J., Hedger, M. P., McLachlan, R. I., & Wreford, N. G. (1997). The effects of gonadotropin-releasing hormone immunization and recombinant follicle-stimulating hormone on the Leydig cell and macrophage populations of the adult rat testis. *Journal of Andrology*, 18(4), 417–423. Retrieved from <http://europepmc.org/abstract/MED/92839553>.
17. Duckett, R. J., Wreford, N. G., Meachem, S. J., McLachlan, R. I., & Hedger, M. P. (1997). Effect of Chorionic Gonadotropin and Flutamide on Leydig Cell and Macrophage Populations in the Testosterone-Estradiol-Implanted Adult Rat. *Journal of Andrology*, 18(6), 656–662. <https://doi.org/https://doi.org/10.1002/j.1939-4640.1997.tb02442.x>.
18. DeFalco, T., Potter, S. J., Williams, A. V., Waller, B., Kan, M. J., & Capel, B. (2015). Macrophages Contribute to the Spermatogonial Niche in the Adult Testis. *Cell Reports*, 12(7), 1107–1119. <https://doi.org/10.1016/j.celrep.2015.07.015>.
19. Goluža, T., Boscanin, A., Cvetko, J., Kozina, V., Kosović, M., Bernat, M. M., Ježek, D. (2014). Macrophages and Leydig cells in testicular biopsies of azoospermic men. *BioMed Research International*, 2014, 828697. <https://doi.org/10.1155/2014/828697>.
20. Medawar, P. B. (1948). Immunity to homologous grafted skin; the fate of skin homografts transplanted to the brain, to subcutaneous tissue, and to the anterior chamber of the eye. *British Journal of Experimental Pathology*, 29(1), 58–69..
21. Benhar, Inbal, London, A., & Schwartz, M. (2012). The privileged immunity of immune privileged organs: the case of the eye . *Frontiers in Immunology* . Retrieved from <https://www.frontiersin.org/article/10.3389/fimmu.2012.00296>.
22. Meinhardt, A., & Hedger, M. P. (2011). Immunological, paracrine and endocrine aspects of testicular immune privilege. *Molecular and Cellular Endocrinology*, 335(1), 60–68. <https://doi.org/https://doi.org/10.1016/j.mce.2010.03.022>.
23. Fijak, M., & Meinhardt, A. (2006). The testis in immune privilege. *Immunological Reviews*, 213, 66–81. <https://doi.org/10.1111/j.1600-065X.2006.00438.x>.
24. Fijak M., Bhushan S., Meinhardt A. (2010) Immunoprivileged Sites: The Testis. In: Cuturi M., Anegón I. (eds) *Suppression and Regulation of Immune Responses. Methods in Molecular Biology (Methods and Protocols)*, vol 677. Humana Press, Totowa, NJ. [https://doi.org/10.1007/978-1-60761-869-0\\_29](https://doi.org/10.1007/978-1-60761-869-0_29).
25. Fijak, M., Zeller, T., Huys, T., Klug, J., Wahle, E., Linder, M., ... Meinhardt, A. (2014). Autoantibodies against protein disulfide isomerase ER-60 are a diagnostic marker for low-grade testicular inflammation. *Human Reproduction*, 29(11), 2382–2392. <https://doi.org/10.1093/humrep/deu226>.
26. Tung, K. S. K., Goldberg, E. H., & Goldberg, E. (1979). Immunobiological consequence of immunization of female mice with homologous spermatozoa: Induction of infertility. *Journal of Reproductive Immunology*, 1(3), 145–158. [https://doi.org/https://doi.org/10.1016/0165-0378\(79\)90015-9](https://doi.org/https://doi.org/10.1016/0165-0378(79)90015-9).
27. Fijak, M., Pilatz, A., Hedger, M. P., Nicolas, N., Bhushan, S., Michel, V., Meinhardt, A. (2018). Infectious, inflammatory and “autoimmune” male factor infertility: how do rodent models inform clinical practice? *Human Reproduction Update*, 24(4), 416–441. <https://doi.org/10.1093/humupd/dmy009>.

# REFERENCE

28. Meinhardt, A., Wang, M., Schulz, C., & Bhushan, S. (2018). Microenvironmental signals govern the cellular identity of testicular macrophages. *Journal of Leukocyte Biology*, 104(4), 757–766. <https://doi.org/https://doi.org/10.1002/JLB.3MR0318-086RR>.
29. Ní Chasaide, C., & Lynch, M. A. (2020). The role of the immune system in driving neuroinflammation. *Brain and Neuroscience Advances*, 4, 2398212819901082. <https://doi.org/10.1177/2398212819901082>.
30. Qin, Y., Garrison, B. S., Ma, W., Wang, R., Jiang, A., Li, J., Springer, T. A. (2018). A Milieu Molecule for TGF- $\beta$  Required for Microglia Function in the Nervous System. *Cell*, 174(1), 156–171.e16. <https://doi.org/10.1016/j.cell.2018.05.027>.
31. Easley-Neal, C., Foreman, O., Sharma, N., Zarrin, A. A., & Weimer, R. M. (2019). CSF1R Ligands IL-34 and CSF1 Are Differentially Required for Microglia Development and Maintenance in White and Gray Matter Brain Regions . *Frontiers in Immunology* . Retrieved from <https://www.frontiersin.org/article/10.3389/fimmu.2019.02199>.
32. Vinoth Kumar, R., Oh, T. W., & Park, Y.-K. (2016). Anti-Inflammatory Effects of Ginsenoside-Rh2 Inhibits LPS-Induced Activation of Microglia and Overproduction of Inflammatory Mediators Via Modulation of TGF- $\beta$ 1/Smad Pathway. *Neurochemical Research*, 41(5), 951–957. <https://doi.org/10.1007/s11064-015-1804-x>.
33. Nathan, C. F., Murray, H. W., Wiebe, M. E., & Rubin, B. Y. (1983). Identification of interferon-gamma as the lymphokine that activates human macrophage oxidative metabolism and antimicrobial activity. *The Journal of Experimental Medicine*, 158(3), 670–689. <https://doi.org/10.1084/jem.158.3.670>.
34. Mills, C. D. (2012). M1 and M2 Macrophages: Oracles of Health and Disease. *Critical Reviews in Immunology*, 32(6), 463–488. <https://doi.org/10.1615/critrevimmunol.v32.i6.10>.
35. Parisi, L., Gini, E., Baci, D., Tremolati, M., Fanuli, M., Bassani, B., Mortara, L. (2018). Macrophage Polarization in Chronic Inflammatory Diseases: Killers or Builders? *Journal of Immunology Research*, 2018, 8917804. <https://doi.org/10.1155/2018/8917804>.
36. Gordon, S., Plüddemann, A., & Martinez Estrada, F. (2014). Macrophage heterogeneity in tissues: phenotypic diversity and functions. *Immunological Reviews*, 262(1), 36–55. <https://doi.org/10.1111/imr.12223>.
37. Saradna, A., Do, D. C., Kumar, S., Fu, Q.-L., & Gao, P. (2018). Macrophage polarization and allergic asthma. *Translational Research : The Journal of Laboratory and Clinical Medicine*, 191, 1–14. <https://doi.org/10.1016/j.trsl.2017.09.002>.
38. Murray, P. J., & Wynn, T. A. (2011). Protective and pathogenic functions of macrophage subsets. *Nature Reviews. Immunology*, 11(11), 723–737. <https://doi.org/10.1038/nri3073>.
39. Röszer, T. (2015). Understanding the Mysterious M2 Macrophage through Activation Markers and Effector Mechanisms. *Mediators of Inflammation*, 2015, 816460. <https://doi.org/10.1155/2015/816460>.
40. Hoeffel, G., Chen, J., Lavin, Y., Low, D., Almeida, F. F., See, P., Ginhoux, F. (2015). C-Myb(+) erythro-myeloid progenitor-derived fetal monocytes give rise to adult tissue-resident macrophages. *Immunity*, 42(4), 665–678. <https://doi.org/10.1016/j.immuni.2015.03.011>.
41. Schulz, C., Gomez Perdiguero, E., Chorro, L., Szabo-Rogers, H., Cagnard, N., Kierdorf, K., Geissmann, F. (2012). A lineage of myeloid cells independent of Myb and hematopoietic stem cells. *Science (New York, N.Y.)*, 336(6077), 86–90. <https://doi.org/10.1126/science.1219179>.

# REFERENCE

42. Yona, S., Kim, K.-W., Wolf, Y., Mildner, A., Varol, D., Breker, M., Jung, S. (2013). Fate mapping reveals origins and dynamics of monocytes and tissue macrophages under homeostasis. *Immunity*, 38(1), 79–91. <https://doi.org/10.1016/j.immuni.2012.12.001>.
43. Sieweke, M. H., & Allen, J. E. (2013). Beyond Stem Cells: Self-Renewal of Differentiated Macrophages. *Science*, 342(6161), 1242974. <https://doi.org/10.1126/science.1242974>.
44. Röszer, T. (2018). Understanding the Biology of Self-Renewing Macrophages. *Cells*, 7(8). <https://doi.org/10.3390/cells7080103>.
45. Gosselin, D., Link, V. M., Romanoski, C. E., Fonseca, G. J., Eichenfield, D. Z., Spann, N. J., Glass, C. K. (2014). Environment drives selection and function of enhancers controlling tissue-specific macrophage identities. *Cell*, 159(6), 1327–1340. <https://doi.org/10.1016/j.cell.2014.11.023>.
46. Amit, I., Winter, D. R., & Jung, S. (2016). The role of the local environment and epigenetics in shaping macrophage identity and their effect on tissue homeostasis. *Nature Immunology*, 17(1), 18–25. <https://doi.org/10.1038/ni.3325>.
47. Okabe, Y., & Medzhitov, R. (2016). Tissue biology perspective on macrophages. *Nature Immunology*, 17(1), 9–17. <https://doi.org/10.1038/ni.3320>.
48. Mossadegh-Keller, N., & Sieweke, M. H. (2019). Characterization of Mouse Adult Testicular Macrophage Populations by Immunofluorescence Imaging and Flow Cytometry. *Bio-Protocol*, 9(5), 10.21769/BioProtoc.3178. <https://doi.org/10.21769/BioProtoc.3178>.
49. DeFalco, T., Potter, S. J., Williams, A. V., Waller, B., Kan, M. J., & Capel, B. (2015). Macrophages Contribute to the Spermatogonial Niche in the Adult Testis. *Cell Reports*, 12(7), 1107–1119. <https://doi.org/10.1016/j.celrep.2015.07.015>.
50. Mossadegh-Keller, N., & Sieweke, M. H. (2018). Testicular macrophages: Guardians of fertility. *Cellular Immunology*, 330, 120–125. <https://doi.org/10.1016/j.cellimm.2018.03.009>.
51. Mossadegh-Keller, N., Gentek, R., Gimenez, G., Bigot, S., Mailfert, S., & Sieweke, M. H. (2017). Developmental origin and maintenance of distinct testicular macrophage populations. *The Journal of Experimental Medicine*, 214(10), 2829–2841. <https://doi.org/10.1084/jem.20170829>.
52. Jablonski, K. A., Amici, S. A., Webb, L. M., Ruiz-Rosado, J. de D., Popovich, P. G., Partida-Sanchez, S., & Guerau-de-Arellano, M. (2015). Novel Markers to Delineate Murine M1 and M2 Macrophages. *PloS One*, 10(12), e0145342. <https://doi.org/10.1371/journal.pone.0145342>.
53. Chakarov, S., Lim, H. Y., Tan, L., Lim, S. Y., See, P., Lum, J., Ginhoux, F. (2019). Two distinct interstitial macrophage populations coexist across tissues in specific subtissular niches. *Science*, 363(6432), eaau0964. <https://doi.org/10.1126/science.aau0964>.
54. Bhushan, S., & Meinhardt, A. (2017). The macrophages in testis function. *Journal of Reproductive Immunology*, 119, 107–112. <https://doi.org/10.1016/j.jri.2016.06.008>.
55. Bhushan, S., Tchatalbachev, S., Lu, Y., Fröhlich, S., Fijak, M., Vijayan, V., Meinhardt, A. (2015). Differential Activation of Inflammatory Pathways in Testicular Macrophages Provides a Rationale for Their Subdued Inflammatory Capacity. *The Journal of Immunology*, 194(11), 5455 LP – 5464. <https://doi.org/10.4049/jimmunol.1401132>.
56. Bryniarski, K., Szewczyk, K., Ptak, M., Bobek, M., & Ptak, W. (2002). A two step procedure to fractionate mouse testicular macrophages with different cytokine profiles. *Archivum Immunologiae et Therapiae Experimentalis*, 50(3), 225–229.
57. Bryniarski, K., Szczepanik, M., Ptak, M., & Ptak, W. (2005). Modulation of testicular macrophage activity by collagenase. *Folia Histochemica et Cytobiologica*, 43 1, 37–41..

## REFERENCE

58. Bryniarski, K., Szczepanik, M., Ptak, M., & Ptak, W. (2005). The influence of collagenase treatment on the production of TNF- $\alpha$ , IL-6 and IL-10 by testicular macrophages. *Journal of Immunological Methods*, 301(1–2), 186–189. <https://doi.org/10.1016/j.jim.2005.04.002>.
59. an den Bossche J, Baardman J, Otto NA, van der Velden S, Neele AE, van den Berg SM et al. Mitochondrial Dysfunction Prevents Repolarization of Inflammatory Macrophages. *Cell Reports*. 2016;17(3):684–696. <https://doi.org/10.1016/j.celrep.2016.09.008>.
60. Cook, A. D., Louis, C., Robinson, M. J., Saleh, R., Sleeman, M. A., & Hamilton, J. A. (2016). Granulocyte macrophage colony-stimulating factor receptor  $\alpha$  expression and its targeting in antigen-induced arthritis and inflammation. *Arthritis Research & Therapy*, 18(1), 287. <https://doi.org/10.1186/s13075-016-1185-9>.
61. Lin, H., Lee, E., Hestir, K., Leo, C., Huang, M., Bosch, E., Williams, L. T. (2008). Discovery of a cytokine and its receptor by functional screening of the extracellular proteome. *Science (New York, N.Y.)*, 320(5877), 807–811. <https://doi.org/10.1126/science.1154370>.
62. Bézie, S., Picarda, E., Ossart, J., Tesson, L., Usal, C., Renaudin, K., Guillonnet, C. (2015). IL-34 is a Treg-specific cytokine and mediates transplant tolerance. *The Journal of Clinical Investigation*, 125(10), 3952–3964. <https://doi.org/10.1172/JCI81227>.
63. Wei, S., Nandi, S., Chitu, V., Yeung, Y.-G., Yu, W., Huang, M., Stanley, E. R. (2010). Functional overlap but differential expression of CSF-1 and IL-34 in their CSF-1 receptor-mediated regulation of myeloid cells. *Journal of Leukocyte Biology*, 88(3), 495–505. <https://doi.org/10.1189/jlb.1209822>.
64. Nandi, S., Cioce, M., Yeung, Y.-G., Nieves, E., Tesfa, L., Lin, H., Stanley, E. R. (2013). Receptor-type protein-tyrosine phosphatase  $\zeta$  is a functional receptor for interleukin-34. *The Journal of Biological Chemistry*, 288(30), 21972–21986. <https://doi.org/10.1074/jbc.M112.442731>.
65. Stanley, E. R., & Chitu, V. (2014). CSF-1 receptor signaling in myeloid cells. *Cold Spring Harbor Perspectives in Biology*, 6(6). <https://doi.org/10.1101/cshperspect.a021857>.
66. Mouchemore, K. A., & Pixley, F. J. (2012). CSF-1 signaling in macrophages: pleiotrophy through phosphotyrosine-based signaling pathways. *Critical Reviews in Clinical Laboratory Sciences*, 49(2), 49–61. <https://doi.org/10.3109/10408363.2012.666845>.
67. Kondo, Y., Lemere, C. A., & Seabrook, T. J. (2007). Osteopetrotic (op/op) mice have reduced microglia, no A $\beta$  deposition, and no changes in dopaminergic neurons. *Journal of Neuroinflammation*, 4, 31. <https://doi.org/10.1186/1742-2094-4-31>.
68. Wang, Y., & Colonna, M. (2014). Interleukin-34, a cytokine crucial for the differentiation and maintenance of tissue resident macrophages and Langerhans cells. *European Journal of Immunology*, 44(6), 1575–1581. <https://doi.org/10.1002/eji.201344365>.
69. Nissen, J. C., Thompson, K. K., West, B. L., & Tsirka, S. E. (2018). Csf1R inhibition attenuates experimental autoimmune encephalomyelitis and promotes recovery. *Experimental Neurology*, 307, 24–36. <https://doi.org/10.1016/j.expneurol.2018.05.021>.
70. Merry, T. L., Brooks, A. E. S., Masson, S. W., Adams, S. E., Jaiswal, J. K., Jamieson, S. M. F., & Shepherd, P. R. (2020). The CSF1 receptor inhibitor pexidartinib (PLX3397) reduces tissue macrophage levels without affecting glucose homeostasis in mice. *International Journal of Obesity* (2005), 44(1), 245–253. <https://doi.org/10.1038/s41366-019-0355-7>.
71. DeNardo, D. G., Brennan, D. J., Rexhepaj, E., Ruffell, B., Shiao, S. L., Madden, S. F., Coussens, L. M. (2011). Leukocyte complexity predicts breast cancer survival and functionally regulates response to chemotherapy. *Cancer Discovery*, 1(1), 54–67. <https://doi.org/10.1158/2159-8274.CD-10-0028>.

# REFERENCE

72. Kuse, Y., Ohuchi, K., Nakamura, S., Hara, H., & Shimazawa, M. (2018). Microglia increases the proliferation of retinal precursor cells during postnatal development. *Molecular Vision*, 24, 536–545. Retrieved from <https://pubmed.ncbi.nlm.nih.gov/30090016>.
73. Pollard, J. W. (2009). Trophic macrophages in development and disease. *Nature Reviews. Immunology*, 9(4), 259–270. <https://doi.org/10.1038/nri2528>.
74. Hamilton, J. A. (2008). Colony-stimulating factors in inflammation and autoimmunity. *Nature Reviews. Immunology*, 8(7), 533–544. <https://doi.org/10.1038/nri2356>.
75. Lacey, D. C., Achuthan, A., Fleetwood, A. J., Dinh, H., Roiniotis, J., Scholz, G. M., Hamilton, J. A. (2012). Defining GM-CSF- and macrophage-CSF-dependent macrophage responses by in vitro models. *Journal of Immunology* (Baltimore, Md. : 1950), 188(11), 5752–5765. <https://doi.org/10.4049/jimmunol.1103426>.
76. Fleetwood, A. J., Dinh, H., Cook, A. D., Hertzog, P. J., & Hamilton, J. A. (2009). GM-CSF- and M-CSF-dependent macrophage phenotypes display differential dependence on type I interferon signaling. *Journal of Leukocyte Biology*, 86(2), 411–421. <https://doi.org/10.1189/jlb.1108702>.
77. Schneider, K. M., Watson, N. B., Minchenberg, S. B., & Massa, P. T. (2018). The influence of macrophage growth factors on Theiler's Murine Encephalomyelitis Virus (TMEV) infection and activation of macrophages. *Cytokine*, 102, 83–93. <https://doi.org/10.1016/j.cyto.2017.07.015>.
78. Ohradanova-Repic, A., Machacek, C., Charvet, C., Lager, F., Le Roux, D., Platzer, R., Stockinger, H. (2018). Extracellular Purine Metabolism Is the Switchboard of Immunosuppressive Macrophages and a Novel Target to Treat Diseases With Macrophage Imbalances. *Frontiers in Immunology*, 9, 852. <https://doi.org/10.3389/fimmu.2018.00852>.
79. Na, Y. R., Gu, G. J., Jung, D., Kim, Y. W., Na, J., Woo, J. S., Seok, S. H. (2016). GM-CSF Induces Inflammatory Macrophages by Regulating Glycolysis and Lipid Metabolism. *Journal of Immunology* (Baltimore, Md. : 1950), 197(10), 4101–4109. <https://doi.org/10.4049/jimmunol.1600745>.
80. Lukic, A., Larssen, P., Fauland, A., Samuelsson, B., Wheelock, C. E., Gabrielsson, S., & Radmark, O. (2017). GM-CSF- and M-CSF-primed macrophages present similar resolving but distinct inflammatory lipid mediator signatures. *FASEB Journal : Official Publication of the Federation of American Societies for Experimental Biology*, 31(10), 4370–4381. <https://doi.org/10.1096/fj.201700319R>.
81. Karmaus, P. W. F., Herrada, A. A., Guy, C., Neale, G., Dhungana, Y., Long, L., Chi, H. (2017). Critical roles of mTORC1 signaling and metabolic reprogramming for M-CSF-mediated myelopoiesis. *The Journal of Experimental Medicine*, 214(9), 2629–2647. <https://doi.org/10.1084/jem.20161855>.
82. Pearce, E. L., & Pearce, E. J. (2013). Metabolic pathways in immune cell activation and quiescence. *Immunity*, 38(4), 633–643. <https://doi.org/10.1016/j.immuni.2013.04.005>.
83. O'Neill, L. A. J., & Hardie, D. G. (2013). Metabolism of inflammation limited by AMPK and pseudo-starvation. *Nature*, 493(7432), 346–355. <https://doi.org/10.1038/nature11862>.
84. Tan, Z., Xie, N., Cui, H., Moellering, D. R., Abraham, E., Thannickal, V. J., & Liu, G. (2015). Pyruvate dehydrogenase kinase 1 participates in macrophage polarization via regulating glucose metabolism. *Journal of Immunology* (Baltimore, Md. : 1950), 194(12), 6082–6089. <https://doi.org/10.4049/jimmunol.1402469>.
85. Ayala, T. S., Tessaro, F. H. G., Jannuzzi, G. P., Bella, L. M., Ferreira, K. S., & Martins, J. O. (2019). High Glucose Environments Interfere with Bone Marrow-Derived Macrophage Inflammatory Mediator Release, the TLR4 Pathway and Glucose Metabolism. *Scientific Reports*, 9(1), 11447. <https://doi.org/10.1038/s41598-019-47836-8>.

# REFERENCE

86. Viola, A., Munari, F., Sánchez-Rodríguez, R., Sclaro, T., & Castegna, A. (2019). The Metabolic Signature of Macrophage Responses . *Frontiers in Immunology* . Retrieved from <https://www.frontiersin.org/article/10.3389/fimmu.2019.01462>.
87. Ikonen, E. (2008). Cellular cholesterol trafficking and compartmentalization. *Nature Reviews. Molecular Cell Biology*, 9(2), 125–138. <https://doi.org/10.1038/nrm2336>.
88. Cyster, J. G., Dang, E. V., Reboldi, A., & Yi, T. (2014). 25-Hydroxycholesterols in innate and adaptive immunity. *Nature Reviews. Immunology*, 14(11), 731–743. <https://doi.org/10.1038/nri3755>.
89. Liu, S.-Y., Sanchez, D. J., Aliyari, R., Lu, S., & Cheng, G. (2012). Systematic identification of type I and type II interferon-induced antiviral factors. *Proceedings of the National Academy of Sciences*, 109(11), 4239 LP – 4244. <https://doi.org/10.1073/pnas.1114981109>.
90. Kandutsch, A. A., Chen, H. W., & Heiniger, H. J. (1978). Biological activity of some oxygenated sterols. *Science*, 201(4355), 498 LP – 501. <https://doi.org/10.1126/science.663671>.
91. Diczfalusy, U., Olofsson, K. E., Carlsson, A.-M., Gong, M., Golenbock, D. T., Rooyackers, O., Björkbacka, H. (2009). Marked upregulation of cholesterol 25-hydroxylase expression by lipopolysaccharide. *Journal of Lipid Research*, 50(11), 2258–2264. <https://doi.org/10.1194/jlr.M900107-JLR200>.
92. McDonald, J. G., & Russell, D. W. (2010). Editorial: 25-Hydroxycholesterol: a new life in immunology. *Journal of Leukocyte Biology*, 88(6), 1071–1072. <https://doi.org/10.1189/jlb.0710418>.
93. Park, K., & Scott, A. L. (2010). Cholesterol 25-hydroxylase production by dendritic cells and macrophages is regulated by type I interferons. *Journal of Leukocyte Biology*, 88(6), 1081–1087. <https://doi.org/10.1189/jlb.0610318>.
94. Li, C., Deng, Y.-Q., Wang, S., Ma, F., Aliyari, R., Huang, X.-Y., Cheng, G. (2017). 25-Hydroxycholesterol Protects Host against Zika Virus Infection and Its Associated Microcephaly in a Mouse Model. *Immunity*, 46(3), 446–456. <https://doi.org/https://doi.org/10.1016/j.immuni.2017.02.012>.
95. Shrivastava-Ranjan, P., Bergeron, É., Chakrabarti, A. K., Albariño, C. G., Flint, M., Nichol, S. T., & Spiropoulou, C. F. (2016). 25-Hydroxycholesterol Inhibition of Lassa Virus Infection through Aberrant GP1 Glycosylation. *MBio*, 7(6), e01808-16. <https://doi.org/10.1128/mBio.01808-16>.
96. Park, K., & Scott, A. L. (2010). Cholesterol 25-hydroxylase production by dendritic cells and macrophages is regulated by type I interferons. *Journal of Leukocyte Biology*, 88(6), 1081–1087. <https://doi.org/10.1189/jlb.0610318>.
97. Blanc, M., Hsieh, W. Y., Robertson, K. A., Kropp, K. A., Forster, T., Shui, G., Ghazal, P. (2013). The transcription factor STAT-1 couples macrophage synthesis of 25-hydroxycholesterol to the interferon antiviral response. *Immunity*, 38(1), 106–118. <https://doi.org/10.1016/j.immuni.2012.11.004>.
98. Matsumiya, T., & Imaizumi, T. (2013). How are STAT1 and cholesterol metabolism associated in antiviral responses? *JAK-STAT*, 2(3), e24189–e24189. <https://doi.org/10.4161/jkst.24189>.
99. Liu, S.-Y., Aliyari, R., Chikere, K., Li, G., Marsden, M. D., Smith, J. K., Cheng, G. (2013). Interferon-inducible cholesterol-25-hydroxylase broadly inhibits viral entry by production of 25-hydroxycholesterol. *Immunity*, 38(1), 92–105. <https://doi.org/10.1016/j.immuni.2012.11.005>.
100. Bauman, D. R., Bitmansour, A. D., McDonald, J. G., Thompson, B. M., Liang, G., & Russell, D. W. (2009). 25-Hydroxycholesterol secreted by macrophages in response to Toll-like receptor activation suppresses immunoglobulin A production. *Proceedings of the National Academy of*

# REFERENCE

- Sciences of the United States of America, 106(39), 16764–16769.  
<https://doi.org/10.1073/pnas.0909142106>.
101. Gold, E. S., Ramsey, S. A., Sartain, M. J., Selinummi, J., Podolsky, I., Rodriguez, D. J., Aderem, A. (2012). ATF3 protects against atherosclerosis by suppressing 25-hydroxycholesterol-induced lipid body formation. *The Journal of Experimental Medicine*, 209(4), 807–817.  
<https://doi.org/10.1084/jem.20111202>.
102. Park, K., & Scott, A. L. (2010). Cholesterol 25-hydroxylase production by dendritic cells and macrophages is regulated by type I interferons. *Journal of Leukocyte Biology*, 88(6), 1081–1087.  
<https://doi.org/10.1189/jlb.0610318>.
103. Gold, E. S., Diercks, A. H., Podolsky, I., Podyminogin, R. L., Askovich, P. S., Treuting, P. M., & Aderem, A. (2014). 25-Hydroxycholesterol acts as an amplifier of inflammatory signaling. *Proceedings of the National Academy of Sciences*, 111(29), 10666 LP – 10671.  
<https://doi.org/10.1073/pnas.1404271111>.
104. Tuong, Z. K., Lau, P., Yeo, J. C., Pearen, M. A., Wall, A. A., Stanley, A. C., Muscat, G. E. O. (2013). Disruption of *Rora*1 and Cholesterol 25-Hydroxylase Expression Attenuates Phagocytosis in Male *Rora*sg/sg Mice. *Endocrinology*, 154(1), 140–149. <https://doi.org/10.1210/en.2012-1889>.
105. Ludigs, K., Parfenov, V., Du Pasquier, R. A., & Guarda, G. (2012). Type I IFN-mediated regulation of IL-1 production in inflammatory disorders. *Cellular and Molecular Life Sciences : CMLS*, 69(20), 3395—3418. <https://doi.org/10.1007/s00018-012-0989-2>.
106. Guarda, G., Braun, M., Staehli, F., Tardivel, A., Mattmann, C., Förster, I., Tschopp, J. (2011). Type I interferon inhibits interleukin-1 production and inflammasome activation. *Immunity*, 34(2), 213–223. <https://doi.org/10.1016/j.immuni.2011.02.006>.
107. Dang, E. V, McDonald, J. G., Russell, D. W., & Cyster, J. G. (2017). Oxysterol Restraint of Cholesterol Synthesis Prevents AIM2 Inflammasome Activation. *Cell*, 171(5), 1057-1071.e11.  
<https://doi.org/https://doi.org/10.1016/j.cell.2017.09.029>.
108. Diczfalusy, U., Olofsson, K. E., Carlsson, A.-M., Gong, M., Golenbock, D. T., Rooyackers, O., Björkbacka, H. (2009). Marked upregulation of cholesterol 25-hydroxylase expression by lipopolysaccharide. *Journal of Lipid Research*, 50(11), 2258–2264.  
<https://doi.org/10.1194/jlr.M900107-JLR200>.
109. Nes, W. D., Lukyanenko, Y. O., Jia, Z. H., Quideau, S., Howald, W. N., Pratum, T. K., Hutson, J. C. (2000). Identification of the lipophilic factor produced by macrophages that stimulates steroidogenesis. *Endocrinology*, 141(3), 953–958. <https://doi.org/10.1210/endo.141.3.7350>.
110. Lukyanenko, Y. O., Chen, J. J., & Hutson, J. C. (2001). Production of 25-hydroxycholesterol by testicular macrophages and its effects on Leydig cells. *Biology of Reproduction*, 64(3), 790–796.  
<https://doi.org/10.1095/biolreprod64.3.790>.
111. Kimura, T., Nada, S., Takegahara, N., Okuno, T., Nojima, S., Kang, S., Kumanogoh, A. (2017). Erratum: Polarization of M2 macrophages requires Lamtor1 that integrates cytokine and amino-acid signals. *Nature Communications*, 8(1), 14711. <https://doi.org/10.1038/ncomms14711>.
112. Trinchieri, G. (2010). Type I interferon: friend or foe? *The Journal of Experimental Medicine*, 207(10), 2053–2063. <https://doi.org/10.1084/jem.20101664>.
113. Pestka, S., Krause, C. D., & Walter, M. R. (2004). Interferons, interferon-like cytokines, and their receptors. *Immunological Reviews*, 202, 8–32. <https://doi.org/10.1111/j.0105-2896.2004.00204.x>.
114. Ivashkiv, L. B., & Donlin, L. T. (2014). Regulation of type I interferon responses. *Nature Reviews. Immunology*, 14(1), 36–49. <https://doi.org/10.1038/nri3581>.



# REFERENCE

115. MacMicking, J. D. (2012). Interferon-inducible effector mechanisms in cell-autonomous immunity. *Nature Reviews. Immunology*, 12(5), 367–382. <https://doi.org/10.1038/nri3210>.
116. Stark, G. R., & Darnell, J. E. J. (2012). The JAK-STAT pathway at twenty. *Immunity*, 36(4), 503–514. <https://doi.org/10.1016/j.immuni.2012.03.013>.
117. Schoggins, J. W., Wilson, S. J., Panis, M., Murphy, M. Y., Jones, C. T., Bieniasz, P., & Rice, C. M. (2011). A diverse range of gene products are effectors of the type I interferon antiviral response. *Nature*, 472(7344), 481–485. <https://doi.org/10.1038/nature09907>.
118. Saka, H. A., & Valdivia, R. (2012). Emerging roles for lipid droplets in immunity and host-pathogen interactions. *Annual Review of Cell and Developmental Biology*, 28, 411–437. <https://doi.org/10.1146/annurev-cellbio-092910-153958>.
119. van Boxel-Dezaire, A. H. H., Rani, M. R. S., & Stark, G. R. (2006). Complex modulation of cell type-specific signaling in response to type I interferons. *Immunity*, 25(3), 361–372. <https://doi.org/10.1016/j.immuni.2006.08.014>.
120. Oshiumi, H., Matsumoto, M., Funami, K., Akazawa, T., & Seya, T. (2003). TICAM-1, an adaptor molecule that participates in Toll-like receptor 3-mediated interferon-beta induction. *Nature Immunology*, 4(2), 161–167. <https://doi.org/10.1038/ni886>.
121. Yamamoto, M., Sato, S., Mori, K., Hoshino, K., Takeuchi, O., Takeda, K., & Akira, S. (2002). Cutting edge: a novel Toll/IL-1 receptor domain-containing adapter that preferentially activates the IFN-beta promoter in the Toll-like receptor signaling. *Journal of Immunology (Baltimore, Md. : 1950)*, 169(12), 6668–6672. <https://doi.org/10.4049/jimmunol.169.12.6668>.
122. Meylan, E., Burns, K., Hofmann, K., Blancheteau, V., Martinon, F., Kelliher, M., & Tschopp, J. (2004). RIP1 is an essential mediator of Toll-like receptor 3-induced NF-kappa B activation. *Nature Immunology*, 5(5), 503–507. <https://doi.org/10.1038/ni1061>.
123. Häcker, H., & Karin, M. (2006). Regulation and function of IKK and IKK-related kinases. *Science's STKE : Signal Transduction Knowledge Environment*, 2006(357), re13. <https://doi.org/10.1126/stke.3572006re13>.
124. Oganessian, G., Saha, S. K., Guo, B., He, J. Q., Shahangian, A., Zarnegar, B., Cheng, G. (2006). Critical role of TRAF3 in the Toll-like receptor-dependent and -independent antiviral response. *Nature*, 439(7073), 208–211. <https://doi.org/10.1038/nature04374>.
125. Fitzgerald, K. A., Rowe, D. C., Barnes, B. J., Caffrey, D. R., Visintin, A., Latz, E., Golenbock, D. T. (2003). LPS-TLR4 signaling to IRF-3/7 and NF-kappaB involves the toll adapters TRAM and TRIF. *The Journal of Experimental Medicine*, 198(7), 1043–1055. <https://doi.org/10.1084/jem.20031023>.
126. Sharma, S., tenOever, B. R., Grandvaux, N., Zhou, G.-P., Lin, R., & Hiscott, J. (2003). Triggering the interferon antiviral response through an IKK-related pathway. *Science (New York, N.Y.)*, 300(5622), 1148–1151. <https://doi.org/10.1126/science.1081315>.
127. Akira, S., Uematsu, S., & Takeuchi, O. (2006). Pathogen recognition and innate immunity. *Cell*, 124(4), 783–801. <https://doi.org/10.1016/j.cell.2006.02.015>.
128. Reboldi, A., Dang, E. V., McDonald, J. G., Liang, G., Russell, D. W., & Cyster, J. G. (2014). Inflammation. 25-Hydroxycholesterol suppresses interleukin-1-driven inflammation downstream of type I interferon. *Science (New York, N.Y.)*, 345(6197), 679–684. <https://doi.org/10.1126/science.1254790>.
129. Scheller, M., Foerster, J., Heyworth, C. M., Waring, J. F., Löhler, J., Gilmore, G. L., Horak, I. (1999). Altered Development and Cytokine Responses of Myeloid Progenitors in the Absence of

# REFERENCE

- Transcription Factor, Interferon Consensus Sequence Binding Protein. *Blood*, 94(11), 3764–3771. <https://doi.org/10.1182/blood.V94.11.3764>.
130. RLu, R., & Pitha, P. M. (2001). Monocyte differentiation to macrophage requires interferon regulatory factor 7. *The Journal of Biological Chemistry*, 276(48), 45491–45496. <https://doi.org/10.1074/jbc.C100421200>.
131. Symons, J. A., Alcamí, A., & Smith, G. L. (1995). Vaccinia virus encodes a soluble type I interferon receptor of novel structure and broad species specificity. *Cell*, 81(4), 551–560. [https://doi.org/10.1016/0092-8674\(95\)90076-4](https://doi.org/10.1016/0092-8674(95)90076-4).
132. Vancová, I., La Bonnardiere, C., & Kontsek, P. (1998). Vaccinia virus protein B18R inhibits the activity and cellular binding of the novel type interferon-delta. *The Journal of General Virology*, 79 ( Pt 7), 1647–1649. <https://doi.org/10.1099/0022-1317-79-7-1647>.
133. Bego, M. G., Mercier, J., & Cohen, E. A. (2012). Virus-activated interferon regulatory factor 7 upregulates expression of the interferon-regulated BST2 gene independently of interferon signaling. *Journal of Virology*, 86(7), 3513–3527. <https://doi.org/10.1128/JVI.06971-11>.
134. Litvak, V., Ratushny, A. V., Lampano, A. E., Schmitz, F., Huang, A. C., Raman, A., Aderem, A. (2012). A FOXO3-IRF7 gene regulatory circuit limits inflammatory sequelae of antiviral responses. *Nature*, 490(7420), 421–425. <https://doi.org/10.1038/nature11428>.
135. Owens, B. M. J., Moore, J. W. J., & Kaye, P. M. (2012). IRF7 Regulates TLR2-Mediated Activation of Splenic CD11chi Dendritic Cells. *PLOS ONE*, 7(7), e41050. Retrieved from <https://doi.org/10.1371/journal.pone.0041050>.
136. Honda, K., Yanai, H., Negishi, H., Asagiri, M., Sato, M., Mizutani, T., Taniguchi, T. (2005). IRF-7 is the master regulator of type-I interferon-dependent immune responses. *Nature*, 434(7034), 772–777. <https://doi.org/10.1038/nature03464>.
137. Cohen, M., Matcovitch, O., David, E., Barnett-Itzhaki, Z., Keren-Shaul, H., Blecher-Gonen, R., Schwartz, M. (2014). Chronic exposure to TGFβ1 regulates myeloid cell inflammatory response in an IRF7-dependent manner. *The EMBO Journal*, 33(24), 2906–2921. <https://doi.org/10.15252/embj.201489293>.
138. Tang, Y., Shi, Y., Gao, Y., Xu, X., Han, T., Li, J., & Liu, C. (2019). Oxytocin system alleviates intestinal inflammation by regulating macrophages polarization in experimental colitis. *Clinical Science (London, England : 1979)*, 133(18), 1977—1992. <https://doi.org/10.1042/cs20190756>.
139. Cavalcante, P. A. M., Alenina, N., Budu, A., Freitas-Lima, L. C., Alves-Silva, T., Agudelo, J. S. H., Araújo, R. C. (2019). Nephropathy in Hypertensive Animals Is Linked to M2 Macrophages and Increased Expression of the YM1/Chi3l3 Protein. *Mediators of Inflammation*, 2019, 9086758. <https://doi.org/10.1155/2019/9086758>.
140. Shuhui, L., Mok, Y.-K., & Wong, W. S. F. (2009). Role of Mammalian Chitinases in Asthma. *International Archives of Allergy and Immunology*, 149(4), 369–377. <https://doi.org/10.1159/000205583>.
141. Welch, J. S., Escoubet-Lozach, L., Sykes, D. B., Liddiard, K., Greaves, D. R., & Glass, C. K. (2002). TH2 cytokines and allergic challenge induce Ym1 expression in macrophages by a STAT6-dependent mechanism. *The Journal of Biological Chemistry*, 277(45), 42821–42829. <https://doi.org/10.1074/jbc.M205873200>.
142. Starossom, S. C., Campo Garcia, J., Woelfle, T., Romero-Suarez, S., Olah, M., Watanabe, F., Khoury, S. J. (2019). Chi3l3 induces oligodendrogenesis in an experimental model of autoimmune neuroinflammation. *Nature Communications*, 10(1), 217. <https://doi.org/10.1038/s41467-018-08140-7>.

## REFERENCE

143. Moslehi, A., Farahabadi, M., Chavoshzadeh, S. A., Barati, A., Ababzadeh, S., & Mohammadbeigi, A. (2018). The Effect of Amygdalin on Endoplasmic Reticulum (ER) Stress Induced Hepatic Steatosis in Mice. *The Malaysian Journal of Medical Sciences : MJMS*, 25(1), 16–23. <https://doi.org/10.21315/mjms2018.25.1.3>.
144. Osborne, L. C., Monticelli, L. A., Nice, T. J., Sutherland, T. E., Siracusa, M. C., Hepworth, M. R., Artis, D. (2014). Coinfection. Virus-helminth coinfection reveals a microbiota-independent mechanism of immunomodulation. *Science (New York, N.Y.)*, 345(6196), 578–582. <https://doi.org/10.1126/science.1256942>.
145. Couper, K. N., Blount, D. G., & Riley, E. M. (2008). IL-10: the master regulator of immunity to infection. *Journal of Immunology (Baltimore, Md. : 1950)*, 180(9), 5771–5777. <https://doi.org/10.4049/jimmunol.180.9.5771>.
146. Klein, B., Bhushan, S., Günther, S., Middendorff, R., Loveland, K. L., Hedger, M. P., & Meinhardt, A. (2020). Differential tissue-specific damage caused by bacterial epididymo-orchitis in the mouse. *Molecular Human Reproduction*, 26(4), 215–227. <https://doi.org/10.1093/molehr/gaaa011>.
147. Eftekharian, M. M., Noroozi, R., Sayad, A., Sarrafzadeh, S., Toghi, M., Azimi, T., Mirfakhraie, R. (2016). RAR-related orphan receptor A (RORA): A new susceptibility gene for multiple sclerosis. *Journal of the Neurological Sciences*, 369, 259–262. <https://doi.org/10.1016/j.jns.2016.08.045>.
148. Saijo, K., Winner, B., Carson, C. T., Collier, J. G., Boyer, L., Rosenfeld, M. G., Glass, C. K. (2009). A Nurrl/CoREST pathway in microglia and astrocytes protects dopaminergic neurons from inflammation-induced death. *Cell*, 137(1), 47–59. <https://doi.org/10.1016/j.cell.2009.01.038>.
149. Jetten, A. M. (2009). Retinoid-related orphan receptors (RORs): critical roles in development, immunity, circadian rhythm, and cellular metabolism. *Nuclear Receptor Signaling*, 7, e003. <https://doi.org/10.1621/nrs.07003>.
150. Wu, T., Ma, F., Ma, X., Jia, W., Pan, E., Cheng, G., Sun, C. (2018). Regulating Innate and Adaptive Immunity for Controlling SIV Infection by 25-Hydroxycholesterol . *Frontiers in Immunology* . Retrieved from <https://www.frontiersin.org/article/10.3389/fimmu.2018.02686>.
151. Rinaldi, V. D., Donnard, E., Gellatly, K., Rasmussen, M., Kucukural, A., Yukselen, O., Rando, O. J. (2020). An atlas of cell types in the mouse epididymis and vas deferens. *ELife*, 9, e55474. <https://doi.org/10.7554/eLife.55474>.
152. Browne, J. A., Leir, S.-H., Eggner, S. E., & Harris, A. (2018). Region-specific innate antiviral responses of the human epididymis. *Molecular and Cellular Endocrinology*, 473, 72–78. <https://doi.org/10.1016/j.mce.2018.01.004>.
153. Zhou, S., Cerny, A. M., Fitzgerald, K. A., Kurt-Jones, E. A., & Finberg, R. W. (2012). Role of interferon regulatory factor 7 in T cell responses during acute lymphocytic choriomeningitis virus infection. *Journal of Virology*, 86(20), 11254–11265. <https://doi.org/10.1128/JVI.00576-12>.
154. Dong, D., Zheng, L., Lin, J., Zhang, B., Zhu, Y., Li, N., Huang, Z. (2019). Structural basis of assembly of the human T cell receptor-CD3 complex. *Nature*, 573(7775), 546–552. <https://doi.org/10.1038/s41586-019-1537-00>.
155. Lee, J.-K., & Tansey, M. G. (2013). Microglia isolation from adult mouse brain. *Methods in Molecular Biology (Clifton, N.J.)*, 1041, 17–23. [https://doi.org/10.1007/978-1-62703-520-0\\_3](https://doi.org/10.1007/978-1-62703-520-0_3).
156. Bowling, N., Matter, W. F., Gadski, R. A., McClure, D. B., Schreyer, T., Dawson, P. A., & Vlahos, C. J. (1996). LY295427, a novel hypocholesterolemic agent, enhances [3H]25-hydroxycholesterol binding to liver cytosolic proteins. *Journal of Lipid Research*, 37(12), 2586–2598.

## REFERENCE

157. Lokka, E., Lintukorpi, L., Cisneros-Montalvo, S., Mäkelä, J.-A., Tyystjärvi, S., Ojasalo, V., Gerke, H., Toppari, J., Rantakari, P., & Salmi, M. (2020). Generation, localization and functions of macrophages during the development of testis. *Nature Communications*, 11(1), 4375. <https://doi.org/10.1038/s41467-020-18206-0>
158. Murray, P. J., & Wynn, T. A. (2011). Protective and pathogenic functions of macrophage subsets. *Nature Reviews. Immunology*, 11(11), 723 – 737. <https://doi.org/10.1038/nri3073>.
159. Röszer, T. (2015). Understanding the Mysterious M2 Macrophage through Activation Markers and Effector Mechanisms. *Mediators of Inflammation*, 2015, 816460. <https://doi.org/10.1155/2015/816460>.
160. Wang, M., Yang, Y., Cansever, D., Wang, Y., Kantores, C., Messiaen, S., Moison, D., Livera, G., Chakarov, S., Weinberger, T., Stremmel, C., Fijak, M., Klein, B., Pleuger, C., Lian, Z., Ma, W., Liu, Q., Klee, K., Händler, K., Bhushan, S. (2021). Two populations of self-maintaining monocyte-independent macrophages exist in adult epididymis and testis. *Proceedings of the National Academy of Sciences of the United States of America*, 118(1). <https://doi.org/10.1073/pnas.2013686117>

# ACKNOWLEDGEMENTS

## 8. ACKNOWLEDGEMENTS

The experimental work of this dissertation was performed at the Department of Anatomy and Cell Biology at Justus-Liebig-University of Giessen, Germany, under the supervisions of Prof. Dr. Andreas Meinhardt and Dr. Sudhanshu Bhushan.

First of all, I would like to thank Prof. Dr. Andreas Meinhardt and Dr. Sudhanshu Bhushan for providing me with this precious opportunity to be a member of this team and to work on this project. I truly appreciate the confidence and patience my supervisors have always shown to me. All of the advice, support and guidance through three years were helpful for me to become an independent researcher.

In particular, I would like to express my deepest gratitude to Dr. Sudhanshu Bhushan for his constant scientific and technical assistance and guidance. His wealth of knowledge in the field of male reproduction and immunology has always given me a lot help.

I am extremely thankful to Dr. Monika Fijak and Dr. Britta Klein. They provided me with numerous suggestions during my lab work. Moreover, I want to thank Dr. Jörg Klug for arranging all basic technique training. I also would like to thank Ms. Suada Fröhlich and Ms. Eva Wahle for technical support during these three years of work. I want to thank Dr. Aileen Harrer for her kind help in the translation of the summary to German.

Additionally, I would like to thank Ms. Eva Wewel and Ms. Pia Jürgens, who helped me a lot with the admission, visa problem and family matters. Ms. Pia Jürgens was kind to help me with all life problem whenever needed.

I sincerely appreciate the kind help from all my other colleges and friends: Julia Bender, Wei Peng, Tao Lei, Ming Wang and Muyao Tang. They were always willing to help me with work problem and life troubles.

I would like to thank my family, my wife, Ying Luo and my son, Junchen Yang. They supported me to study abroad. They went through hardships to accompany me to live together in Germany.

I was impressed by Mrs. Gabriela Michel from the Institute of Clinic Immunology and Transfusion Medicine. She was so patient to help me with the new FACS machine, even during Christmas time.

## ACKNOWLEDGEMENTS

I would like to thank Prof. Douglas F. Covey Developmental Biology, Washington University School of Medicine, St. Louis, United States for the compound of LY295427 as a kind gift.

It is my pleasure to thank Prof. Eveline Baumgart-Vogt and her GGL management team with Dr. Lorna Lueck, who had put a lot of effort in organizing and constantly improving the doctoral training program for us.

In the end, I owe my thanks to my motherland, China, which never forgot us and was always the first to offer help when needed, especially during COVID19. I also appreciate the German government and people, who showed kindness and a just attitude to Chinese students.

## CURRICULUM VITAE

### **9. CURRICULUM VITAE**

The curriculum vitae was removed from the electronic version of the paper.


# EHRENWÖRTLICHE ERKLÄRUNG

## 10. EHRENWÖRTLICHE ERKLÄRUNG

Ich erkläre: Ich habe die vorgelegte Dissertation selbständig und ohne unerlaubte fremde Hilfe und nur mit den Hilfen angefertigt, die ich in der Dissertation angegeben habe. Alle Textstellen, die wörtlich oder sinngemäß aus veröffentlichten oder nicht veröffentlichten Schriften entnommen sind, und alle Angaben, die auf mündlichen Auskünften beruhen, sind als solche kenntlich gemacht. Bei den von mir durchgeführten und in der Dissertation erwähnten Untersuchungen habe ich die Grundsätze guter wissenschaftlicher Praxis, wie sie in der „Satzung der Justus-Liebig-Universität Giessen zur Sicherung guter wissenschaftlicher Praxis“ niedergelegt sind, eingehalten.

I declare that I have completed this dissertation single-handedly without the unauthorized help of a second party and only with the assistance acknowledged therein. I have appropriately acknowledged and referenced all text passages that are derived literally from or are based on the content of published or unpublished work of others, and all information that relates to verbal communications. I have abided by the principles of good scientific conduct laid down in the charter of the Justus Liebig University of Giessen in carrying out the investigations described in the dissertation.

Giessen, den

 28.06.2021

---

Yalong Yang